Exploring cells with targeted biosensors

Diana Pendin,[1,3]* Elisa Greotti,[1,3]* Konstantinos Lefkimmiatis,[1,2] and Tullio Pozzan[1,2,3]

[1]Neuroscience Institute, National Research Council, Padua Section, 35121 Padua, Italy
[2]Venetian Institute of Molecular Medicine, 35129 Padua, Italy
[3]Department of Biomedical Sciences, University of Padua, 35121 Padua, Italy

Cellular signaling networks are composed of multiple pathways, often interconnected, that form complex networks with great potential for cross-talk. Signal decoding depends on the nature of the message as well as its amplitude, temporal pattern, and spatial distribution. In addition, the existence of membrane-bound organelles, which are both targets and generators of messages, add further complexity to the system. The availability of sensors that can localize to specific compartments in live cells and monitor their targets with high spatial and temporal resolution is thus crucial for a better understanding of cell pathophysiology. For this reason, over the last four decades, a variety of strategies have been developed, not only to generate novel and more sensitive probes for ions, metabolites, and enzymatic activity, but also to selectively deliver these sensors to specific intracellular compartments. In this review, we summarize the principles that have been used to target organic or protein sensors to different cellular compartments and their application to cellular signaling.

The Journal of General Physiology

Introduction

A unique characteristic of eukaryotes is the presence of membrane-enclosed compartments that isolate the content within their lumen from the rest of the cell and whose membranes have a high concentration of enzymes or structural proteins that are specific to the function of each compartment. The majority of genetic material in eukaryotic cells is contained in the nucleus, whereas oxidative phosphorylation occurs within mitochondria, and the synthesis and posttranslational modification of membrane proteins or secretory products are performed in the ER, Golgi apparatus (GA), and secretory vesicles. This subcellular heterogeneity relies on both the physical barrier created by internal membranes and the specific localization/accumulation of proteins in distinct subcellular sites. For example, in polarized epithelia, specific transport proteins can be found exclusively in the apical or basolateral membranes, thus ensuring vectorial transport between the lumen and interstice (Mellman and Nelson, 2008). Similarly, signaling events (second messengers, protein phosphorylation, etc.) may occur in specific subcellular compartments, thus creating functionally distinct micro- or macrodomains (Akiyama and Kamiguchi, 2015).

For decades, the existence of spatially confined signaling units was supported mostly by theoretical and indirect experimental evidence. However, the development of sensors able to measure the dynamic changes of molecules as different as ions, metabolites, and modified proteins in living cells dramatically increased our understanding of cell pathophysiology. In addition, these constructs have been targeted to various subcellular compartments, enabling the direct measure of spatially defined actions within living cells in real time. Here, we review the principles underlying how organic and protein sensors are targeted to different cellular compartments. The purpose of this contribution is not to provide a detailed description of all available sensors or even those selectively localized to subcellular compartments. Rather, we aim to critically describe the general features of sensors used in living cells and the principles of their selective localization to specific organelles or cellular regions. We highlight advantages and drawbacks in the application of each strategy, and by focusing on second messenger sensors, we discuss some of the most unexpected findings of organelle-targeted sensors in the fields of Ca^{2+} and cAMP signaling.

General characteristics of intracellular sensors

A "typical" intracellular sensor is a molecule whose physicochemical characteristics are modified by direct binding of a ligand (e.g., an ion). The term sensor, however, can be applied to other molecules that only change their location in the cell (e.g., translocate from cytosol to the plasma membrane [PM]), are accumulated/released in/from a specific compartment (e.g., membrane potential–dependent accumulation), or undergo a conformational change caused by a covalent modifica-

*D. Pendin and E. Greotti contributed equally to this paper.
Correspondence to Tullio Pozzan: tullio.pozzan@unipd.it

Abbreviations used: AC, adenylyl cyclase; AM, acetoxymethyl; BRET, bioluminescence resonance energy transfer; COX, cytochrome *c* oxidase; DG, diacylglycerol; EE, early endosome; FFN, fluorescent false neurotransmitter; FLIM, fluorescence lifetime imaging microscopy; FP, fluorescent protein; FRET, Förster resonance energy transfer; GA, Golgi apparatus; GEI, genetically encoded indicator; IMM, inner mitochondrial membrane; IMS, intermembrane space; LE, late endosome; NLS, nuclear localization sequence; OMM, outer mitochondrial membrane; PA, photoactivatable; PDE, phosphodiesterase; PM, plasma membrane; PSFP, photoswitchable FP; PTS, peroxisome-targeting signal; ROS, reactive oxygen species; sAC, soluble AC; UPR, unfolded protein response.

The Rockefeller University Press $30.00
J. Gen. Physiol. 2017 Vol. 149 No. 1 1–36
https://doi.org/10.1085/jgp.201611654

tion triggered by the event investigated (e.g., cysteine oxidation by H_2O_2 or phosphorylation by an activated kinase). In all cases, the sensor properties (usually its fluorescence intensity/spectrum or localization) monitored in living cells can provide a measure of the observed phenomena. In most cases, these changes are reversible. As discussed in more detail below in this section, sensors can be chemically synthesized (organic dyes) or be protein in nature (genetically encoded indicators [GEIs]).

Biosensors could be divided into four main classes: biosensors based on modifications in the spectral properties or quantum yield of the chromophore (class I) upon changes in ligand concentration, Förster resonance energy transfer (FRET)–based biosensors (class II), biosensors based on translocation/accumulation of fluorophores (class III), and nonfluorescent biosensors (class IV).

In the first class of probes, binding of the ligand results in a change of the sensor molecule itself that in turn causes a modification of its excitation and/or emission intensity/spectrum (or both). The changes in the indicator can be both conformational (usually in protein-based sensors) or in electronic distribution (commonly in organic dyes). This class I of sensors can be further subdivided in two subgroups depending on whether the chromophore spectral properties and/or quantum yield modifications are achieved directly by ligand binding, e.g., protonation/deprotonation (class Ia), or indirectly (class Ib), thanks to the insertion in the probe sequence of a sensing domain and its conformational change. The first subgroup includes mainly probes sensitive to H^+, where functional groups in organic dyes or mutated amino acids, in GFP mutants of GEI, are sensitive to environmental pH. The second subgroup of the first class includes many probes for ions (i.e., Ca^{2+}, Mg^{2+}, K^+, Na^+, heavy metals, and Cl^-). Generally, in this subtype, when the ion binds to the grafted sensing domain, it induces a conformational change of this domain that in turn causes modifications in spectral properties and/or in the quantum yield of the chromophore. Similarly to class Ia, chromophore property modifications are caused by change in its protonation state or in its electronic distribution. Unique cases are represented by sensors, whose fluorescence changes are induced not by ligand binding but by bond modification, e.g., oxidation of key cysteines in the sensor domain (for instance, H_2O_2 sensor [Lukyanov and Belousov, 2014]), by the reorientation of the chromophore in the membrane plane (e.g., some membrane potential dyes [St-Pierre et al., 2014]), or by a conformational change caused by membrane potential modifications (e.g., FlaSh [Siegel and Isacoff, 1997]). In organic dyes, the sensing domain is covalently bounded to the chromophore, whereas in GEIs, the "ligand-binding domain" can be inserted within or at the N/C termini of the fluorescent protein (FP) sequence, thanks to the ability of FPs to tolerate the insertion of entire proteins within their sequence (Baird et al., 1999). With few exceptions (e.g., Camgaroo [Baird et al., 1999]), GEIs that belongs to this second subclass have been mainly generated exploiting circularly permuted FPs, based on the idea that circular permutation makes the fluorophore more accessible to protons and so more susceptible to structural changes induced by conformational changes of the sensing domain.

Among this first class of fluorescent indicators, "intensity-based" and ratiometric sensors have been developed: upon changes in the ligand concentration, an increase/decrease of fluorescence intensity is observed in the first type (e.g., Fluo-4), whereas a shift of the excitation and/or emission peaks (e.g., Fura2, ratiometric pHluorin) is detected in the second. The latter class has important advantages over their single wavelength counterparts: they can be more easily calibrated (e.g., independently of heterogeneity in dye loading, photobleaching, or dye leakage), and they can also correct for changes in focal plane or movement artifacts.

Finally, among this first class of sensors, a specific case is represented by chemiluminescence. In chemiluminescence, binding of the ligand to the chromophore causes an intramolecular reaction in which the cofactor (e.g., coelenterazine in the case of aequorin) is oxidized, leading to photon emission. The rate of photon emission is proportional to the amount of bound ligand.

The second group of sensors takes advantage of another strategy, i.e., the change in FRET status between two fluorescent molecules (most commonly two GFP mutants) that are covalently linked to the sensing domain or domains. In these sensors, ligand binding or their covalent modification (e.g., phosphorylation) does not change the fluorescence characteristics of the two chromophores, but rather their distance and/or orientation and thus FRET efficiency. In living cells, FRET modifications are usually expressed as changes in the ratio between the intensity of the light emitted by the donor and by the acceptor chromophore (upon excitation of the donor), and accordingly, these sensors are intrinsically ratiometric. In a few cases, the efficiency of FRET and its changes is monitored through the measurement of the lifetime of the acceptor or donor molecule using fluorescence lifetime imaging microscopy (FLIM; see conclusion paragraph). FRET sensors can be further divided in two subgroups: (1) intermolecular FRET sensors, in which association and dissociation between two different proteins, one labeled with the donor and the other with the acceptor fluorophore, modulate the FRET signal (e.g., sensors for cAMP, PKCa, and Rac1; reviewed in Miyawaki and Tsien [2000]); (2) intramolecular FRET sensors, in which donor and acceptor FPs are connected by a linker peptide that, upon ligand binding (or covalent modifica-

tions such as phosphorylation), undergoes a conformational change, causing a change in FRET efficiency. The latter case presents the advantage that the stoichiometry of fluorophores is intrinsic to the sensor's primary structure, whereas in intermolecular FRET, the relative amount of each fluorescent molecule depends on the efficiency of cotransfection/coexpression of each part of the sensor. A variety of FRET-based sensors capable of reporting changes in many different cellular parameters (Ca^{2+} [Miyawaki et al., 1997], Zn^{2+} [Lindenburg et al., 2013a], Cl^- [Kuner and Augustine, 2000], Mg^{2+} [Lindenburg et al., 2013b], pH [Li and Tsien, 2012], pyruvate [San Martín et al., 2014], lactate [San Martín et al., 2013], glutamate [Barros et al., 2013], cAMP [reviewed in Paramonov et al., 2015], cGMP [Russwurm et al., 2007], ATP [Berg et al., 2009; Tantama et al., 2013], reactive oxygen species [ROS; reviewed in Wang et al., 2013], InsP3 [Remus et al., 2006], conformational changes in G proteins [Clister et al., 2015], PKA activity [reviewed in Depry and Zhang, 2011], Ras and ERK activation [Harvey et al., 2008; Komatsu et al., 2011], protein phosphorylation [Oldach and Zhang, 2014], etc.) have been generated in the last two decades. For extensive recent reviews on this topic, see Hochreiter et al. (2015), Mohsin et al. (2015), and Germond et al. (2016). In a special case of resonance energy transfer termed bioluminescence resonance energy transfer (BRET), the donor chromophore is a chemiluminescent protein, luciferase (or one of its variants), and the acceptor is a YFP. The relatively low intensity of BRET signals is an important limitation in single cell analysis (for review see Salahpour et al. [2012] and De et al. [2013]).

Recently, attempts have been made to exploit photoswitchable FPs (PSFPs) in class I and II FP-based biosensors. Specific wavelength irradiation induces a change in the spectral properties of PSFPs that can be reversible or irreversible, allowing signal visualization with high spatial and temporal resolution. PSFPs can be classified as photoactivatable (PA), if they increase in their emission intensity upon stimulation, and photoconvertible (PC), if they change their emission spectrum upon irradiation. The possibility to activate/convert a small subset of molecules makes PSFPs a very interesting and innovative tool not only in the field of super-resolution imaging, but also in pulse-chase experiments, organelle tracking, and the study of protein–protein interaction (reviewed in Adam et al. [2014]). Several PC Ca^{2+} sensors have been recently generated (Hoi et al., 2013; Ai et al., 2015; Berlin et al., 2015). An original application of PSFPs is a "calcium (Ca^{2+}) integrator" sensor named "CaMPARI"; this construct undergoes an irreversible green to red conversion when UV irradiated in the presence of an elevated intracellular [Ca^{2+}], allowing the identification of active cells (i.e., cells that undergo large increases in [Ca^{2+}] in a given period of time) in vivo (Fosque et al., 2015). PSFPs have also been used in FRET-based approaches such as of the PA-TNXL construct, a modified Ca^{2+} sensor where the donor is a PA-GFP and the acceptor a FRET quencher (a dim variant of YFP; Matsuda et al., 2013). Interestingly, photoactivation can be achieved also with organic dyes, using caging groups able to change their fluorescence characteristics. Based on this principle, a class of membrane potential sensors called SPOTs (small-molecule PA optical sensors of membrane potential) was recently developed, combining classical voltage-sensitive dyes with a caging group that allows the sensor to fluoresce only after UV irradiation (Grenier et al., 2015). Despite their interesting features, PS-GEIs suffer from some drawbacks: often their fluorescence is very dim before photoactivation, making difficult the identification of expressing cells, particularly in vivo; they often require UV irradiation to be photoactivated/converted; green to red conversion covers an emission spectrum that prevents or makes difficult two-color imaging.

Sensors belonging to class I and II that combine organic dyes and a genetically encoded protein (or peptide) have also been developed. For example, (a) the tetracysteine/biarsenical system and its variants (FlAsH and ReAsH), based on high-affinity interactions between trivalent arsenic compounds and a short peptide sequence containing pairs of closely spaced thiols (Griffin et al., 1998); (b) fluorogen-activating proteins (FAPs) derived from single-chain antibodies able to bind an organic dye (Szent-Gyorgyi et al., 2008); (c) SNAP-tag, Halo-tag, and CLIP-tag composed of a small protein (such as hAGT and halogen dehalogenase) that mediates the covalent binding between the genetically encoded target and the fluorophore (Griffin et al., 1998; Damoiseaux et al., 2001; Zhang et al., 2006; Gautier et al., 2008). The use of these approaches to detect physiological phenomena is still limited (i.e., G protein–coupled receptor activation [Hoffmann et al., 2005] and Ca^{2+} signaling [Bannwarth et al., 2009; Kamiya and Johnsson, 2010]).

A third class of sensors takes advantage of the translocation/accumulation of the probes between cellular compartments. Thus, membrane potential–sensitive probes accumulate within (or are excluded from) the cytosol or mitochondria depending on the membrane potential across their membranes (Nicholls, 2012); weak bases accumulate within acidic organelles, driven by ΔpH (Han and Burgess, 2010). Along the same lines, FPs can translocate between two cellular compartments, depending on the concentration of second messengers: for example, isoforms of GFP-tagged protein kinase C (or GFP-tagged domains from this enzyme) can translocate from the cytosol to the PM upon increases in diacylglycerol (DG) levels at the PM. A sensor based on this principle was developed to monitor the increase in PM of PIP3, by fusing a PIP3-binding domain to GFP (re-

viewed in Tavaré et al. [2001]). These "translocating sensors" are generally used for qualitative measures as their use for gaining quantitative information is difficult. More sensors of this type will be described below in Targeting organic sensors to subcellular compartments (PM and Mitochondrial matrix sections).

A fourth group of sensors does not take advantage of changes in light absorption/emission to monitor changes in the local environment. Examples include (a) Ca^{2+} or Zn^{2+} sensors that change the NMR spectrum upon ion binding (Smith et al., 1983); (b) the local cAMP levels can be measured by the intensity of the cationic current activated in cells expressing (endogenously or upon transfection) cAMP-activated channels (Rich et al., 2015); (c) similarly, local Ca^{2+} levels have been monitored by measuring the ion current through Ca^{2+}-activated K^+ or Cl^- channels (Maruyama et al., 1983; Osipchuk et al., 1990).

A schematic overview of fluorescent biosensors classes and their sensing mechanism is presented in Fig. 1.

Finally, although strictly speaking not intracellular sensors, important key cellular events can be measured with some special biological sensors. One example is the release of neurotransmitters into the extracellular medium that can be measured by a patch pipette (in the outside-in configuration; sniffer-patch) obtained by removing a piece of PM from cells expressing a specific ligand-activated channel (Allen, 1997); in this case, the current is activated in the patch by the molecule (e.g., acetylcholine) released in its proximity. Similarly, sentinel cells (i.e., cells expressing a specific receptor sensitive to a secreted signal), can be used to monitor exocytosis. The changes (e.g., ion current, $[Ca^{2+}]$) in the sentinel cell reveal the release of the molecule of interest (e.g., ATP [Hazama et al., 1998], BDNF [Nakajima et al., 2008], acetylcholine [Nguyen et al., 2010], glutamate, and GABA [Pasti et al., 2001; Christensen et al., 2014]) in its surroundings. The reader interested in this last group of sensors should consult the cited references for more details, as they will not be discussed further here.

Given the abundance of biosensors available, users should carefully evaluate their biophysical properties to select the probes that better match the experimental needs. The most important parameters that should be considered in the sensors selection are (a) the signal to noise ratio that accounts for the ability of an indicator to report changes in fluorescence caused by ligand binding over the fluctuations registered by autofluorescence; (b) for two-color imaging applications, the spectral properties of the sensors should be analyzed to avoid fluorophore cross-talk or bleed through; (c) for in vivo experiments, red-shifted excitation wavelengths are preferred because of their deep penetrance in the tissue; (d) for optogenetic experiments, the sensor excitation/emission wavelength shouldn't overlap with the photostimulation wavelength of the used optogenetic tools; (e) the dynamic range, which is the ratio between the minimal and maximal values a sensor can detect; (f) sensor kinetic properties, which indicate the rate of ligand binding/unbinding to the sensors defining the ability or inability of a sensor to report fast kinetics; (g) selectivity for the ligand, i.e., the specificity of binding of the ligand over other molecules; (h) sensor affinity for the ligand (K_d). As to the last parameter, although for most sensors their ligand affinity in vitro is available, it needs stressing that the environment in situ may significantly affect their K_d and thus any quantitative analysis in living cells. This problem applies to any sensor, and in particular to targeted sensors that localize within subcellular niches whose environment can be grossly different in terms of pH, viscosity, heavy metal concentration, and binding to local proteins. Last, but not least, addition of a targeting peptide may in and of itself affect the properties of the sensor. An accurate measurement of the sensor K_d in situ is therefore essential if any quantitative estimate is necessary. As mentioned above, ratiometric sensors are more easily calibrated than probes that only change signal intensity. In the latter case, the information is generally qualitative and not quantitative.

Although initially sensors were designed to stay in the cytosol, it was soon realized that the spatial complexity of eukaryotic cells and the presence of membrane-bound organelles required the development of efficient strategies for selective sensor targeting. To this end, two different strategies have been pursued, the first exploiting organelle-specific features to target organic dyes, the second using targeting sequences extracted from native proteins specifically localized in the compartment of interest. Plenty of excellent reviews on FPs, ion or redox sensors, and the information obtained through their use on key physiological processes have been published in recent years. This review is focused on the strategies adopted to target the different sensors (organic dyes or GEIs) to specific intracellular locations and the major advantages and pitfalls of each approach. The basic information on the mechanisms of selective protein targeting to different organelles are also briefly summarized. Finally, we discuss some of the most important information (in our biased opinion) obtained with the use of targeted sensors in the field of localized Ca^{2+} and cAMP signaling.

We apologize in advance to those colleagues whose key contributions are not cited; given manuscript length constraints and the enormous amount of literature available, this is an unavoidable corollary.

Targeting organic sensors to subcellular compartments

Organic dyes are low–molecular weight dyes, and different strategies have been used to selectively target them to cellular compartments. We here limit our-

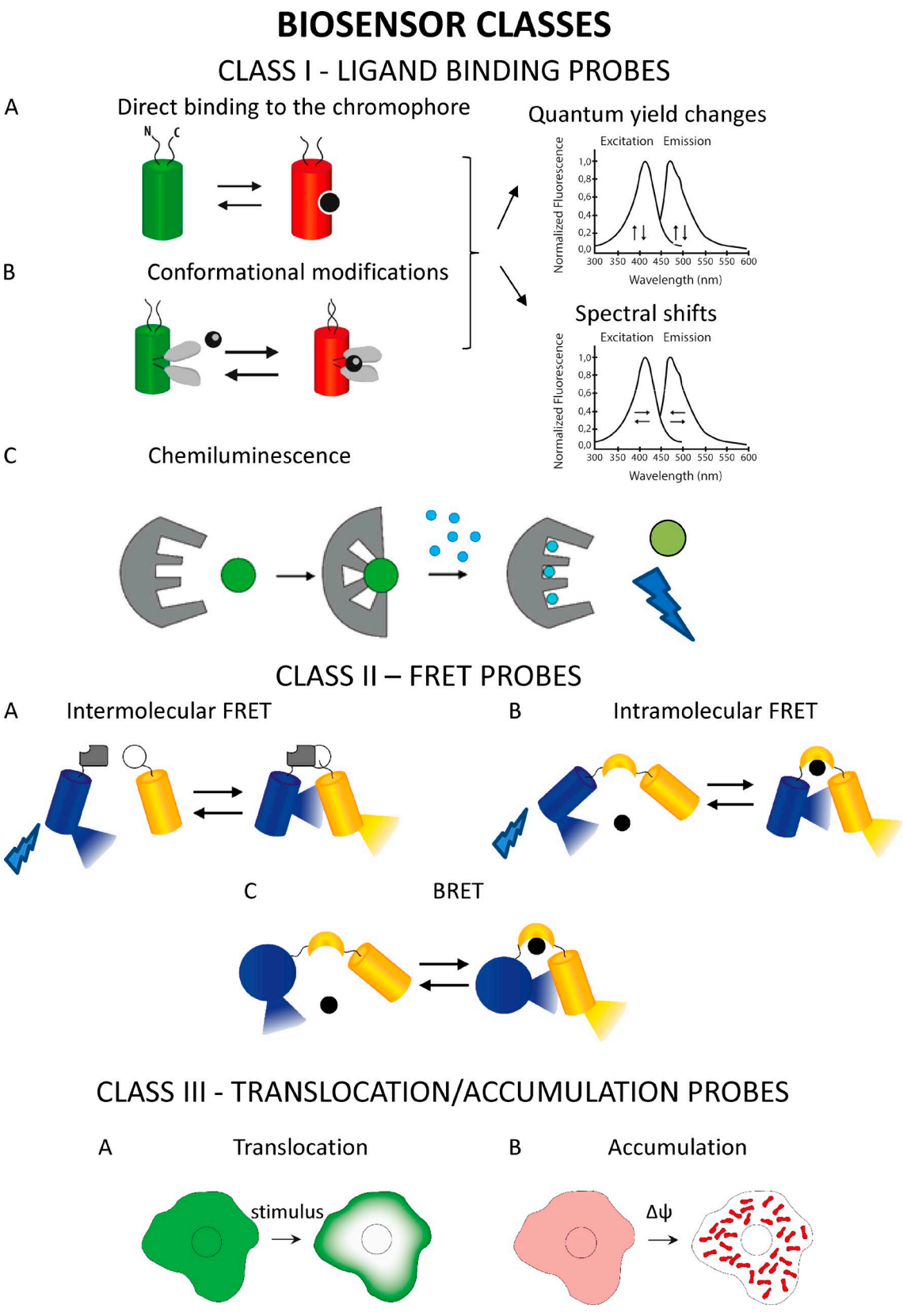

Figure 1. **Fluorescent sensors classes.** *Class I: Ligand-binding sensors.* This first class accounts for probes in which the binding of the ligand results in changes of the physicochemical properties of the sensor such as: (A) FPs that intrinsically respond to a parameter of interest, e.g., pH probes; (B) FPs, in which the binding domain is inserted in the sequence of an FP; (C) intramolecular reaction, as in chemiluminescence, where binding of the ligand causes the oxidation of the cofactor and photon emission. *Class II: FRET-based*

selves to briefly discuss the basic principles used for selective targeting and the most commonly used sensors for each compartment. In Table 1, the main strategies used to target organic dyes to different organelles are summarized.

Mitochondrial matrix. The use of acetoxymethyl (AM) esters to efficiently and easily trap fluorescent Ca^{2+} indicators within living cells (Tsien, 1981; Tsien et al., 1982) has revolutionized our understanding of cellular Ca^{2+} homeostasis, and it is still the most popular method to study Ca^{2+} signaling. The AM esters were intended to allow the trapping of the hydrolyzed dye exclusively in the cytosol of living cells as the concentration of the esterases capable of hydrolyzing the AM groups (thus preventing the release of the probe into the medium) were found to be maximally concentrated in the cytosol. From the beginning, however, it was observed that, at least in part, the hydrolyzed dye was also contained within other intracellular compartments. This extracytosolic localization is variable, often unpredictable, and not organelle specific. The first AM ester designed to be selectively targeted to a cellular subcompartment is Rhod-2 (Fig. 2 A; Minta et al., 1989; Hajnóczky et al., 1995). Rhod-2 localization in the mitochondrial matrix depends on the delocalized positive charge that permits a strong accumulation of the dye, driven by the very negative potential across the inner mitochondrial membrane (IMM). It is still unclear whether the AM hydrolysis depends on the alkaline pH of the matrix (which favors the spontaneous cleavage of the ester bond) and/or on the existence of esterases inside mitochondria.

All other strategies developed to get dye accumulation into mitochondria take advantage of the high potential across the IMM (Yousif et al., 2009). Conjugation to lipophilic cations such as triphenylphosphonium (TPP) has been used and represents a valid strategy to obtain a (relatively) specific mitochondrial targeting (see examples of sensors for Zn^{2+} [Masanta et al., 2011; Sreenath et al., 2011; Liu et al., 2012b; Chyan et al., 2014], thiols [Lim et al., 2011], H_2O_2 [Dickinson and Chang, 2008], pH [Sarkar et al., 2016], and superoxide [Robinson et al., 2006]). Lipophilic fluorescent dyes endowed with a delocalized positive charge have been developed since the '70s to monitor mitochondrial membrane potential in isolated organelles and live cells (TMRM, TMRE, Rhodamine 123, JC-1; reviewed in Nicholls [2012]). Accumulation of the dyes within the matrix results in fluorescence quenching or metachromatic shifts that are somehow proportional to the mitochondrial membrane potential (see Nicholls [2012] for more details). It should be mentioned that, when used in intact live cells, the accumulation in the matrix of membrane potential–sensitive dyes also depends on the PM potential and on the efficacy of their extrusion into the extracellular milieu by the multi-drug resistance proteins. Accordingly, the quantification in absolute terms of mitochondrial membrane potential as well as a comparison among different cells is very hard to achieve. An example of TMRM application is provided in Fig. 2 C.

Another approach proposed to target small molecules to the mitochondrial matrix is the conjugation via a mitochondria-targeting peptide (for a recent example see Si et al. [2015]).

Endo-SR. When added as AM esters, Ca^{2+} indicators are often also trapped in the ER lumen, likely depending on the presence in the lumen of esterases that cleave the AM groups. For this reason, AM esters of low-affinity Ca^{2+} indicators (Mag-Fura-2, Mag-Fluo-4, Fluo-5 N, Mag-Indo 1, and Fluo-4FF) have been used to measure $[Ca^{2+}]$ changes within the ER lumen. In general, however, the amount of dye trapped in the ER is much less than that in the cytosol, and it is thus of no practical use. For this reason, cell permeabilization is often required to ensure the dye release from the cytosol and thus to record the fluorescence signal emitted only by the ER. An example of Mag-Fura2 application, in permeabilized cells, is provided in Fig. 2 D. Different approaches have been used to maximize ER trapping and/or reducing the cytosolic dye. The interested reader is referred to specific papers for experimental details (see for example Hofer et al. [1998] and Landolfi et al. [1998]; and for a review see Landolfi et al. [1998]). One notable exception is the transfection of cells with ER-targeted esterases (Rehberg et al., 2008). Although elegant, this approach has not been used by many groups.

The aforementioned dyes and in particular non-ratiometric dyes are unsuitable to quantitatively evaluate Ca^{2+} in the SR, the specialized ER of skeletal and cardiac muscles. The contraction of the muscle and the unique architecture of this organelle requires the employment of ratiometric dyes. To overcome some of these problems, an interesting approach, called SEER (shifted excitation and emission ratioing), has been de-

sensors. Includes probes where ligand binding changes the FRET efficiency between the two chromophores. They are subdivided into (A) intermolecular FRET sensors; (B) intramolecular FRET sensors; and (C) BRET, the donor chromophore is a chemiluminescent protein and the acceptor is an FP. *Class III: Translocation- or accumulation-based biosensors.* (A) Translocation probe: the GFP-PKC example. The GFP-tagged protein kinase C accumulates at the PM upon increases in DG levels at the PM. (B) Accumulation probe: the TMRM example. This dye accumulates within mitochondria depending on their membrane potential. For other examples such as PM potential dyes that reorient in the plane of the membrane after changes or nonfluorescent probes, see Targeting organic sensors to subcellular compartments (PM section).

Table 1. **Targeting of organic biosensors to organelles: Strategies and most used presently available sensors**

Organelle or compartment	Targeting strategy	Measured parameters
Nucleus	NLS, nuclear microinjection	Ca^{2+} (Allbritton et al., 1994)
ER	Hydrophobicity, alkyl chain	Ca^{2+} (Hofer et al., 1998; Landolfi et al., 1998)
		pH (Reddy G et al., 2015)
		Cu^{2+} (Lee et al., 2014)
PM inner surface	Hydrophobic tail	Ca^{2+} (Vorndran et al., 1995)
		membrane potential (González and Tsien, 1995; Peterka et al., 2011; St-Pierre et al., 2015)
Mitochondrial matrix	Membrane potential	Ca^{2+} (Hajnóczky et al., 1995)
		Zn^{2+} (Masanta et al., 2011; Sreenath et al., 2011; Liu et al., 2012b; Chyan et al., 2014)
		thiols (Lim et al., 2011)
		H_2O_2 (Dickinson and Chang, 2008)
		pH (Sarkar et al., 2016)
		superoxide (Robinson et al., 2006)
		membrane potential (Nicholls, 2012)
Acidic compartments	pH gradient, endocytosis	pH (Zhu et al., 2012; Miao et al., 2013; Lv et al., 2014; Chen et al., 2015; Wang et al., 2015; Yapici et al., 2015)
		thiols (Kand et al., 2015)
		Ca^{2+} (Gilroy and Jones, 1992; Schlatterer et al., 1992)
		vesicle recycling (Gaffield and Betz, 2007; Li et al., 2009)
		neurotransmitter release (Gubernator et al., 2009)

veloped to measure [Ca^{2+}] in the SR of live muscles. Based on the spectral properties of some fluorescent dyes, such as mag-indo-1 and indo-1, this method exploits the dual spectral shifts caused by Ca^{2+} binding, allowing the generation of ratiometric probes with increased accuracy, dynamic range, and sensitivity (Launikonis et al., 2005). SEER can be applied more broadly, and it has already found application to pH (Morgan et al., 2009) and PM voltage measurements (Manno et al., 2013a).

Another approach used to target organic dyes to ER and in general to the secretory pathway is the addition of an alkyl chain (see Lee et al. [2015] as an example of an ER membrane fluidity sensor). These dyes permeate the PM and, depending on the length and saturation of the alkyl chains appended, also distribute to the membranes of ER, GA, and endosomal/lysosomal compartments. Although interesting, this approach does not guarantee a specific ER targeting, usually also resulting in staining of the PM and other membranous compartments.

An important parameter to assess along the secretory pathway is pH. Indeed, pH within the individual organelles of the secretory pathway is crucial for their biosynthetic activity and other physiological functions (e.g., accumulation of neurotransmitters), and the precise measurement of the pH in these compartments is essential. Recently, the generation of a FRET-based, ER-localized probe for pH was reported (Reddy G et al., 2015). Although this and other ER-localized probes (i.e., a probe for Cu^{2+} [Lee et al., 2014]) do not contain a clearly identifiable ER-targeting motif and are probably targeted to ER because of their hydrophobicity, understanding the principles that favor localization of these dyes in the ER would prove valuable for the development of novel ER-targeted sensors. An interesting example in this direction is reported in Meinig et al. (2015), where the structure of a known interactor of the ER-resident protein p97 allowed the design of a novel analogue of the fluorophore rhodol that uniquely accumulates in the ER of mammalian cells.

PM. Theoretical models predict that Ca^{2+} hot spots should be generated on the inner side of the PM in the proximity of open Ca^{2+} channels. Various attempts have been made to quantitatively measure such hot spots. Near-PM versions of tetracarboxylate Ca^{2+} indicators have been created by adding a lipophilic anchor that tethers the dye to the PM inner leaflet (see for example Vorndran et al. [1995]). Because of the limited specificity of PM binding, this approach has been rarely used in recent years.

A series of membrane potential–sensitive dyes have been available since the ‘70s. These dyes are lipophilic cations (carbocyanines) or anions (bis-oxonol) that move from the aqueous extracellular medium to the cell interior/membrane (or vice versa) in response to changes in PM potential, typically displaying a substantial increase in fluorescence inside the cells. A problem with such probes is that although the signal changes are large, the response time is slow, as the dye has to redistribute across the PM.

Another group (i.e., merocyanine dyes) are incorporated in the PM, and changes in the electric field cause the dye to flip from an orientation perpendicular to the cell surface to an orientation where its long axis is parallel to the surface, producing a change in the spectral properties. This mechanism can be very fast, but the

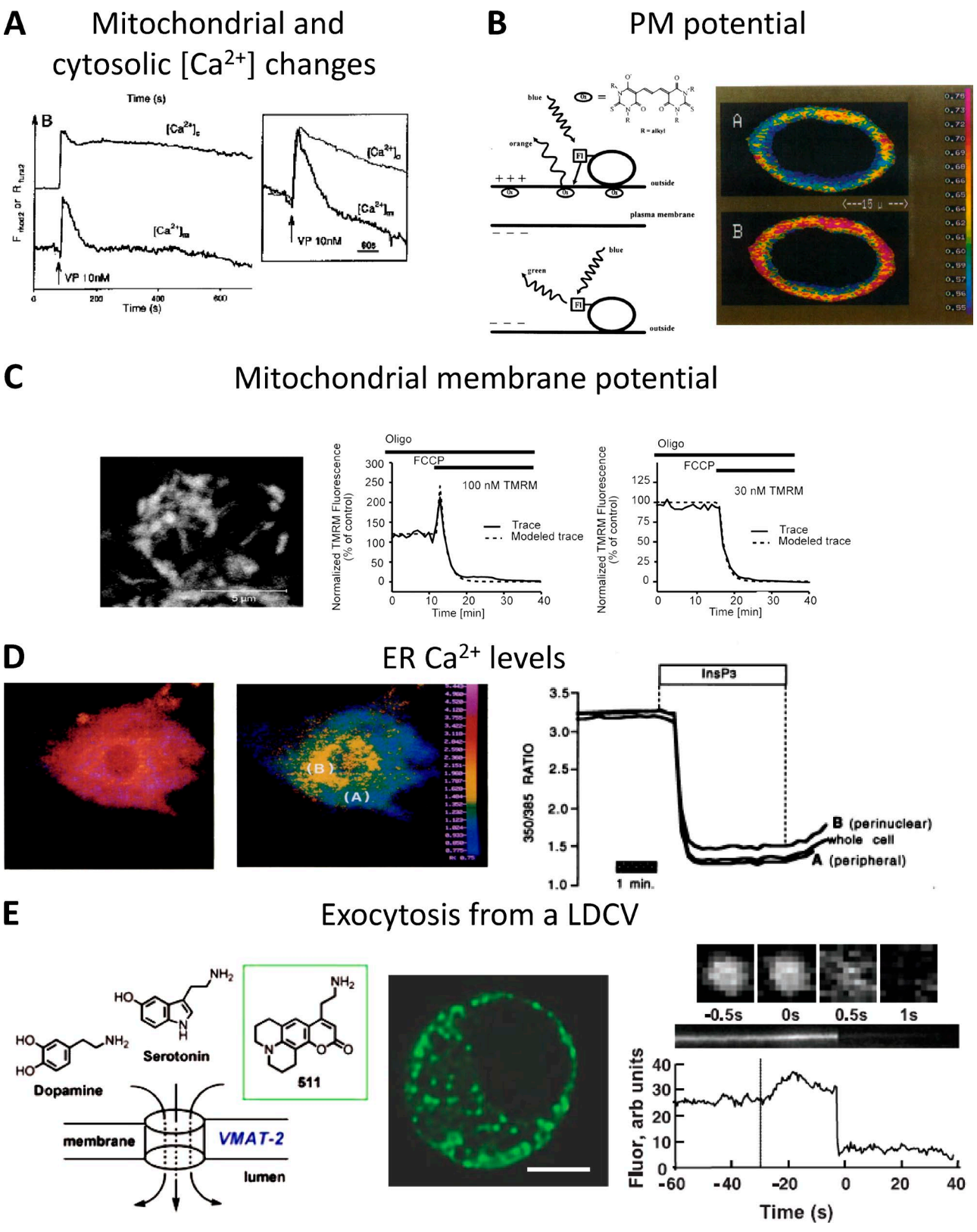

Figure 2. **Targeted synthetic sensors.** (A) Transmission of $[Ca^{2+}]_c$ changes into the mitochondrial matrix of single hepatocytes challenged with a maximal dose of vasopressin (VP). $[Ca^{2+}]_m$ was monitored with dihydro-Rhod 2-AM, and $[Ca^{2+}]_c$ was measured with Fura 2-AM. The inset shows cell population mean responses for $[Ca^{2+}]_c$ and $[Ca^{2+}]_m$. The figure is modified from Hajnóczky et al. (1995) with permission from Elsevier. (B) PM potential measured using the FRET-based sensor. (left) Scheme of the voltage-sensitive FRET mechanism. At resting negative membrane potential (top), the permeable oxonols have a high concentration at the extracellular surface of the PM, and energy transfer from the extracellularly bound FL-WGA (acceptor molecule) is favored. FRET is symbolized as the

fluorescent changes are small, and repetitive measurements are needed to obtain a good record of action potentials (for recent reviews see Peterka et al. [2011] and St-Pierre et al. [2015]). To overcome these limitations, efforts led to the development of potentiometric dyes called hemicyanine or steryl dyes (for a recent review see Loew [2015]), characterized by rapid absorbance and florescence responses to membrane potential. They are based on the electrochromic mechanism of voltage sensitivity. In brief, charge redistribution in steryl dyes causes a spectral shift of the excited dye. Another interesting approach exploited intermolecular FRET to develop a sensor for PM potential that is fast, but with relatively large fluorescence changes. In this system, a fluorophore (a fluorescently labeled lectin) is attached to the outer leaflet of the PM, while a hydrophobic fluorescent (or quencher) anion is incorporated into the membrane. The anion transfers from one side to the other of the PM in response to changes in the transmembrane potential, allowing FRET to happen or not between the two molecules (Fig. 2 B; González and Tsien, 1995). The substitution of the membrane-anchored fluorophore with a variant of GFP formed the first hybrid voltage sensor (hVoS; Chanda et al., 2005), which outperformed existing fully genetically encoded voltage indicators (GEVIs), in particular because of its very fast (sub-millisecond) kinetics.

Acidic compartments. There is a simple method to target, although nonspecifically, cellular compartments with a low luminal pH (pH 4.0–6.0). It consists of incubating cells with fluorescent weakly basic amines that are strongly accumulated in acidic vesicles. With some of these amines, neutral red, acridine orange, and LysoTracker, a strong accumulation of the dye results in a "metachromatic shift" and fluorescence emission changes from green to red, permitting an easy identification of highly acidic compartments (Han and Burgess, 2010; Pierzyńska-Mach et al., 2014). Release of the accumulated dye into the extracellular medium has been used to monitor secretion in different cellular models. Neutralization of the luminal pH by drugs (e.g., monensin) or inhibitors of the H^+ pumps can be simply measured by the decrease in the fluorescence signal (reviewed in Han and Burgess [2010]). More recently, efforts are ongoing to create new and more selectively targeted probes, with better spectral characteristics, to monitor pH (Zhu et al., 2012; Miao et al., 2013; Lv et al., 2014; Chen et al., 2015; Wang et al., 2015; Yapici et al., 2015) and thiols (Kand et al., 2015).

A special case is that of synaptic vesicles that can be visualized using FM1-43, an amphiphilic membrane-impermeable fluorescent dye that inserts into the outer leaflet of the PM, increasing its fluorescence, and is internalized within synaptic vesicles in active neurons during endocytosis (Gaffield and Betz, 2007; Li et al., 2009). FM1-43 has been extensively used to study synaptic vesicle release or recycling. Another class of targeted organic dyes called fluorescent false neurotransmitters (FFNs) have been developed to image neurotransmitter release (Fig. 2 E; Gubernator et al., 2009). As an example, FFN102 is a coumarin dye that accumulates in the secretory granule transported by the vesicular monoamine transporter 2 (VMAT2) that has been used for the measurement of dopamine release (Rodriguez et al., 2013).

Ca^{2+} in endosomes has been instead measured by allowing endocytosis of dextran-bound fluorescent dyes, such as calcium green (Gilroy and Jones, 1992) and fura-2 (Schlatterer et al., 1992). The interpretation of the results is, however, still debated (see Targeting GEIs to organelles, Acidic compartments section).

Nucleus. Nuclear pores are permeable to solutes with molecular mass up to ≅50 kD, and accordingly, any cytosolic dye freely diffuses into the nucleoplasm. The nucleoplasm environment, however, can modify the fluorescence characteristics of the probes (experimentally verified with some Ca^{2+} indicators [Thomas et al., 2000]). In addition, two other problems plague the measurement of nuclear Ca^{2+} levels: (1) the nucleus is generally much brighter than the rest of the cytoplasm simply because of the thickness of the nuclear region, and with non-ratiometric dyes, this can be erroneously

straight arrow from lectin to oxonol. Upon membrane depolarization (bottom), the anions diffuse inside the cell and energy transfer is greatly reduced. (right) Confocal image of a voltage-clamped astrocytoma cell at −70 (A) and 50 mV (B), stained with FLOX6 (from González and Tsien [1995] with permission from Elsevier). (C) Mitochondrial membrane potential measured using TMRM. Cerebellar granule neurons loaded with TMRM (left) were exposed to the uncoupler FCCP and monitored over 60 min using TMRM in both the quenched (100 nM, middle) and nonquenched (30 nM, right) mode (from Ward et al. [2007] with permission from the Society for Neuroscience). (D) $[Ca^{2+}]_{ER}$ measured with Mag-Fura2. (left) Pseudo-color ratio image of permeabilized BHK-21 cells loaded with mag-Fura2. (middle) Same cell of left panel after stimulation with $InsP_3$, causing release of Ca^{2+} from the ER. (right) Representative kinetic of mag-Fura2 ratio collected from selected areas of the cell (from Hofer et al. [1995] with permission from the Federation of American Societies for Experimental Biology). (E) Exocytosis from large dense core vesicles (LDCVs) measured using FFN511. (left) Chemical structure of FFN511. (middle) Multiphoton image of a chromaffin cell shows distribution of FFN511 in LDCVs. Bar, 5 µm. (right) FFN511 exocytosis from an LDCV observed with total internal reflection fluorescence microscopy (TIRFM) images. The upper row shows consecutive images of a single vesicle. Orthogonal section through this vesicle and its integrated intensity are in the middle and bottom panels. The dotted line indicates stimulation by high potassium (from Gubernator et al. [2009] with permission from The American Association for the Advancement of Science).

interpreted as evidence for a nucleus/cytoplasm Ca^{2+} gradient; (2) trapping of the dyes within the lumen of the nuclear membrane (continuous with the ER) and/or its invaginations into the nucleus (Echevarría et al., 2003) can be erroneously interpreted as evidence for localized high $[Ca^{2+}]$ in the nucleus. Specific localization of biosensors in the nucleus was achieved either by nuclear microinjection of dextran-bound Ca^{2+} indicators (too large to pass the nuclear pores) or by nuclear localization signals bound to the dextran particles containing the dye (Allbritton et al., 1994). Using this technique (and see also Targeting GEIs to organelles, Nucleus section for FP probes), it has been demonstrated that nuclear Ca^{2+} levels rapidly equilibrate with the cytosol, with delays of a few hundred of milliseconds.

In conclusion, selective targeting of organic biosensors are now available for several organelles (summarized in Table 1); however, they are mainly limited to probes for Ca^{2+}, membrane potential, vesicle recycling, and pH, and they all suffer from some kind of limitation.

Targeting GEIs to organelles

In 1999, Gunter Blobel was awarded the Nobel Prize for the discovery (Blobel and Dobberstein, 1975a,b) that newly synthesized proteins destined to the secretory pathway are endowed with unique signal sequences that allow their insertion into the ER. In the same period, G. Schatz and co-workers together with other groups demonstrated that most mitochondrial proteins translocate into mitochondria posttranscriptionally because of the presence of a specific targeting signal (Roise and Schatz, 1988; Hartl et al., 1989; Omura, 1998). Decades of research have revealed how proteins are targeted to the correct cellular location and transported across one or more organelle membrane to the compartment where they function. The known targeting strategies involve interactions between a peptide sequence in the protein, localization factors, and various membrane-embedded translocation/retention machineries. The initially identified targeting sequence for the ER, usually composed of a stretch of 3–70 amino acid residues often, but not always, located at the N terminus of the protein, have been flanked by other sequences designated for targeting, found distributed along the polypeptide chain, usually called signal patches (for a review see Dudek et al. [2015]). Despite the number of studies dedicated to unravel the mechanisms governing protein targeting to the different cellular locations, even today not all targeting strategies are known, and the mechanism of localization of many proteins remains unidentified.

In general, proteins can reach the appropriate destination during or after the translation process. Co-translational translocation is typical for secreted, membrane-bound proteins or proteins located in the ER, GA, and endosomes. Posttranslational translocation occurs for some proteins translated in the cytosol and destined to ER, secretory vesicles, or PM. In some cases, posttranslational modifications, such as glycosylation, can work as additional targeting/retention signals. Similarly, proteins targeted to mitochondria, nucleus, or peroxisomes follow specific posttranslational transport pathways, which will be briefly discussed in the corresponding paragraphs.

To the best of our knowledge, the localization of a protein in the cytosol depends on the absence of any signal sequence. Although the targeting mechanism of some specific organellar proteins is still elusive, the general concept is that signal sequences are necessary and sufficient for the selective localization of all (but not cytosolic) proteins within the cell. Appending such signals even to a foreign protein (and thus to protein-based sensors) results in most cases in the selective localization of this chimeric artificial protein into the compartment specified by the targeting sequence. The first example of a selectively targeted GEI is that of mitochondrial aequorin (Rizzuto et al., 1992), and this construct is the prototype of all targeted sensors generated later on. In a few cases, usually because the targeting mechanism to the desired compartment is unknown, selective targeting has been achieved by appending to the sensor either a binding site for a protein localized in the compartment of interest or by fusing the sensor to a protein (or part of it) that is itself selectively localized, through yet incompletely characterized mechanisms. The key advantage of GEI and of this targeting strategy over organic dyes is that localization is, in most cases, highly specific and predicted. Below we briefly describe the targeting strategies for different cellular subcompartments that have been used to selectively localize GEIs (summarized in Fig. 9). Moreover, we provide an overview of the most commonly used targeted biosensors (summarized in Table 2).

IMM and outer mitochondrial membrane (OMM) and matrix. Mitochondria are double membrane-bound organelles forming a dynamic tubular network in the cytosol. The IMM and the OMM define an intermembrane space (IMS). Infoldings of the IMM form the cristae and shape the mitochondrial matrix. The precise targeting to each mitochondrial subcompartment is achieved thanks to the presence of unique signals that mediate the recognition of the protein by specific translocases. With a few exceptions (primarily for proteins localized on the OMM), the mitochondrial signal sequence binds the OMM translocase (TOM) that actively transports the protein across the membrane. The imported protein then binds to the translocase of the IMM (TIM). The mitochondrial matrix targeting or localization signal (MTS) is usually composed by an amphipathic α-helix of 10–70 amino acids fused to the N terminus of the protein with a net positive charge. The positive

Table 2. **Summary of some of the most used organelle-targeted indicators**

GEI	Organelle targeted						
	PM	**Nucleus**	**ER/SR**	**GA**	**Mitochondria**	**Acidic compartments**	**Peroxisomes**
ATP:ADP	Pellegatti et al., 2005	Imamura et al., 2009	Vishnu et al., 2014		Gajewski et al., 2003; Imamura et al., 2009; Nakano et al., 2011; Lefkimmiatis et al., 2013		
Calcium	Marsault et al., 1997; Mao et al., 2008	Brini et al., 1993; Bengtson et al., 2010; Giacomello et al., 2010; Simonetti et al., 2013	Kendall et al., 1992; Palmer et al., 2004; Tang et al., 2011; Kipanyula et al., 2012; de la Fuente et al., 2013; Rodriguez-Garcia et al., 2014; Suzuki et al., 2014; Henderson et al., 2015; Rodríguez-Prados et al., 2015; Waldeck-Weiermair et al., 2015; Navas-Navarro et al., 2016	Pinton et al., 1998; Lissandron et al., 2010; Wong et al., 2013; Aulestia et al., 2015; Rodríguez-Prados et al., 2015	Rizzuto et al., 1992, 1994; Arnaudeau et al., 2001; Griesbeck et al., 2001; Nagai et al., 2001; Rapizzi et al., 2002; Filippin et al., 2003, 2005; Palmer et al., 2006; Giacomello et al., 2010; Park et al., 2010; Alam et al., 2012; Jean-Quartier et al., 2012; Loro et al., 2012; Akerboom et al., 2013	Mitchell et al., 2001; Shen et al., 2012; McCue et al., 2013; Albrecht et al., 2015; Ronco et al., 2015	Drago et al., 2008; Lasorsa et al., 2008
cAMP	DiPilato et al., 2004; Dyachok et al., 2006; Terrin et al., 2006	DiPilato et al., 2004			DiPilato et al., 2004; Terrin et al., 2006; Di Benedetto et al., 2013; Lefkimmiatis et al., 2013		
DG	Sato et al., 2006		Sato et al., 2006	Sato et al., 2006	Sato et al., 2006		
ERK activity		Harvey et al., 2008					
Glucose		Fehr et al., 2004	Fehr et al., 2005				
Hydrogen Peroxide (H_2O_2)		Malinouski et al., 2011	Merksamer et al., 2008		Belousov et al., 2006; Malinouski et al., 2011; Ermakova et al., 2014		Malinouski et al., 2011
Phosphoinositides ($PI3P_2$, $PI3P_3$)	Sato, 2014	Ananthanarayanan et al., 2005	Sato, 2014	Sato, 2014	Sato, 2014		
$InsP_3$		Sato et al., 2005; Kapoor et al., 2014					
Lactate		Barros et al., 2013					
Mg^{2+}		Lindenburg et al., 2013b					
NADH-NAD^+		Zhao et al., 2011			Hung et al., 2011; Zhao et al., 2011; Bilan et al., 2014		
pH	Mukhtarov et al., 2013			Llopis et al., 1998; Miesenböck et al., 1998; Wu et al., 2000	Kneen et al., 1998; Llopis et al., 1998; Abad et al., 2004; Porcelli et al., 2005; Azarias and Chatton, 2011; Poburko et al., 2011; Tantama et al., 2011	Miesenböck et al., 1998; Ohara-Imaizumi et al., 2002; Zhu et al., 2009; Li and Tsien, 2012	Jankowski et al., 2001; Lasorsa et al., 2008
PKA	Allen and Zhang, 2006; Depry et al., 2011	Allen and Zhang, 2006	Liu et al., 2011		Allen and Zhang, 2006; Lefkimmiatis et al., 2013		
PKC	Gallegos et al., 2006	Gallegos et al., 2006		Gallegos et al., 2006	Gallegos et al., 2006		
Redox state/ROS			van Lith et al., 2011		Hanson et al., 2004; Gutscher et al., 2008; Liu et al., 2012a; Albrecht et al., 2014		Yano et al., 2010
Voltage	Storace et al., 2016						
Zn^{2+}			Qin et al., 2011	Qin et al., 2011	Dittmer et al., 2009; Miranda et al., 2012	Vinkenborg et al., 2009	

References are provided for original works or reviews. For most of these sensors, the cytosolic forms are available and are not included in this table. Sensors for glutamate (Marvin et al., 2013), pyruvate (San Martín et al., 2014), G protein activation (van Unen et al., 2016), cGMP (Russwurm et al., 2007), and phosphate (Gu et al., 2006) are currently available only in the form localized in the cytosol.

charge is essential as import of the proteins into the matrix is fueled by the negative membrane potential of the IMM. A complex associated with TIM, called PAM (presequence translocase-associated motor), actively transports the protein into the matrix, where a mitochondrial matrix peptidase cleaves the MTS. Proteins targeted to the IMS cross OMM thanks to TOM as hairpin loops and then they can follow the same route of matrix proteins, staying in the IMS thanks to the presence of a hydrophobic sequence, or they are recognized and modified by the IMS assembly machinery, called the MIA (mitochondrial IMS assembly machinery) pathway. A few proteins are localized in mitochondria because of yet unknown targeting sequences. For a general review on mitochondria targeting of proteins, see Harbauer et al. (2014).

Most of the available mitochondrial GEI have been localized in the matrix using the targeting sequence of cytochrome *c* oxidase (COX) subunits. Our group and others used the 36 amino acids of N-terminal sequence of human subunit VIII (COX8; Rizzuto et al., 1992) or the 12 amino acids of subunit IV of yeast COX (COX4; Nagai et al., 2001). More rarely, other targeting sequences have been used to localize probes in the mitochondrial matrix (Hanson et al., 2004; Zhao et al., 2011; Liu et al., 2012a). Appending a single copy of these targeting peptides appears sufficient for an effective localization of relatively small sensors in the matrix (GFP or its mutants, monomeric RFPs, or aequorins). However, it has been observed that in order to achieve an efficient targeting of some molecules (such as Cameleons or cAMP sensors), multiple copies of the signal peptides (from two to eight copies, most commonly four) are required. It is advisable to include an efficient cleavage site downstream the targeting signal because inappropriate cleavage of it could affect the properties of the probes. Indeed, Filippin et al. (2005) showed that if uncleaved, the leader peptide impaired both the Ca^{2+} affinity and the dynamic range of Pericam. The authors speculated that the uncleaved N-terminal segment affects the Ca^{2+}-dependent M13-calmodulin interaction either directly, e.g., causing differences in the probe conformation of these N-terminal tails, or indirectly, e.g., causing "undesired" interaction with other proteins (Filippin et al., 2005).

Different strategies have been used to localize sensors on the outer surface of the OMM, i.e., fusion of the sensors to a fragment of an endogenous OMM localized protein (Allen and Zhang, 2006; Giacomello et al., 2010). As for targeting to the IMS, sensors have been fused to full proteins or domains anchoring to the IMM (Rizzuto et al., 1998; Porcelli et al., 2005; Malinouski et al., 2011).

Mitochondria are involved in many different cellular processes: (a) ATP synthesis, (b) Ca^{2+} homeostasis, (c) ROS production, (d) cellular death program regulation, and (e) "pro-survival programs" such as autophagy and mitophagy, only to mention the best known. Given this variety of mitochondrial functions, many mitochondria-targeted sensors are available nowadays. The parameters that can now be measured with these sensors include pH, Ca^{2+}, ATP, cAMP, ROS, PKA activity (all these sensors are reviewed in De Michele et al. [2014]), and mitophagy (Dolman et al., 2013). Although practically all the mitochondrial functions are directly or indirectly dependent on the maintenance of membrane potential across the IMM, GEIs for quantitative measurement of mitochondrial membrane potential are still missing. Other parameters that still lack specific biosensors include Na^{+}, K^{+}, and respiratory chain activity.

A schematic overview of mitochondria-targeting strategies and of the available sensors is provided in Fig. 3 A.

ER membrane and lumen. All proteins processed by the ER, whether destined to be retained in this compartment or to enter the secretory or lysosomal pathways, are synthesized in the cytosol. Nascent proteins are targeted to and translocated across the membrane of the ER through the binding of the cytosolic signal recognition particle (SRP) to N-terminal signal peptide emerging from the ribosome. This complex then interacts with the ER-localized SRP receptor, targeting the nascent protein toward the Sec61 translocon channel. Through this channel, the nascent chain can be directly conveyed into the lumen of the ER, where it can then fold into its final conformation. Transmembrane proteins are inserted into the membrane by translocation through the Sec61 complex, where membrane-spanning stretches enter the lipid bilayer laterally. A few proteins are targeted to and inserted into the ER membrane only after their synthesis is complete (for a review on ER targeting see Dudek et al. [2015]).

Based on this information, the classical approach used for targeting of exogenous proteins (including biosensors) to the ER lumen is achieved by appending an ER-targeting sequence to the N-terminal end of the indicator's sequence. The addition of specific C-terminal sequences ensures retrieval from post-ER compartments by virtue of retrograde transport mechanisms. The most frequently used retrieval sequences are lysine–aspartic acid–glutamic acid–leucine (KDEL) for luminal proteins and lysine-lysine-X-X (KKXX) for membrane proteins. Sensors targeted to ER lumen have been developed mainly following this strategy to measure Ca^{2+} (Cameleons [Palmer et al., 2004; Sztretye et al., 2011; Kipanyula et al., 2012; Waldeck-Weiermair et al., 2015; Greotti et al., 2016], GCamPer [Henderson et al., 2015], CatchER [Tang et al., 2011], G-CEPIA1er [Suzuki et al., 2014], er-GAPs [Rodriguez-Garcia et al., 2014; Rodríguez-Prados et al., 2015; Navas-Navarro et al., 2016]), redox state (roGFP1-iL–KDEL [van Lith et al., 2011]), pH (AV–KDEL plus Flubida [Wu et al.,

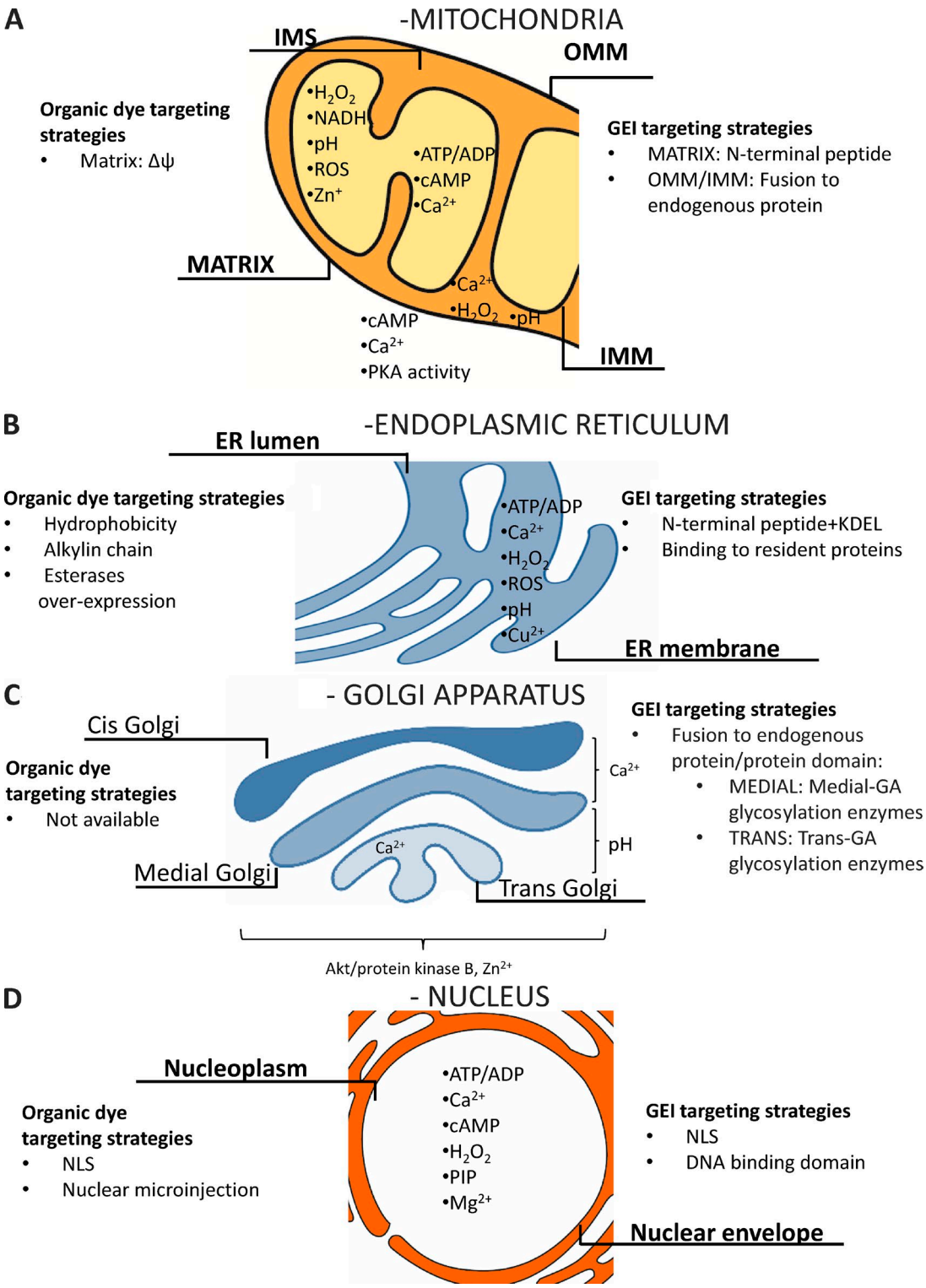

Figure 3. **Schematic representation of targeting strategies.** Targeting strategies used to achieve selective mitochondria-targeted biosensors (A), ER-targeted probes (B), Golgi-targeted sensors (C), and nuclear-targeted sensors (D) and localization of the available sensors.

2000]), and ATP (ERAT4.01 [Vishnu et al., 2014]). Noteworthy, the most used aequorin-based ER sensors have been developed using a different retention strategy, i.e., the insertion of N-terminal domain that specifically binds to the ER-resident protein Bip (Montero et al., 1995, 1997; de la Fuente et al., 2013). This strategy

was adopted because the C-terminal modification of aequorin results in a major modification of the chemiluminescent characteristics of the protein that prevents its use in the high Ca^{2+} environment typical of the ER lumen. Similarly, to specifically target a Ca^{2+} sensor to the SR, the SR-resident protein calsequestrin was fused to the N terminus of Cameleon variant D4cpv probe (Sztretye et al., 2011).

The ER is the site of folding of membrane and secreted proteins, and it is known that physiological or pathological processes that disturb this process cause ER stress and activate the signaling pathway of the unfolded protein response (UPR). A limited number of fluorescence- or luminescence-based sensors have been developed to dynamically measure this phenomenon. In this case, the design strategy does not imply the traditional targeting by fusion at the N terminus of a signal peptide. Instead, ER stress–dependent splicing of the transcriptional activator XBP1 has been used to develop fluorescent reporter constructs by fusing XBP1 sequence to a GFP variant. Under normal conditions, the mRNA of the fusion gene is not spliced. However, during ER stress, splicing leads to a frame shift of the chimeric XBP1-FP mRNA, and a fusion protein is translated, allowing the detection of cells experiencing ER stress by monitoring fluorescence. Examples of ER stress sensors are ERAI (Iwawaki et al., 2004), NanoLuc (Hikiji et al., 2015), and the dual-luciferase UPR reporter system (Fang et al., 2015).

As a general consideration, when generating ER-targeted FP-based sensors, the characteristic features of both ER and FPs need to be considered, namely the ER oxidizing environment and glycosylation ability and FP oligomerization tendency. Indeed, expressing FPs in the ER oxidizing environment can impair folding, generating nonfluorescent disulfide-linked oligomers, leading to severely decreased fluorescence. Moreover, proteins can be glycosylated, a modification that can interfere with correct protein folding, mobility, retention, and half-life. Lastly, and especially critical for outer surface ER-targeted sensors, FPs need to be monomeric. When targeted to ER membrane, the weakly dimerizing EGFP causes a reorganization of the ER tubular network with the formation of stacked cisternal membranes and sinusoidal and crystalloid membranes (Snapp et al., 2003). To overcome these obstacles, the highly efficient folding capability of monomeric superfolder GFP (sfGFP) has been exploited, generating a very stable and bright FP when targeted to the lumen or the surface of ER (Pédelacq et al., 2006; Aronson et al., 2011; Hoseki et al., 2016; Summerville et al., 2016).

A schematic overview of ER targeting strategies and of the available sensors is provided in Fig. 3 B, with the exception of UPR sensors.

Golgi compartments. Once inside the ER lumen or membrane, proteins can proceed to the secretory pathway through vesicular transport. The first stop is the GA, which serves as the major protein sorting hub, receiving de novo synthesized proteins from the ER that are destined for secretion, for the endocytic compartments, the lysosomes, or the PM. In most eukaryotes, the GA is made up of a series of cisternae that, based on their morphology, function, and unique set of resident proteins, have been categorized in cis-, medial-, and trans-Golgi network (TGN). The GA faces the unique challenge of maintaining its protein composition (and the distinct properties of its subcompartments) while dealing with a constant influx and efflux of proteins. Targeting and retention in the GA rely on many different mechanisms, in particular protein–protein interactions, composition, and length of the transmembrane domain, the cytosolic tail, and luminal region (Borgese, 2016). The strategies used for targeting GEIs implicate the fusion of the sensors with specific resident proteins (or their targeting sequence), most frequently the N-terminal fusion to cytosolic tail and transmembrane domain of glycosylation enzymes. To the best of our knowledge, GA-targeted sensors have been generated for Ca^{2+} (Aequorins [Pinton et al., 1998; Aulestia et al., 2015], Cameleons [Lissandron et al., 2010; Wong et al., 2013], GAP [Rodríguez-Prados et al., 2015]), pH (GT-EGFP and variants [Llopis et al., 1998] and pHluorin (Miesenböck et al., 1998]), a targeted biotin plus fluorescent avidin (Wu et al., 2000), Zn^{2+} (Qin et al., 2011), and Akt/protein kinase B (Sasaki et al., 2003).

A schematic overview of GA-targeting strategies and of the available sensors is provided in Fig. 3 C.

Nucleus. The import of soluble cargos into the nucleus has been extensively studied in many eukaryotic systems (Goldfarb et al., 1986). Although small molecules can enter the nucleus without regulation, macromolecules such as proteins larger than ≅50 kD require a nuclear localization sequence (NLS), typically composed of a few basic amino acid residues, essentially lysines or arginines that appear either in the form of a single stretch or as two smaller clusters separated by about a dozen amino acid residues. These sequences are recognized by a class of karyopherins called importins, which mediates the translocation through the nuclear pore complexes (NPCs) via interactions with NPC proteins nucleoporins. Once in the nucleus, the dissociation of the cargo from the karyopherin relies on the small GTPase Ran (Ras-related nuclear protein) that allows the directionality of transport. NLSs are not cleaved from these nuclear proteins.

Targeting of Ca^{2+} sensors to the nucleoplasm was achieved by fusing (in general at the N terminus of the probe) an NLS derived from classical nuclear proteins. Some constructs also contain a DNA-binding domain to prevent back diffusion of the probe into the cytosol. Sensors have been developed for Ca^{2+} (Aequorin [Brini

et al., 1993], Cameleon [Giacomello et al., 2010], GCamPs [Bengtson et al., 2010], and TN-XXL [Simonetti et al., 2013]), ATP (Imamura et al., 2009), H_2O_2 (Malinouski et al., 2011), and phosphoinositides (Ananthanarayanan et al., 2005).

A schematic overview of nuclear targeting strategies and of the available sensors is provided in Fig. 3 D.

Outer and inner PM. For targeting to the PM, proteins use two mechanisms, namely sequence domains and lipid modifications. Selection and movement along the secretory pathway to the PM of membrane proteins inserted into the ER depends on organellar targeting motifs within the proteins themselves, as well as on interactions with adaptors. Many other proteins that require membrane attachment to perform their biological activity need a hydrophobic posttranslational lipid modification to bind to the PM. Four major types of lipid modifications have been identified among proteins destined for PM: acylation by saturated fatty acids, prenylation by polyunsaturated isoprenoid groups, esterification by cholesterol, and conjugation by glycosylphosphatidylinositol (GPI). GPI modification is most common in proteins that attach to the exterior of the cell membrane. In contrast, proteins that reside at the inner leaflet of the PM frequently use acyl and prenyl modifications for membrane binding. Targeting of GEI to the PM has been obtained most commonly by introducing prenylation "CAAX" boxes or palmitoylation motifs in the sequence of the protein of interest. Frequently, a sequence of 12–16 amino acids is used to incorporate more lipidation motifs to ensure effective retention at the membrane. Another strategy applied to target sensors to the inner leaflet of PM consists in fusing the sensor to the domain facing the cytosol of a known integral or peripheral PM protein.

Sensors have been targeted to the external side of PM, e.g., ATP (Pellegatti et al., 2005), and the sub-plasmalemmal rim (for Ca^{2+} [Marsault et al., 1997; Mao et al., 2008], Cl^-/pH [Mukhtarov et al., 2013], PKC activity [Violin et al., 2003], and endocytosis [Galperin and Sorkin, 2003]). Also, different types of GEI sensitive to PM potential have been developed, mainly by fusing an FP variant with a voltage-sensitive domain that resides in the PM (for a review see Storace et al. [2016]).

A subtype of PM-targeted probes was developed to study the transient PM nanodomains known as lipid rafts (recently reviewed in Carquin et al. [2016]). Interesting examples of lipid raft–targeted GEIs are FRET-based sensors generated to study protein segregation in this PM subdomain. These sensors were generated by fusing CFP or YFP to different lipid anchors, such as MyrPalm (myristoylated and palmitoylated), GerGer (geranylgeranylated), PalmPalm (tandemly palmitoylated), and caveolin (full-length bovine caveolin-1, triply palmitoylated with a putative membrane-embedded hairpin loop; Zacharias et al., 2002).

It is important to stress that in a few cases, PM-targeted GEIs can be mistargeted or form intracellular aggregates. Trafficking strategies (such as the introduction of GA trafficking signals or ER export motifs) are needed to favor their transport along the secretory pathway to the cell surface (Mutoh et al., 2011).

A schematic overview of fundamental PM targeting strategies and of the available sensors is provided in Fig. 4 A.

Among PM-targeted GEIs, it is possible to classify a distinct subclass of constructs targeted to cilia. These sensory organelles, composed of microtubules and projected from the apical surface of numerous cell types, can be distinguished in primary and motile cilia. Cilia are involved in the mechanosensation of different stimuli on specialized structure, for instance, blood on vasculature or urine on nephron (reviewed in Prasad et al. [2014]). To the best of our knowledge, sensors targeted to cilia have been developed to measure Ca^{2+} (Su et al., 2013; Delling et al., 2016) and cAMP (Mukherjee et al., 2016). The latter probe was expressed in sperm cells by placing the cAMP sensor under the control of protamine-1 promoter and allowing measurement in motile cilia, whereas Ca^{2+} GEIs have been targeted specifically to primary cilia by linking such indictor to ciliary targeting signals (CTSs), a sequence element recognized by the ciliar sorting machinery (reviewed in Nachury et al. [2010]).

Acidic compartments. Acidic compartments are a group of organelles characterized by a luminal pH <7, usually from 6 to 4. Imaging intracellular acidic compartments is becoming an important topic in biology, given the physiological role of these organelles in autophagy, removal of cytotoxic macromolecules, receptor recycling, and internalization. Moreover, acidic compartments are emerging as important players in pathologies such as neurodegenerative diseases, inflammation, lysosomal disease accumulation, and cancer. Internal pH is an important issue to address because it is the main parameter that affects the properties of a chromophore.

Endosomes. Endosomes are characterized by a mild acidic pH (~6.0); they arise from the PM-containing molecules or ligands destined to the GA or to lysosomes for degradation. Endosomes can also originate from the TGN, directed to lysosomes and PM. Immediately after their formation, endosomes become part of a dynamic vesicular-tubular network classified as early endosomes (EEs). Their homotypic fusion generates larger vesicles called multi-vesicular bodies (MVBs) or late endosomes (LEs) that can be degraded through the fusion with lysosomes or recycled, generating recycling endosomes (REs). Along this path, endosomes undergo

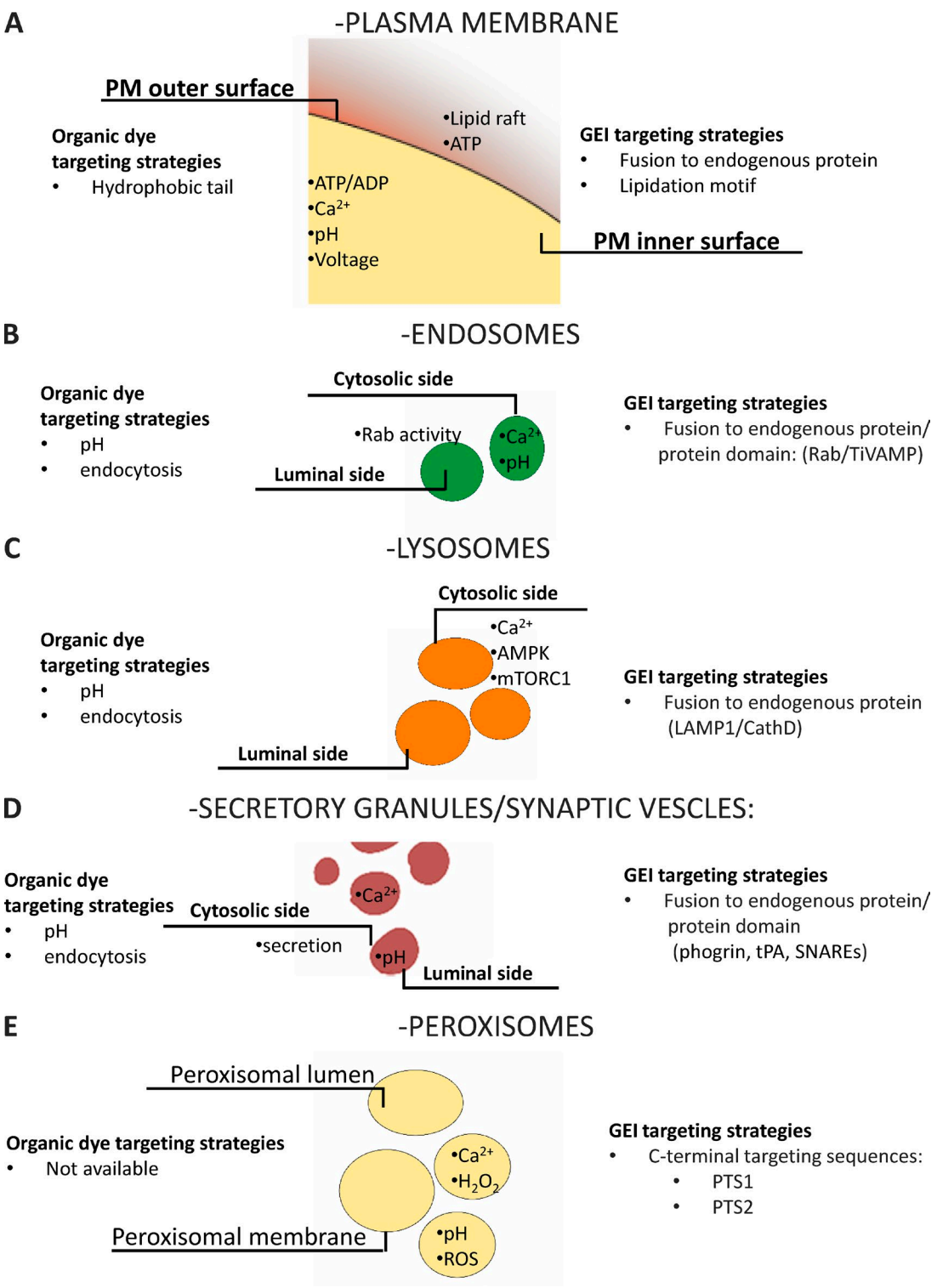

Figure 4. **Schematic representation of targeting strategies.** Targeting strategies used to generate probes selectively targeted to PM (A), endosomes (B), lysosomes (C), secretory granules/synaptic vesicles (D), and peroxisomes (E) and localization of the available probes.

acidification through the activity of V-ATPase (for a general review see Villaseñor et al. [2016]). Generally, EEs are visualized by fusing the C terminus of FPs to Rab4, Rab5, and RhoB, whereas LEs are visualized by fusion with Rab7. Proteins of the Rab superfamily are guanosine nucleotide–dependent proteins located on the cytosolic surface of EEs that regulate budding, delivery, tethering, and fusion of the vesicle membrane with that

of the target compartment (Wandinger-Ness and Zerial, 2014). Rab proteins have been used to generate FRET sensors to monitor Rab activity (Galperin and Sorkin, 2003). To the best of our knowledge, the only sensors targeted to the luminal side of endosomes have been developed using the C terminus of TiVAMP to generate a Ca^{2+} sensor (Albrecht et al., 2015).

The role of endosomes in receptor signaling and recycling contributes to the spatio-temporal complexity of subcellular signaling. Despite the importance of these organelles in cell physiology, their fast maturation and the acidic pH have prevented the generation of a broad spectrum of biosensors. Moreover, the biosensors available are mainly able to detect changes on the cytosolic face of endosomes, thus precluding the possibility to investigate luminal phenomena. However, the emerging importance of these subcompartments in determining cell functions and pathologies calls for further efforts to explore the "luminal side of endosomes."

A schematic overview of acidic compartment–targeting strategies and of the available sensors is provided in Fig. 4 B.

Lysosomes. Lysosomes are well known for containing hydrolytic enzymes (hydrolases) deputed to breaking down biomolecules of intra- and extracellular origin. Hydrolases are inactive, and their activation depends on processes, such as fusion or kiss-and-run contacts with LEs, generating endolysosomes. Lysosomes are key players in phagocytosis, endocytosis, and autophagy, but they are also involved in homeostatic processes such as secretion, PM repair, cell signaling, and energy metabolism. Indeed, the classical definition of lysosome as "suicide bags" of the cell is no longer used (Ballabio, 2016). The acidic (pH ∼4.5) lysosomal matrix is optimal for its enzymes. These proteins are encoded by nuclear genes, synthesized in rough ER, and released from the GA thanks to the presence of a specific lysosomal tag (mannose 6-phosphate [M6P]), ensuring their delivery to endosomes that finally undergo internal acidification leading to maturation into full lysosomes. There are also enzymes and structural proteins that follow an M6P-independent pathway, usually recognized by the lysosomal integral membrane protein LIMP-2 or sortilin. Sorting of cargo receptors and lysosomal transmembrane proteins is ensured by di-leucine–based motifs and tyrosine-based motifs that act as sorting signals. These domains are able to interact with components of clathrin coats or adaptor protein complexes that ultimately fuse to endosomes (reviewed in Braulke and Bonifacino [2009]).

Also, vesicles that bud from the trans-GA and are part of the constitutive secretory pathway are equipped with specific membrane proteins, and their localization depends on the same pathways described for lysosomes (Gadila and Kim, 2016). We are not aware of GEIs specifically targeted to the lumen of these organelles.

Lysosome localization can be achieved by fusing the lysosomal-resident membrane protein LAMP1 to the probe, allowing the development of sensors able to report changes in the cytosolic face of these organelles. This strategy has been used to generate sensors for Ca^{2+} (Shen et al., 2012; McCue et al., 2013; Ronco et al., 2015), mTORC1 activity (Zhou et al., 2015), and AMPK (Miyamoto et al., 2015).

A schematic overview of acidic compartment–targeting strategies and of the available sensors is provided in Fig. 4 C.

Secretory vesicles. Secretory granules (pH ∼5.8) contain products to be released into the extracellular medium, such as insulin in β cells, histamine in mast cells, or digestive enzymes in pancreatic acinar cells. They originate from the trans-GA and can fuse with the PM constitutively or in a regulated manner (for a general review see Martin-Urdiroz et al. [2016]). The targeting signal for the secretory pathway is usually formed by 5–30 hydrophobic amino acids that form an α-helical structure at the N terminus of the protein. Sequences from proteins physiologically located in these organelles (e.g., phogrin, plasminogen activator [tPA]) have been used to target GEIs; examples include sensors for Ca^{2+} (phogrin-Ycam2 [Emmanouilidou et al., 1999 and D1-SG [Dickson et al., 2012]) and pH (phogrin-pHluorin [Ohara-Imaizumi et al., 2002]). Targeting of aequorin to insulin granules in β cells was achieved by fusing at the N terminus of aequorin the sequence of VAMP-2 (synaptobrevin; Mitchell et al., 2001).

A unique type of secretory organelle is represented by synaptic vesicles. They are much smaller than classical secretory granules, are expressed almost exclusively in neurons, and they store and release neurotransmitters essential for neuronal functionality. Selective targeting of GEIs to synaptic vesicles can be achieved by using sequences derived from VAMP-3 (cellulobrevin) and synaptophysin. The latter can tolerate insertion of sequences, e.g., biosensors, between its transmembrane domains. Using these strategies, different sensors have been generated for pH (Zhu et al., 2009) and secretion (Miesenböck et al., 1998). Moreover, a new red indicator for synaptic vesicle labeling was developed to facilitate multicolor imaging and integration with optogenetic actuators to study regulated secretion (Li and Tsien, 2012). Finally, a new optogenetic tool to monitor and control pH within secretory vesicles, called pHoenix, was recently developed. It was obtained by inserting within the fourth synaptophysin helix: the pH-sensitive GFP pHluorin (located in the luminal side of the vesicles); the proton pump Archaerhodopsin-3 (Arch3) fused to mKate, an FP variant; the transmembrane helix of the rat gastric H^+/K^+ ATPase β-subunit fused before

the fourth helix of synaptophysin, to maintain the correct transmembrane topology of Arch3 (Rost et al., 2015).

A schematic overview of acidic compartment–targeting strategies and of the available sensors is provided in Fig. 4 D.

Peroxisomes. Peroxisomes are membrane-bound organelles involved in specific metabolism pathways, such as hydrogen peroxide conversion to water, β-oxidation, synthesis of bile acid, and plasmalogens. They are at the crossroads between inflammation, lipid metabolism, and redox signaling (reviewed in Tripathi and Walker [2016]).

Proteins destined to peroxisomes can reach these organelles because of the presence of peroxisome-targeting signals (PTS). Two types of PTS have been identified: PTS1, located at the protein's C terminus, usually composed by the tripeptide serine-lysine-leucine (SKL); PTS2, a nonapeptide located at the N terminus (Gould et al., 1989). Both of these sequences can be fused to biosensors to achieve their targeting and have been exploited to generate GEIs to measure pH (Jankowski et al., 2001; Lasorsa et al., 2008), Ca^{2+} (Drago et al., 2008; Lasorsa et al., 2008), and redox state (Yano et al., 2010). It was also shown that addition of the sequence KVK between the sensor and the SKL sequence improved peroxisomal targeting (Drago et al., 2008). PTS1 targeting sequences have been conjugated also to organic dyes to generate peptide probes (Dansen et al., 2000; Pap et al., 2001). To tether sensors at the peroxisomal membrane, the C terminus of PEX16 was used to develop a GFP-based sensor for peroxisome maturation (Kim et al., 2006).

Although we are beginning to understand the peroxisomal complexity, it is becoming increasingly clear that the development of pH-insensitive and multicolor probes will be crucial for dissecting the cross-talk not only within peroxisomes but also between peroxisomes and other organelles.

A schematic overview of peroxisomal targeting strategies and available sensors is provided in Fig. 4 E.

What have we learned from targeted sensors?

After more than 25 yr of judicious use of targeted sensors, the information accrued about cellular spatial complexity is so vast that it is impossible to summarize it in a single paper. We are now able to directly and quantitatively monitor the dynamics of ions and second messenger levels in living cells within a tissue or even intact animals; we can directly measure the movement of a protein from one compartment to another in real time; we can measure the dynamics of metabolites or the fusion of single vesicles with the PM; we can monitor the phosphorylation/dephosphorylation of kinase/phosphatase targets or the conformational change in some proteins. A major general concept has emerged from all these data: the key characteristic of living cells is the spatial and temporal heterogeneity of signaling molecules or protein and metabolite concentration/distribution. Such a heterogeneity in space and time had been postulated on the basis of indirect evidence, but in some cases, their discovery was largely unexpected. Below we will provide a few examples in which the use of selectively targeted sensors produced the most unexpected results, focusing solely on the most commonly used Ca^{2+} and cAMP sensors.

Ca^{2+} sensors. The spatial heterogeneity of Ca^{2+} levels among cellular compartments was predicted long before the advent of targeted sensors. It was, in fact, well known that organelles such as the ER/SR are endowed with Ca^{2+} pumps that allow Ca^{2+} accumulation in their lumen (at the expense of ATP hydrolysis) and Ca^{2+} release channels (IP_3 and Ryanodine receptors) activated upon stimulation. Targeted sensors have allowed the confirmation of the hypothesized Ca^{2+} spatial heterogeneity but have also led to a dynamic measurement of the kinetics of the process in living cells and to its quantification (see Fig. 5 for some examples of organellar Ca^{2+}).

For other cellular organelles, such as GA, secretory granules, endosomes, or peroxisomes, the available indirect evidence before the use of targeted Ca^{2+} sensors was fragmentary or simply nonexistent. Selectively targeting Ca^{2+} GEIs to the different GA subcompartments revealed that this organelle is endowed with an unexpected intra-organelle Ca^{2+} handling complexity, with the cis-GA very similar to the ER, the trans-GA with unique Ca^{2+} uptake and release characteristics, and the intermediate GA with a mixture of the two (Fig. 6; Lissandron et al., 2010; Wong et al., 2013).

Secretory granules largely resemble the trans-GA, whereas peroxisomes appear to be in rapid equilibrium with Ca^{2+} levels in the cytosol. The latter point is still subject to debate because Ca^{2+} signaling in peroxisomes has just started to be investigated. Indeed, although our group found similar resting Ca^{2+} level in cytosol and peroxisomes and passive Ca^{2+} diffusion into peroxisomes upon rises in cytosolic $[Ca^{2+}]$ (Fig. 7; Drago et al., 2008; Costa et al., 2010), an aequorin-based study showed higher $[Ca^{2+}]$ in peroxisomes at resting level and the ability of these organelles to actively take up Ca^{2+} upon Ca^{2+} release from the intracellular stores (Lasorsa et al., 2008).

There has been a long debate about the possible existence of Ca^{2+} gradients between the cytosol and nucleus, but over the last years the general consensus appears to be that the two compartments are in rapid equilibrium, with a small delay in the nuclear Ca^{2+} increase caused by the diffusion of the ion across the nuclear pores (Fig. 5 A; Brini et al., 1993; Miyawaki et al., 1997; Manjarrés et al., 2008). On the contrary, the mechanism of

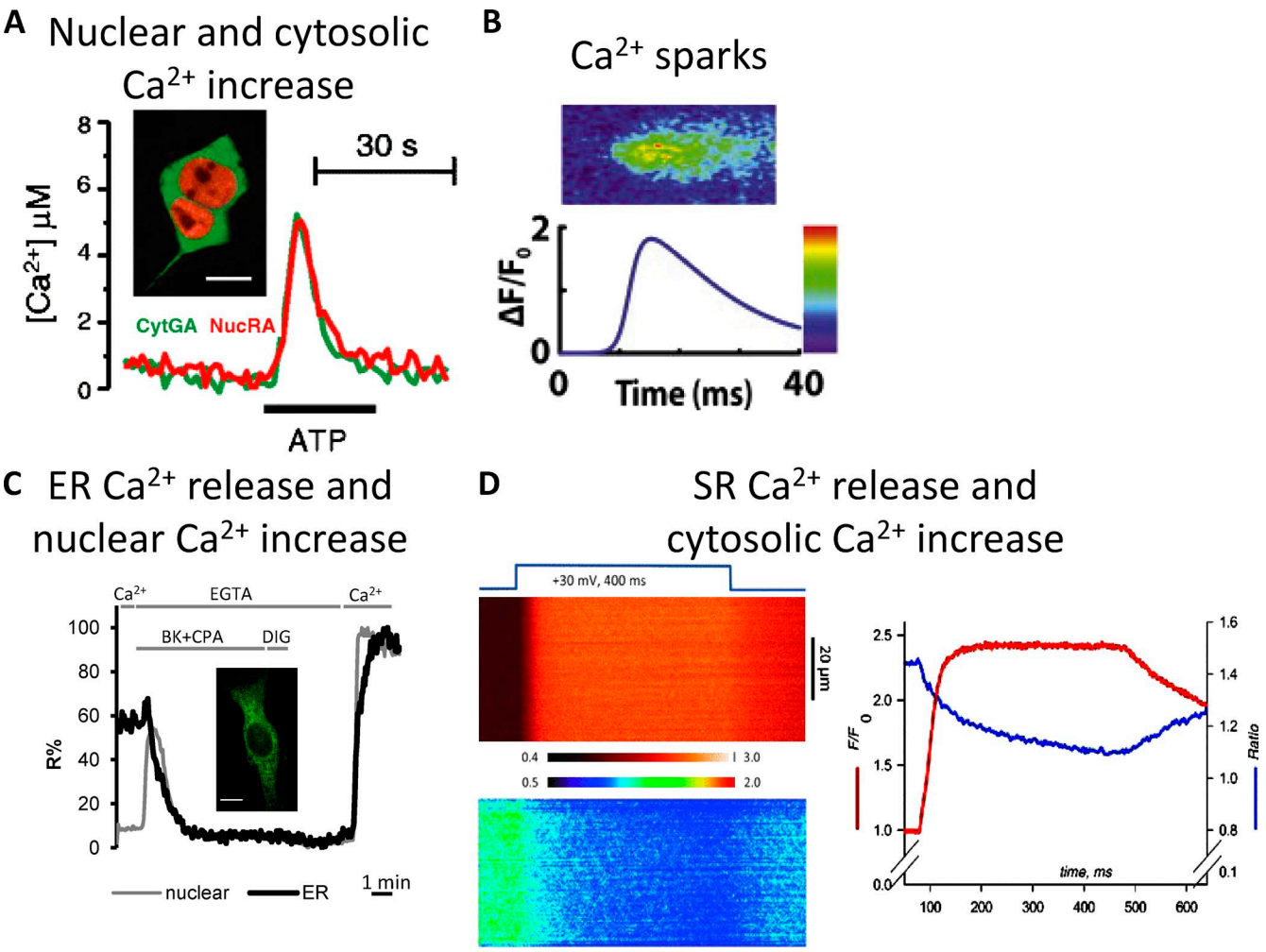

Figure 5. **Ca^{2+} dynamics in different cellular compartments.** (A) Cytosolic and nuclear Ca^{2+} dynamics evaluated using cytosolic green aequorin (CytGA) and nuclear red aequorin (NucRA). (A, inset) CytGA and NucRA localization in HEK293T cells. Bar, 10 µm. (A) Representative kinetics of $[Ca^{2+}]_C$ and $[Ca^{2+}]_N$ (from Manjarrés et al. [2008] with permission from Springer). (B) Microscopic SR calcium release, the so-called Ca^{2+} sparks, evaluated using Fluo-3 (from Cannell and Kong [2012] with permission from Elsevier). (C) Measurements of nuclear and ER Ca^{2+}dynamics using the D3 and D4 Cameleons variants, respectively. (inset) D4ER fluorescence (green). Bar, 10 µm. Representative kinetics of nuclear (gray) and ER (black) fluorescent signals in a single BHK cell coexpressing H2B-D3cpv and D4ER and stimulated with bradykinin (BK) and the SERCA inhibitor, cyclopiazonic acid (CPA), in a Ca^{2+}-free medium (from Greotti et al. [2016] with permission from MDPI AG). (D) SR Ca^{2+} release and cytosolic Ca^{2+} increase in flexor digitorum brevis (FDB) monitored using the FRET-based D4cpv-Casq1 SR sensor and the cytosolic dye X-rhod-1. FDB was voltage-clamped and subjected to depolarization as indicated. (left, top) Normalized line scan of fluorescence of X-rhod-1 (cytosolic signal). (bottom) FRET ratio ($R(x,t)$) of D4cpv-Casq1 (SR signal). (right) Plot of the line averages (from Manno et al. [2013b] with permission from The Physiological Society).

Ca^{2+} uptake and release in the endosome/lysosome compartment is still highly debated (recently reviewed in Morgan [2016]). This is because of significant limitations caused by the very acidic environment (that strongly affects both the fluorescence and Ca^{2+} affinity of the probes) and the difficulties in identifying optimal targeting strategies.

Heterogeneity in Ca^{2+} levels is also found in different strategic regions of the cytosol, e.g., in the proximity of PM or ER/SR Ca^{2+} channels. Indeed, upon channel opening, Ca^{2+} flows from an area with a high cation concentration, such as the extracellular space or the ER, into an area with a much lower $[Ca^{2+}]$, the cytosol. The generated Ca^{2+} gradient is modulated by different cellular players, such as Ca^{2+} buffers and pumps/exchanger, and by the frequency and the temporal extent of the channels opening, allowing the formation of the so-called microdomains. Their role in cell physiology had been predicted a long time before they could be experimentally addressed.

Of special interest are the localized microdomains in the active zones of the presynaptic membrane and the local microdomains close to open PM Ca^{2+} channels (see for example Augustine and Neher [1992]; Deisseroth et al. [1996]; Marsault et al. [1997]; Nakahashi et al. [1997]; Dolmetsch et al. [2001]; Kornhauser et al.

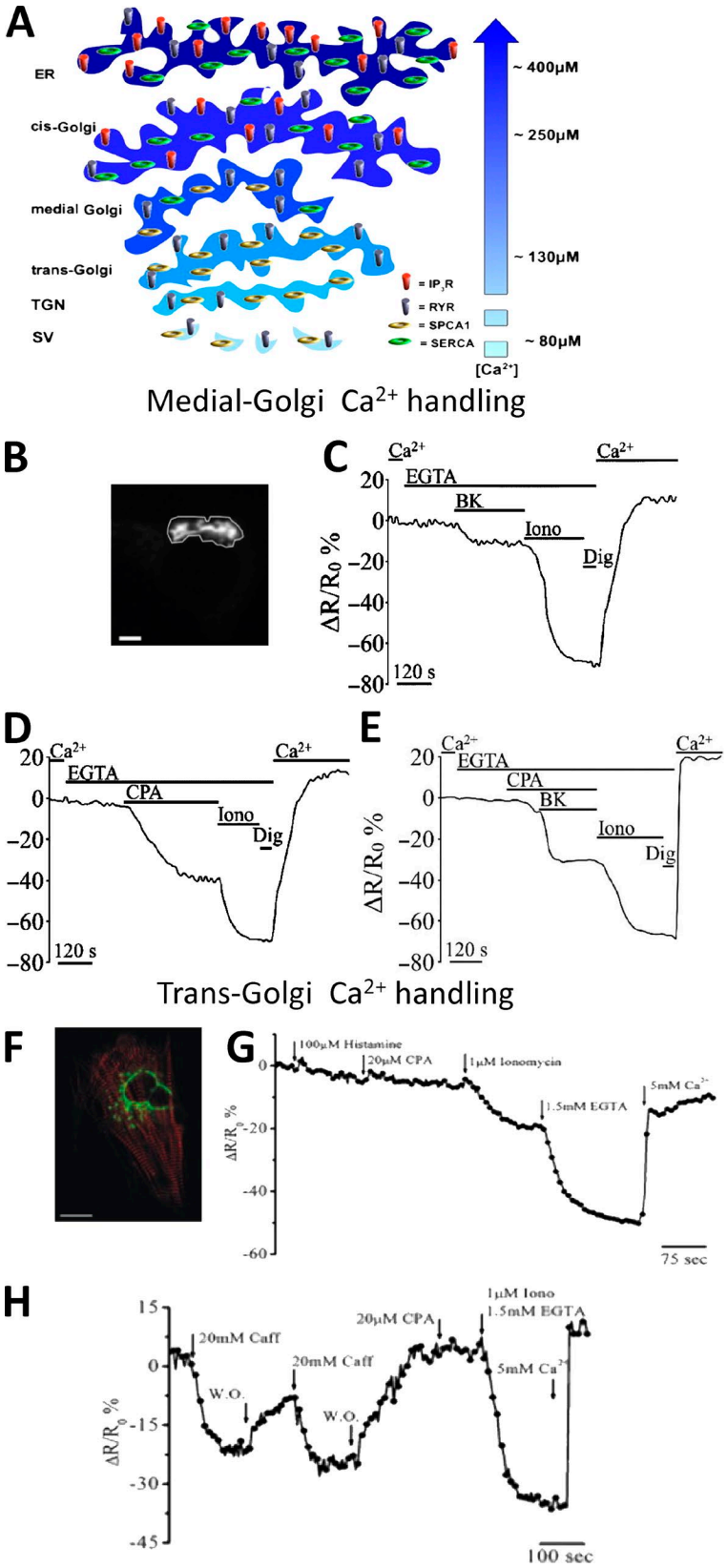

Figure 6. **The heterogeneity of GA in Ca^{2+} handling.** (A) $[Ca^{2+}]$ and molecular toolkit along the secretory pathway. The GA can be divided in three distinct subcompartments: the cis-Golgi, with a luminal $[Ca^{2+}]$ around 250 µM, the medial Golgi, with a luminal $[Ca^{2+}]$ lower compared with that of the cis-Golgi (i.e., ~150–200 µM), and trans-Golgi, with a luminal $[Ca^{2+}]$ around 130 µM. The efflux and influx Ca^{2+} toolkit is also shown. TGN, trans-Golgi network; SV, secretory vesicles (from Pizzo et al. [2011] with permission from Elsevier). (B–E) Ca^{2+} handling by medial Golgi in intact cells monitored with a targeted Cameleon probe: (B) the fluorescence microscope image of a medial-Go-D1cpv–expressing SH-SY5Y cell. Bar, 10 µm. (C–E) SHSY-5Y cells were incubated in medium supplemented or not with 1 mM $CaCl_2$ or 300 µM EGTA and challenged with the indicated stimuli: (C) bradykinin (BK), demonstrating the presence of an IP_3 sensitive pool; (D) cyclopiazonic acid (CPA), demonstrating the presence of the SERCA pump; (E) ionomycin (Iono), a ionophore demonstrating the presence of another molecular component besides IP_3Rs and SERCA, such as SPCA1 (from Wong et al. [2013] with permission from Oxford University Press). (F–H) Ca^{2+} handling by trans-Golgi in single intact cells monitored with a targeted Cameleon probe: (F) confocal microscopy image of a cardiomyocyte cell expressing trans-Go-D1cpv and the mRFP-Zasp construct (red). Bar, 10 µm. (G and H) HeLa cells (G) and cardiac myocytes (H) were exposed to different stimuli demonstrating that this compartment is enriched of SPCA1 (ionomycin-sensitive pool) and RyRs (caffeine-sensitive pool), but neither SERCA (CPA-sensitive pool) nor IP_3Rs (histamine-sensitive pool) are present (from Lissandron et al. [2010] with permission from the National Academy of Sciences).

[2002]). One of the most unexpected results regarding high Ca^{2+} cytosolic microdomains, however, came from the application of Ca^{2+} sensors to mitochondria. The ability of these organelles to accumulate large amounts of Ca^{2+} was known since the '60s, but until the use of mitochondrial aequorin, the consensus was that, given

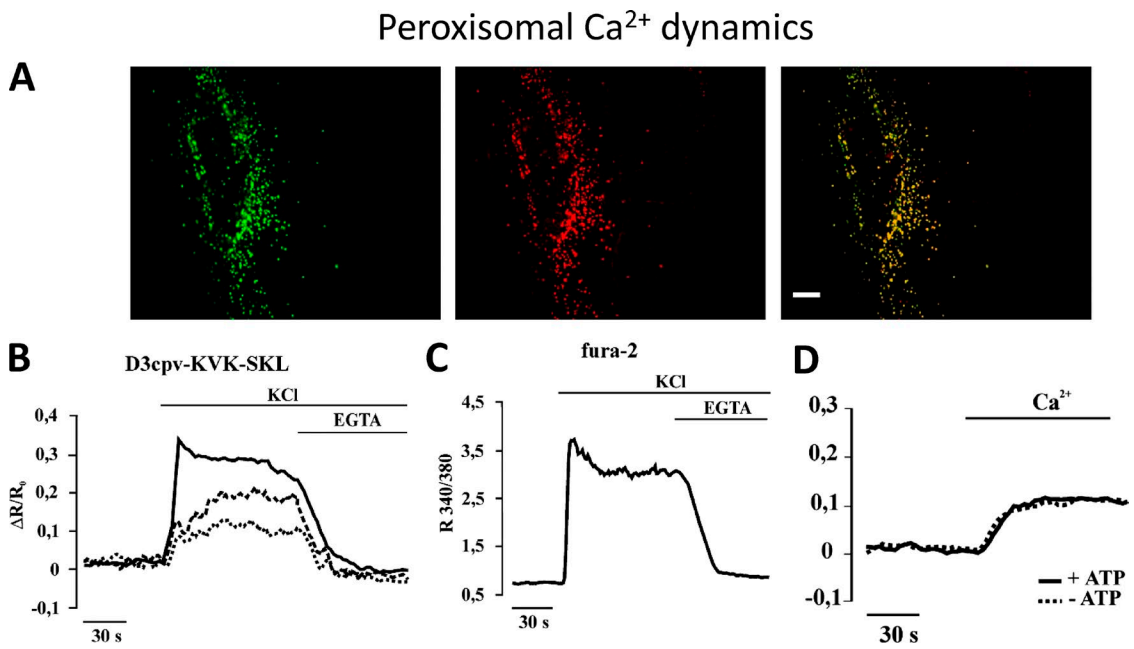

Figure 7. **Peroxisomal Ca^{2+} dynamics.** Peroxisomal Ca^{2+} dynamics explored using a targeted Cameleon. (A) Colocalization of transiently expressed D3cpv-SKL and the peroxisome marker catalase in HeLa cells. Bar, 10 µm. (B and C) Increases in $[Ca^{2+}]_c$ are followed by a slow rise in intraperoxisomal $[Ca^{2+}]$. Fluorescence changes of GH3 cells transiently expressing D3cpv-KVK-SKL selectively within peroxisomes (two cells, dashed and dotted traces), mistargeted to the cytosol (continuous trace; B), or loaded with fura-2 (C). Where indicated, 30 mM KCl and 2 mM EGTA were added. (D) Cells permeabilized with digitonin. The experiment shows that no driving force supplied by ATP is needed for Ca^{2+} to enter peroxisomes (from Drago et al. [2008] with permission from The American Society for Biochemistry and Molecular Biology).

the low affinity of their Ca^{2+} uptake mechanism, mitochondria in live cells played only a minor role in cellular Ca^{2+} homeostasis. Matrix-localized aequorin showed that, instead, mitochondria in living cells take up Ca^{2+} very rapidly and efficiently (Rizzuto et al., 1992, 1993). This paradox was solved by the demonstration that mitochondria are specifically located in close proximity to Ca^{2+} channels (ER/SR or PM) where they are transiently exposed to the microdomains of high Ca^{2+} generated close to the channel mouths (Fig. 8; Rizzuto et al., 1998; Giacomello et al., 2010; for review see Rizzuto and Pozzan [2006]).

This discovery has revolutionized our understanding of mitochondrial pathophysiology, and this field has become one of the most active in the recent years. Other examples of localized cytosolic domains of Ca^{2+} are represented by acinar cells from the pancreas (Tinel et al., 1999) and by leukocytes such as cytotoxic T lymphocytes or granulocytes (see for example Poenie et al. [1987]; Tsai et al. [2014]). In these latter cases, localized cytosolic $[Ca^{2+}]$ increases depend on a high local concentration of IP_3Rs or on a combination of local activation of PM Ca^{2+} extrusion and localization of the IP_3Rs.

A schematic overview of cellular $[Ca^{2+}]$ heterogeneity among compartments is presented in Fig. 9 along with a schematic overview of the method to target GEIs to different organelles.

cAMP sensors. In the late '70s, several studies were published demonstrating that similar levels of cAMP (as measured by classical radio immunoassays from cell extracts) can induce drastically different functional outcomes, depending on the agonist that elicited its production (Hayes et al., 1979, 1980). The proposed explanation was that the distinct functional responses to cAMP were caused by the subcellular heterogeneity of the second messenger levels, dependent on the signaling pathway activated. Although significant efforts were made using biochemical and electrophysiological approaches, the precise topology of intracellular cAMP levels in the live cells could not be unveiled. Nevertheless, evidence supporting the existence of local cAMP microdomains was provided by the measurement of the cation current through cAMP activated channels (Rich et al., 2000). Indirect, strong evidence in favor of the existence of cAMP microdomains has been obtained by Jurevicius and Fischmeister (1996) in adult cardiac cells.

The existence of cAMP microdomains was consolidated when direct measurement of cAMP levels, in living cells, became eventually possible through the use of cAMP-sensitive GEIs. First, using recombinant PKA labeled in vitro with organic dyes and microinjected (Backskai et al., 1993) and later using GFP-tagged PKA to transfect cells (Zaccolo et al., 2000; Zaccolo and Pozzan, 2002). These sensors, when expressed in neonatal rat ventricular myocytes (NRVMs), appeared localized in

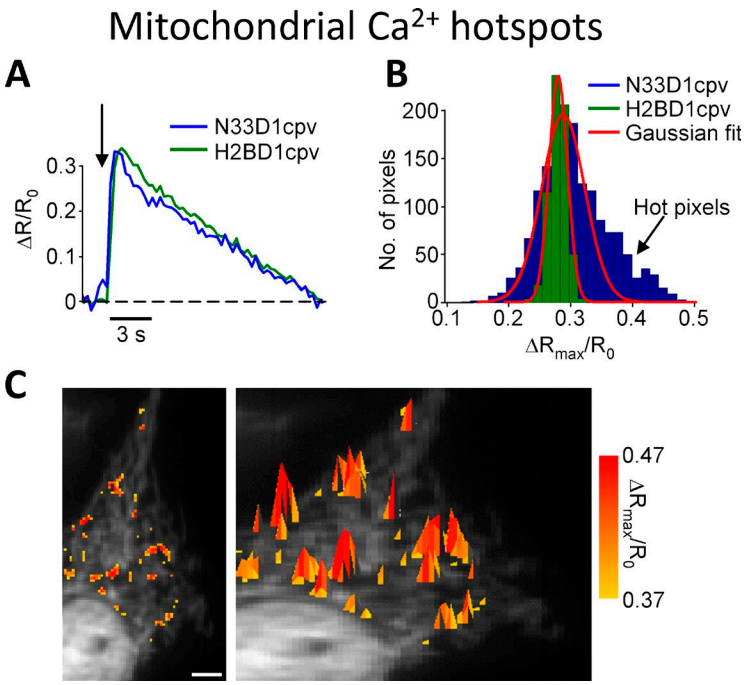

Figure 8. **Mitochondrial [Ca^{2+}] hotspots.** Pixel by pixel correlation showing the presence of Ca^{2+} microdomains on mitochondrial outer membrane (OMM) upon stimulation. HeLa cells cotransfected with nuclear (H2BD1cpv)- and OMM (N33D1cpv)-targeted Cameleons were treated with 100 µM histamine where indicated by the arrow in A. (A) The average [Ca^{2+}] rises, expressed as $\Delta R/R_0$, of nucleus (green trace) and OMM (blue trace) are very similar. (B) The number and intensity of single pixels, expressed as $\Delta R_{max}/\Delta R_0$ of single pixels, of the nucleus (green) or OMM (blue) reached during the first 4 s after histamine stimulation were plotted. The Gaussian fit of the nuclear (green) and OMM (red) pixel distribution highlights the right tail caused by hot-spot formation on OMM upon cellular stimulation. (C) Yellow to red color representation of $\Delta R_{max}/R_0$ spatial distribution of pixels in 2D (left) and 3D (right), superimposed to YFP fluorescence image. Only pixels that during the 4 s after the histamine challenge have a $\Delta R_{max}/R_0$ exceeding by 125% the $\Delta R/R_0$ of the whole compartment were color coded. Bar, 5 µm (from Giacomello et al. [2010] with permission from Elsevier).

specific cellular structures corresponding to the sarcomeric Z lines (Zaccolo and Pozzan, 2002). Interestingly, cAMP elevations in response to β-adrenergic agonists were significantly higher at the level of Z-lines (T-tubule/SR) than in the bulk cytosol. Importantly, these differences were abrogated when phosphodiesterases (PDEs) were inhibited, suggesting both the existence of cAMP microdomains and the crucial role of PDEs in their formation. Additional evidence supporting the existence of highly localized microdomains in adult cardiac cells was subsequently provided by an elegant study by Nikolaev et al. (2010) (Fig. 10, A–C). These authors showed that the local cAMP increases elicited by β-adrenergic stimulation differ substantially in the proximity of β1 or β2 adrenergic receptors. Along the same line, Röder et al. (2010) showed that, in vivo in mouse skeletal muscles, local cAMP microdomains are generated by activation of calcitonin gene-related peptide (CGRP) receptors in the postsynaptic neuromuscular junction.

The ability of different PKA regulatory subunits to localize to specific subcellular compartments was further exploited with PKA-based sensors targeted to different subcellular compartments and later on with targeted, EPAC-based, cAMP FRET sensors (Mongillo et al., 2004; Di Benedetto et al., 2008; Terrin et al., 2012). These constructs provided further evidence that around specific PKA subtypes intracellular cAMP signals are spatially restricted and distinctly regulated (Di Benedetto et al., 2008). A step beyond these seminal studies was recently taken with the generation of a transgenic animal model expressing a targeted cAMP FRET sensor. Using this transgenic animal in combination with a disease model, the authors were able to study how disease affects cAMP signaling within specific microdomains (Sprenger et al., 2015).

It is noteworthy that originally it was thought that cAMP concentration increases rather uniformly within the cytosol, so the hypothesis of cAMP microdomains initially was not very popular. Moreover, the existence of cAMP microdomains was in contrast with the accepted notion that cAMP diffusion within the cell was very rapid (diffusion coefficient of ∼500 $\mu m^2\ s^{-1}$ [Dworkin and Keller, 1977]) and the cAMP buffering capacity relatively modest, at least in comparison with that of Ca^{2+}.

More recent data, however, have demonstrated that the cAMP diffusion rate in adult cardiac myocytes is significantly slower than previously measured (i.e., ∼35 $\mu m^2\ s^{-1}$; Fig. 10, D and E; Richards et al., 2016); this latter value is in agreement with that calculated for a fluorescently tagged cAMP analogue (∼10 $\mu m^2\ s^{-1}$) in the same cell model using a different approach (Agarwal et al., 2016). Although both studies agree on slow diffusing cAMP, they propose different underlying mechanisms. Agarwal et al. (2016) propose that cAMP buffering at the level of the OMM is the primary reason for slow cAMP diffusion, whereas Richards et al. (2016) provide evidence that intracellular tortuosity is the main cause for slow diffusion.

Targeted degradation of cAMP by PDEs is considered the most relevant among the molecular mechanisms that allow the formation of cAMP microdomains. However, mathematical models predict that even with slow diffusing cAMP (∼10–35 $\mu m^2\ s^{-1}$) the sole PDE action is not sufficient to generate microdomains (Yang et al., 2016). These data would suggest that the formation of cAMP microdomains is likely to be a multi-parametric

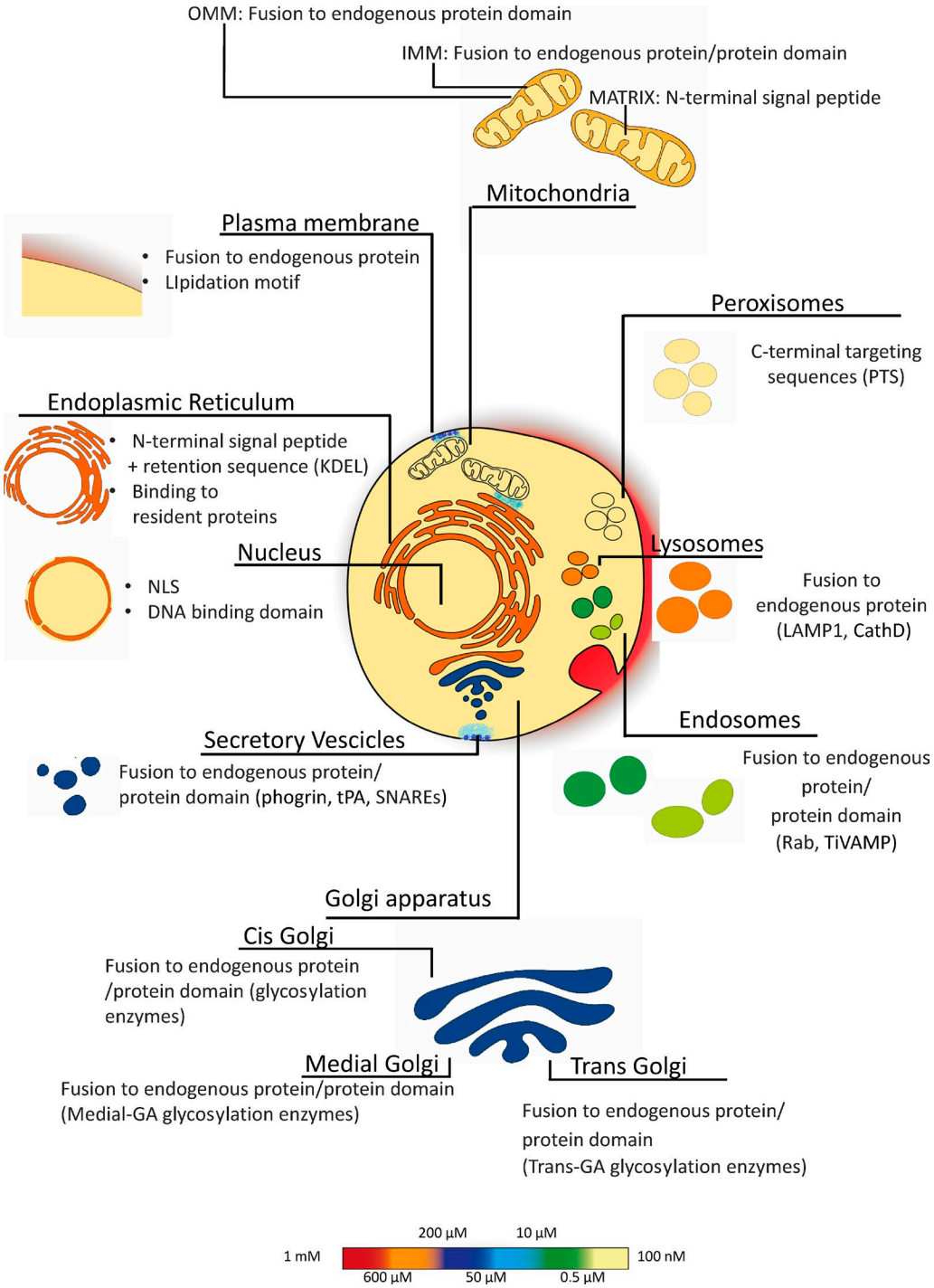

Figure 9. **Intracellular resting [Ca^{2+}] and GEI-targeted mechanism.** In resting conditions, cells maintain a [Ca^{2+}] gradient between the cytosol ([Ca^{2+}] ~100 nM) and the extracellular medium ([Ca^{2+}] ~1.5–2 mM) and some organelles. The [Ca^{2+}] of each compartment is color coded (bar on the right). The figure also includes a schematic representation illustrating the targeting mechanisms used to target GEIs to the different cell compartments.

phenomenon where more than one mechanism such as enrichment in selected subcellular compartments of different types of adenylyl cyclases (ACs) and effectors, physical barriers (Richards et al., 2016), and cAMP buffering (Agarwal et al., 2016) that limit cAMP diffusion, along with specific localization of PDEs and PKA co-occur to ensure the existence of distinct cAMP events within the cell. Interested readers are referred to a recent review for a more detailed discussion of this topic (Feinstein et al., 2012; Saucerman et al., 2014).

The levels and dynamics of cAMP in organelles have been, on the contrary, scarcely investigated until re-

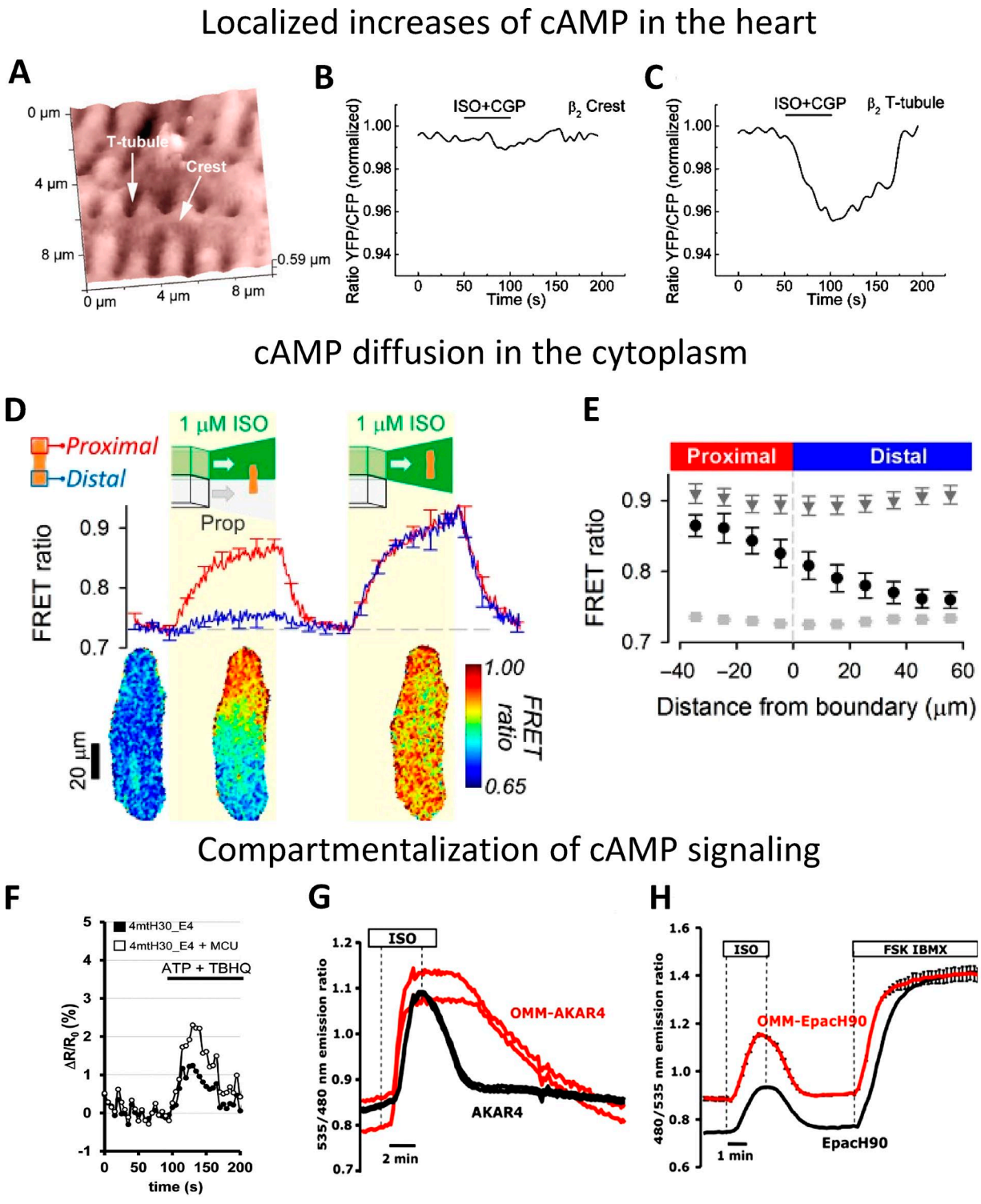

Figure 10. **cAMP signaling.** (A–C) Localized increases of cAMP. (A) Scanning ion conductance microscopy image and corresponding cAMP level obtained in cardiomyocytes expressing Epac1-cAMP sensor upon local β2-adrenergic receptors (β_2AR) stimulation in the cell crest (B) and in the T-tubule (C). Cells were stimulated with a β_2AR agonist (ISO and CGP) in the presence of a β_1AR antagonist, showing β2-cAMP signals only in T-tubules, whereas no cAMP signal was detected in cell crest (from Nikolaev et al. [2010] with permission from The American Association for the Advancement of Science). (D and E) cAMP diffusion is low in the cytoplasm of adult rat ventricular myocytes. GEI for cAMP Epac^{SH187} (from Klarenbeek et al. [2015] with permission from PLOS) was expressed in myocytes stimulated with β-adrenoceptor agonist and antagonist to investigate cAMP diffusion. (D) Time course of FRET ratio in proximal and distal ROIs (top) and pseudocolor representative image (bottom); (E) longitudinal profile of FRET ratio, relative to boundary position, measured under resting conditions (light gray squares), during the last 10 s of β-agonist and β-antagonist additions (black circles) to one end of the cell, and during the last 10 s of uniform exposure to β-agonist (dark gray triangles). The

cently. The first attempts to use targeted FRET-based sensors to measure cAMP in the mitochondrial matrix led to the conclusion that cAMP from the cytosol could freely diffuse into the mitochondrial matrix (DiPilato et al., 2004). However, when a different set of cAMP FRET sensors very selectively targeted to the mitochondrial matrix was used, it was unambiguously demonstrated that cAMP produced outside mitochondria cannot reach the matrix. These studies also demonstrated that cAMP can be produced in situ within the mitochondrial matrix by a soluble AC (sAC) opening the possibility of an independent cAMP signaling cascade within this compartment (Fig. 10, F–H; Di Benedetto et al., 2013; Lefkimmiatis et al., 2013). Similarly to PM-bound ACs, which are controlled by Ca^{2+} (Halls and Cooper, 2011), matrix sAC is activated by mitochondrial Ca^{2+} uptake in synergy with the other well-known sAC activator HCO_3^-. When FRET-based sensors able to measure PKA activity were targeted to the mitochondrial matrix and to the OMM, it became obvious that the cAMP/PKA axes present within these two subregions are drastically different. A matrix-targeted construct, sensitive to PKA-dependent phosphorylation, was unable to detect any PKA activity in this compartment (Lefkimmiatis et al., 2013). In agreement with this finding, it was recently shown that EPAC1, the other major cAMP effector, may be responsible for the effects of matrix-generated cAMP (Wang et al., 2016). On the contrary, a PKA sensor targeted to the cytosolic surface of the OMM demonstrated that this region contains high levels of PKA activity, but it also showed that the kinetics of cAMP-dependent phosphorylation decay (upon decrease of cAMP) are clearly distinct (much slower) from those occurring in the cytosol (Lefkimmiatis et al., 2013).

As to the functional consequences of cAMP increase in mitochondria, it has been clearly demonstrated that phosphorylation of OMM-localized PKA targets results in modification of the organelle shape and inhibition of apoptosis (Harada et al., 1999; Chang and Blackstone, 2007; Cribbs and Strack, 2007; Kim et al., 2011); as to the role of cAMP in the matrix, recent evidence suggests that it may regulate O_2 consumption, ATP production, and aldosterone production (the latter in adrenal medulla cells), although the molecular nature of the mitochondrial cAMP effector is still debated.

In conclusion, similarly to Ca^{2+}, plenty of direct and indirect evidence supports the notion that cAMP microdomains are generated in living cells with different amplitudes, rising and decay kinetics. These problems are, however, still incompletely investigated, and more sensitive and sophisticated tools are needed for a detailed understanding of this fascinating topic.

Conclusions and future perspectives

In the last two decades, the cumulative knowledge about the physiological mechanisms of protein import and targeting, paralleled by the development of new fluorescent indicators and dyes, have expanded the palette of available organelle-targeted sensors and allowed the discovery of unexpected physiological features about subcellular compartments. Further expanding our knowledge of endogenous organelle-targeting mechanisms could be not only useful for generating better sensors for cell biology studies, but also fundamentally important for other scientifically relevant tasks including development of new strategies for drug delivery.

Despite the existence of different targeted biosensors, many challenges are still unsolved. Concerning synthetic indicators, further efforts should be devoted to generate pH-insensitive biosensors and organic dyes able to specifically accumulate in organelles. As far as GEIs are concerned, the generation of PAFPs could help in the visualization of microdomain dynamics and in coupling super-resolution techniques with dynamic imaging. Recently, the development of red-shifted sensors, improving tissue penetration while decreasing phototoxicity, opened up the possibility of dual- or multicolor imaging and the concomitant use of optogenetic tools (Oheim et al., 2014). However, despite the potential interest of these probes, they have been exploited only limitedly yet.

Besides the most commonly used intensity/FRET-based imaging, FLIM has found interesting applications in cell physiology. FLIM is intrinsically quantitative, allowing measurements independent of fluorophore concentration, excitation intensity fluctuations, sample thickness, and photobleaching. Moreover, lifetime mea-

experiment shows the low cAMP diffusion in the cytoplasm of adult ventricular myocyte (from Richards et al. [2016] with permission from Oxford University Press). (F–H) Kinetics of cAMP levels and cAMP-dependent phosphorylation in the cytosol and on the OMM. (F) cAMP and mitochondria. Representative kinetics of intramitochondrial cAMP levels (expressed as $\Delta R/R_0$ changes) in control cells or in cells overexpressing MCU (mitochondrial Ca^{2+} uniporter). Where indicated, the cells were stimulated with an IP_3-generating agonist (ATP) and a SERCA pump inhibitor (tert-Butylhydroquinone [TBHQ]) to induce a massive Ca^{2+} accumulation within the mitochondrial matrix. The data demonstrate that the amplitude of the cAMP increase in the mitochondria depends on the amplitude of the Ca^{2+} increase within the matrix (from Di Benedetto et al. [2013] with permission from Elsevier). (G) Kinetics of cAMP-dependent phosphorylation of the sensor AKAR4 localized in the cytosol or on the OMM; (H) kinetics of the cAMP increase with sensors localized in the cytosol or on the OMM. The data demonstrate that the kinetics of the sensor phosphorylation is very different in the cytosol and OMM (G), whereas the amplitude and kinetics of cAMP levels in the two compartments are very similar (H; from Lefkimmiatis et al. [2013] with permission from The Rockefeller University Press).

surements can differentiate fluorophores presenting juxtaposition in their emission spectra, allowing the possibility of directly visualizing several probes at the same time to monitor the interplay among different organelles or signaling events (Niehörster et al., 2016). Until now, FLIM has not been extensively used in the study of live cell signaling, largely because of the low temporal resolution that prevents the analysis of rapid dynamic events. Only recently has this major limitation been overcome through the use of the so-called single image frequency-domain FLIM, siFLIM. This novel approach has been used to measure Ca^{2+} and cAMP dynamics in living cells at rest and upon stimulation using specific GEIs with a time resolution down to 50 ms (Raspe et al., 2016).

The field of dynamic measurement of cellular processes is developing very rapidly, and the challenge for the near future is that of more extensive application of the tools and methodologies described here (in particular of subcellular targeted sensors) to the most integrated models, i.e., living and freely moving animals.

ACKNOWLEDGMENTS

We are indebted to our colleagues Paola Pizzo, Cristina Fasolato, and Paulo Magalhães for helpful discussions and critical reading of the manuscript.

The original work by the authors has been supported by grants to T. Pozzan from the National Research Council of Italy, the Ministry of Education, University, and Research, the Foundation Cariparo, the Italian Institute of Technology, the University of Padova, and the Veneto Region; and by a grant to K. Lefkimmiatis from the British Heart Foundation Centre of Research Excellence, Oxford (RE/13/1/30181).

The authors declare no competing financial interests.

Eduardo Ríos served as editor.

Submitted: 28 June 2016
Revised: 26 October 2016
Accepted: 1 December 2016

REFERENCES

Abad, M.F., G. Di Benedetto, P.J. Magalhães, L. Filippin, and T. Pozzan. 2004. Mitochondrial pH monitored by a new engineered green fluorescent protein mutant. *J. Biol. Chem.* 279:11521–11529. http://dx.doi.org/10.1074/jbc.M306766200

Adam, V., R. Berardozzi, M. Byrdin, and D. Bourgeois. 2014. Phototransformable fluorescent proteins: Future challenges. *Curr. Opin. Chem. Biol.* 20:92–102. http://dx.doi.org/10.1016/j.cbpa.2014.05.016

Agarwal, S.R., C.E. Clancy, and R.D. Harvey. 2016. Mechanisms restricting diffusion of intracellular cAMP. *Sci. Rep.* 6:19577. http://dx.doi.org/10.1038/srep19577

Ai, M., H. Mills, M. Kanai, J. Lai, J. Deng, E. Schreiter, L. Looger, T. Neubert, and G. Suh. 2015. Green-to-red photoconversion of GCaMP. *PLoS One.* 10:e0138127. http://dx.doi.org/10.1371/journal.pone.0138127

Akerboom, J., N. Carreras Calderón, L. Tian, S. Wabnig, M. Prigge, J. Tolö, A. Gordus, M.B. Orger, K.E. Severi, J.J. Macklin, et al. 2013. Genetically encoded calcium indicators for multi-color neural activity imaging and combination with optogenetics. *Front. Mol. Neurosci.* 6:2. http://dx.doi.org/10.3389/fnmol.2013.00002

Akiyama, H., and H. Kamiguchi. 2015. Second messenger networks for accurate growth cone guidance. *Dev. Neurobiol.* 75:411–422. http://dx.doi.org/10.1002/dneu.22157

Alam, M.R., L.N. Groschner, W. Parichatikanond, L. Kuo, A.I. Bondarenko, R. Rost, M. Waldeck-Weiermair, R. Malli, and W.F. Graier. 2012. Mitochondrial Ca^{2+} uptake 1 (MICU1) and mitochondrial Ca^{2+} uniporter (MCU) contribute to metabolism-secretion coupling in clonal pancreatic β-cells. *J. Biol. Chem.* 287:34445–34454. http://dx.doi.org/10.1074/jbc.M112.392084

Albrecht, S.C., M.C. Sobotta, D. Bausewein, I. Aller, R. Hell, T.P. Dick, and A.J. Meyer. 2014. Redesign of genetically encoded biosensors for monitoring mitochondrial redox status in a broad range of model eukaryotes. *J. Biomol. Screen.* 19:379–386. http://dx.doi.org/10.1177/1087057113499634

Albrecht, T., Y. Zhao, T.H. Nguyen, R.E. Campbell, and J.D. Johnson. 2015. Fluorescent biosensors illuminate calcium levels within defined beta-cell endosome subpopulations. *Cell Calcium.* 57:263–274. http://dx.doi.org/10.1016/j.ceca.2015.01.008

Allbritton, N.L., E. Oancea, M.A. Kuhn, and T. Meyer. 1994. Source of nuclear calcium signals. *Proc. Natl. Acad. Sci. USA.* 91:12458–12462. http://dx.doi.org/10.1073/pnas.91.26.12458

Allen, T.G. 1997. The 'sniffer-patch' technique for detection of neurotransmitter release. *Trends Neurosci.* 20:192–197. http://dx.doi.org/10.1016/S0166-2236(96)01039-9

Allen, M.D., and J. Zhang. 2006. Subcellular dynamics of protein kinase A activity visualized by FRET-based reporters. *Biochem. Biophys. Res. Commun.* 348:716–721. http://dx.doi.org/10.1016/j.bbrc.2006.07.136

Ananthanarayanan, B., Q. Ni, and J. Zhang. 2005. Signal propagation from membrane messengers to nuclear effectors revealed by reporters of phosphoinositide dynamics and Akt activity. *Proc. Natl. Acad. Sci. USA.* 102:15081–15086. http://dx.doi.org/10.1073/pnas.0502889102

Arnaudeau, S., W.L. Kelley, J.V. Walsh Jr., and N. Demaurex. 2001. Mitochondria recycle Ca^{2+} to the endoplasmic reticulum and prevent the depletion of neighboring endoplasmic reticulum regions. *J. Biol. Chem.* 276:29430–29439. http://dx.doi.org/10.1074/jbc.M103274200

Aronson, D.E., L.M. Costantini, and E.L. Snapp. 2011. Superfolder GFP is fluorescent in oxidizing environments when targeted via the Sec translocon. *Traffic.* 12:543–548. http://dx.doi.org/10.1111/j.1600-0854.2011.01168.x

Augustine, G.J., and E. Neher. 1992. Neuronal Ca^{2+} signalling takes the local route. *Curr. Opin. Neurobiol.* 2:302–307. http://dx.doi.org/10.1016/0959-4388(92)90119-6

Aulestia, F.J., M.T. Alonso, and J. García-Sancho. 2015. Differential calcium handling by the cis and trans regions of the Golgi apparatus. *Biochem. J.* 466:455–465. http://dx.doi.org/10.1042/BJ20141358

Azarias, G., and J.Y. Chatton. 2011. Selective ion changes during spontaneous mitochondrial transients in intact astrocytes. *PLoS One.* 6:e28505. http://dx.doi.org/10.1371/journal.pone.0028505

Bacskai, B.J., B. Hochner, M. Mahaut-Smith, S.R. Adams, B.K. Kaang, E.R. Kandel, and R.Y. Tsien. 1993. Spatially resolved dynamics of cAMP and protein kinase A subunits in Aplysia sensory neurons. *Science.* 260:222–226. http://dx.doi.org/10.1126/science.7682336

Baird, G.S., D.A. Zacharias, and R.Y. Tsien. 1999. Circular permutation and receptor insertion within green fluorescent proteins. *Proc. Natl. Acad. Sci. USA.* 96:11241–11246. http://dx.doi.org/10.1073/pnas.96.20.11241

Ballabio, A. 2016. The awesome lysosome. *EMBO Mol. Med.* 8:73–76. http://dx.doi.org/10.15252/emmm.201505966

Bannwarth, M., I.R. Correa, M. Sztretye, S. Pouvreau, C. Fellay, A. Aebischer, L. Royer, E. Rois, and K. Johnsson. 2009. Indo-1 derivatives for local calcium sensing. *ACS Chem. Biol.* 4:179–190. http://dx.doi.org/10.1021/cb800258g

Barros, L.F., A. San Martín, T. Sotelo-Hitschfeld, R. Lerchundi, I. Fernández-Moncada, I. Ruminot, R. Gutiérrez, R. Valdebenito, S. Ceballo, K. Alegría, et al. 2013. Small is fast: astrocytic glucose and lactate metabolism at cellular resolution. *Front. Cell. Neurosci.* 7:27. http://dx.doi.org/10.3389/fncel.2013.00027

Belousov, V.V., A.F. Fradkov, K.A. Lukyanov, D.B. Staroverov, K.S. Shakhbazov, A.V. Terskikh, and S. Lukyanov. 2006. Genetically encoded fluorescent indicator for intracellular hydrogen peroxide. *Nat. Methods.* 3:281–286. http://dx.doi.org/10.1038/nmeth866

Bengtson, C.P., H.E. Freitag, J.M. Weislogel, and H. Bading. 2010. Nuclear calcium sensors reveal that repetition of trains of synaptic stimuli boosts nuclear calcium signaling in CA1 pyramidal neurons. *Biophys. J.* 99:4066–4077. http://dx.doi.org/10.1016/j.bpj.2010.10.044

Berg, J., Y.P. Hung, and G. Yellen. 2009. A genetically encoded fluorescent reporter of ATP:ADP ratio. *Nat. Methods.* 6:161–166. http://dx.doi.org/10.1038/nmeth.1288

Berlin, S., E.C. Carroll, Z.L. Newman, H.O. Okada, C.M. Quinn, B. Kallman, N.C. Rockwell, S.S. Martin, J.C. Lagarias, and E.Y. Isacoff. 2015. Photoactivatable genetically encoded calcium indicators for targeted neuronal imaging. *Nat. Methods.* 12:852–858. http://dx.doi.org/10.1038/nmeth.3480

Bilan, D.S., M.E. Matlashov, A.Y. Gorokhovatsky, C. Schultz, G. Enikolopov, and V.V. Belousov. 2014. Genetically encoded fluorescent indicator for imaging NAD^+/NADH ratio changes in different cellular compartments. *Biochim. Biophys. Acta.* 1840:951–957. http://dx.doi.org/10.1016/j.bbagen.2013.11.018

Blobel, G., and B. Dobberstein. 1975a. Transfer of proteins across membranes. I. Presence of proteolytically processed and unprocessed nascent immunoglobulin light chains on membrane-bound ribosomes of murine myeloma. *J. Cell Biol.* 67:835–851. http://dx.doi.org/10.1083/jcb.67.3.835

Blobel, G., and B. Dobberstein. 1975b. Transfer of proteins across membranes. II. Reconstitution of functional rough microsomes from heterologous components. *J. Cell Biol.* 67:852–862. http://dx.doi.org/10.1083/jcb.67.3.852

Borgese, N. 2016. Getting membrane proteins on and off the shuttle bus between the endoplasmic reticulum and the Golgi complex. *J. Cell Sci.* 129:1537–1545. http://dx.doi.org/10.1242/jcs.183335

Braulke, T., and J.S. Bonifacino. 2009. Sorting of lysosomal proteins. *Biochim. Biophys. Acta.* 1793:605–614. http://dx.doi.org/10.1016/j.bbamcr.2008.10.016

Brini, M., M. Murgia, L. Pasti, D. Picard, T. Pozzan, and R. Rizzuto. 1993. Nuclear Ca2+ concentration measured with specifically targeted recombinant aequorin. *EMBO J.* 12:4813–4819.

Cannell, M.B., and C.H. Kong. 2012. Local control in cardiac E-C coupling. *J. Mol. Cell. Cardiol.* 52:298–303. http://dx.doi.org/10.1016/j.yjmcc.2011.04.014

Carquin, M., L. D'Auria, H. Pollet, E.R. Bongarzone, and D. Tyteca. 2016. Recent progress on lipid lateral heterogeneity in plasma membranes: From rafts to submicrometric domains. *Prog. Lipid Res.* 62:1–24. http://dx.doi.org/10.1016/j.plipres.2015.12.004

Chanda, B., R. Blunck, L.C. Faria, F.E. Schweizer, I. Mody, and F. Bezanilla. 2005. A hybrid approach to measuring electrical activity in genetically specified neurons. *Nat. Neurosci.* 8:1619–1626. http://dx.doi.org/10.1038/nn1558

Chang, C.R., and C. Blackstone. 2007. Cyclic AMP-dependent protein kinase phosphorylation of Drp1 regulates its GTPase activity and mitochondrial morphology. *J. Biol. Chem.* 282:21583–21587. http://dx.doi.org/10.1074/jbc.C700083200

Chen, X., Y. Bi, T. Wang, P. Li, X. Yan, S. Hou, C.E. Bammert, J. Ju, K.M. Gibson, W.J. Pavan, and L. Bi. 2015. Lysosomal targeting with stable and sensitive fluorescent probes (Superior LysoProbes): applications for lysosome labeling and tracking during apoptosis. *Sci. Rep.* 5:9004. http://dx.doi.org/10.1038/srep09004

Christensen, R.K., A.V. Petersen, N. Schmitt, and J.F. Perrier. 2014. Fast detection of extrasynaptic GABA with a whole-cell sniffer. *Front. Cell. Neurosci.* 8:133. http://dx.doi.org/10.3389/fncel.2014.00133

Chyan, W., D.Y. Zhang, S.J. Lippard, and R.J. Radford. 2014. Reaction-based fluorescent sensor for investigating mobile Zn^{2+} in mitochondria of healthy versus cancerous prostate cells. *Proc. Natl. Acad. Sci. USA.* 111:143–148. http://dx.doi.org/10.1073/pnas.1310583110

Clister, T., S. Mehta, and J. Zhang. 2015. Single-cell analysis of G-protein signal transduction. *J. Biol. Chem.* 290:6681–6688. http://dx.doi.org/10.1074/jbc.R114.616391

Costa, A., I. Drago, S. Behera, M. Zottini, P. Pizzo, J.I. Schroeder, T. Pozzan, and F. Lo Schiavo. 2010. H_2O_2 in plant peroxisomes: an in vivo analysis uncovers a Ca^{2+}-dependent scavenging system. *Plant J.* 62:760–772. http://dx.doi.org/10.1111/j.1365-313X.2010.04190.x

Cribbs, J.T., and S. Strack. 2007. Reversible phosphorylation of Drp1 by cyclic AMP-dependent protein kinase and calcineurin regulates mitochondrial fission and cell death. *EMBO Rep.* 8:939–944. http://dx.doi.org/10.1038/sj.embor.7401062

Damoiseaux, R., A. Keppler, and K. Johnsson. 2001. Synthesis and applications of chemical probes for human O6-alkylguanine-DNA alkyltransferase. *ChemBioChem.* 2:285–287. http://dx.doi.org/10.1002/1439-7633(20010401)2:4<285::AID-CBIC285>3.0.CO;2-N

Dansen, T.B., K.W. Wirtz, R.J. Wanders, and E.H. Pap. 2000. Peroxisomes in human fibroblasts have a basic pH. *Nat. Cell Biol.* 2:51–53.

De, A., A. Jasani, R. Arora, and S.S. Gambhir. 2013. Evolution of BRET biosensors from live cell to tissue-scale in vivo imaging. *Front. Endocrinol. (Lausanne).* 4:131.

Deisseroth, K., H. Bito, and R.W. Tsien. 1996. Signaling from synapse to nucleus: postsynaptic CREB phosphorylation during multiple forms of hippocampal synaptic plasticity. *Neuron.* 16:89–101. http://dx.doi.org/10.1016/S0896-6273(00)80026-4

de la Fuente, S., R.I. Fonteriz, M. Montero, and J. Alvarez. 2013. Ca^{2+} homeostasis in the endoplasmic reticulum measured with a new low-Ca^{2+}-affinity targeted aequorin. *Cell Calcium.* 54:37–45. http://dx.doi.org/10.1016/j.ceca.2013.04.001

Delling, M., A.A. Indzhykulian, X. Liu, Y. Li, T. Xie, D.P. Corey, and D.E. Clapham. 2016. Primary cilia are not calcium-responsive mechanosensors. *Nature.* 531:656–660. http://dx.doi.org/10.1038/nature17426

De Michele, R., F. Carimi, and W.B. Frommer. 2014. Mitochondrial biosensors. *Int. J. Biochem. Cell Biol.* 48:39–44. http://dx.doi.org/10.1016/j.biocel.2013.12.014

Depry, C., and J. Zhang. 2011. Using FRET-based reporters to visualize subcellular dynamics of protein kinase A activity. *Methods Mol. Biol.* 756:285–294. http://dx.doi.org/10.1007/978-1-61779-160-4_16

Depry, C., M.D. Allen, and J. Zhang. 2011. Visualization of PKA activity in plasma membrane microdomains. *Mol. Biosyst.* 7:52–58. http://dx.doi.org/10.1039/C0MB00079E

Di Benedetto, G., A. Zoccarato, V. Lissandron, A. Terrin, X. Li, M.D. Houslay, G.S. Baillie, and M. Zaccolo. 2008. Protein kinase A type I and type II define distinct intracellular signaling compartments. *Circ. Res.* 103:836–844. http://dx.doi.org/10.1161/CIRCRESAHA.108.174813

Di Benedetto, G., E. Scalzotto, M. Mongillo, and T. Pozzan. 2013. Mitochondrial Ca^{2+} uptake induces cyclic AMP generation in the

matrix and modulates organelle ATP levels. *Cell Metab.* 17:965–975. http://dx.doi.org/10.1016/j.cmet.2013.05.003

Dickinson, B.C., and C.J. Chang. 2008. A targetable fluorescent probe for imaging hydrogen peroxide in the mitochondria of living cells. *J. Am. Chem. Soc.* 130:9638–9639. http://dx.doi.org/10.1021/ja802355u

Dickson, E.J., J.G. Duman, M.W. Moody, L. Chen, and B. Hille. 2012. Orai-STIM-mediated Ca^{2+} release from secretory granules revealed by a targeted Ca^{2+} and pH probe. *Proc. Natl. Acad. Sci. USA.* 109:E3539–E3548. http://dx.doi.org/10.1073/pnas.1218247109

DiPilato, L.M., X. Cheng, and J. Zhang. 2004. Fluorescent indicators of cAMP and Epac activation reveal differential dynamics of cAMP signaling within discrete subcellular compartments. *Proc. Natl. Acad. Sci. USA.* 101:16513–16518. http://dx.doi.org/10.1073/pnas.0405973101

Dittmer, P.J., J.G. Miranda, J.A. Gorski, and A.E. Palmer. 2009. Genetically encoded sensors to elucidate spatial distribution of cellular zinc. *J. Biol. Chem.* 284:16289–16297. http://dx.doi.org/10.1074/jbc.M900501200

Dolman, N.J., K.M. Chambers, B. Mandavilli, R.H. Batchelor, and M.S. Janes. 2013. Tools and techniques to measure mitophagy using fluorescence microscopy. *Autophagy.* 9:1653–1662. http://dx.doi.org/10.4161/auto.24001

Dolmetsch, R.E., U. Pajvani, K. Fife, J.M. Spotts, and M.E. Greenberg. 2001. Signaling to the nucleus by an L-type calcium channel-calmodulin complex through the MAP kinase pathway. *Science.* 294:333–339. http://dx.doi.org/10.1126/science.1063395

Drago, I., M. Giacomello, P. Pizzo, and T. Pozzan. 2008. Calcium dynamics in the peroxisomal lumen of living cells. *J. Biol. Chem.* 283:14384–14390. http://dx.doi.org/10.1074/jbc.M800600200

Dudek, J., S. Pfeffer, P.H. Lee, M. Jung, A. Cavalié, V. Helms, F. Förster, and R. Zimmermann. 2015. Protein transport into the human endoplasmic reticulum. *J. Mol. Biol.* 427:1159–1175. http://dx.doi.org/10.1016/j.jmb.2014.06.011

Dworkin, M., and K.H. Keller. 1977. Solubility and diffusion coefficient of adenosine 3′:5′-monophosphate. *J. Biol. Chem.* 252:864–865.

Dyachok, O., Y. Isakov, J. Sågetorp, and A. Tengholm. 2006. Oscillations of cyclic AMP in hormone-stimulated insulin-secreting β-cells. *Nature.* 439:349–352. http://dx.doi.org/10.1038/nature04410

Echevarría, W., M.F. Leite, M.T. Guerra, W.R. Zipfel, and M.H. Nathanson. 2003. Regulation of calcium signals in the nucleus by a nucleoplasmic reticulum. *Nat. Cell Biol.* 5:440–446. http://dx.doi.org/10.1038/ncb980

Emmanouilidou, E., A.G. Teschemacher, A.E. Pouli, L.I. Nicholls, E.P. Seward, and G.A. Rutter. 1999. Imaging Ca^{2+} concentration changes at the secretory vesicle surface with a recombinant targeted cameleon. *Curr. Biol.* 9:915–918. http://dx.doi.org/10.1016/S0960-9822(99)80398-4

Ermakova, Y.G., D.S. Bilan, M.E. Matlashov, N.M. Mishina, K.N. Markvicheva, O.M. Subach, F.V. Subach, I. Bogeski, M. Hoth, G. Enikolopov, and V.V. Belousov. 2014. Red fluorescent genetically encoded indicator for intracellular hydrogen peroxide. *Nat. Commun.* 5:5222. http://dx.doi.org/10.1038/ncomms6222

Fang, Z., X. Kuang, Y. Zhang, P. Shi, and Z. Huang. 2015. A novel HAC1-based dual-luciferase reporter vector for detecting endoplasmic reticulum stress and unfolded protein response in yeast *Saccharomyces cerevisiae*. *Plasmid.* 79:48–53. http://dx.doi.org/10.1016/j.plasmid.2015.04.002

Fehr, M., S. Lalonde, D.W. Ehrhardt, and W.B. Frommer. 2004. Live imaging of glucose homeostasis in nuclei of COS-7 cells. *J. Fluoresc.* 14:603–609. http://dx.doi.org/10.1023/B:JOFL.0000039347.94943.99

Fehr, M., H. Takanaga, D.W. Ehrhardt, and W.B. Frommer. 2005. Evidence for high-capacity bidirectional glucose transport across the endoplasmic reticulum membrane by genetically encoded fluorescence resonance energy transfer nanosensors. *Mol. Cell. Biol.* 25:11102–11112. http://dx.doi.org/10.1128/MCB.25.24.11102-11112.2005

Feinstein, W.P., B. Zhu, S.J. Leavesley, S.L. Sayner, and T.C. Rich. 2012. Assessment of cellular mechanisms contributing to cAMP compartmentalization in pulmonary microvascular endothelial cells. *Am. J. Physiol. Cell Physiol.* 302:C839–C852. http://dx.doi.org/10.1152/ajpcell.00361.2011

Filippin, L., P.J. Magalhães, G. Di Benedetto, M. Colella, and T. Pozzan. 2003. Stable interactions between mitochondria and endoplasmic reticulum allow rapid accumulation of calcium in a subpopulation of mitochondria. *J. Biol. Chem.* 278:39224–39234. http://dx.doi.org/10.1074/jbc.M302301200

Filippin, L., M.C. Abad, S. Gastaldello, P.J. Magalhães, D. Sandonà, and T. Pozzan. 2005. Improved strategies for the delivery of GFP-based Ca^{2+} sensors into the mitochondrial matrix. *Cell Calcium.* 37:129–136. http://dx.doi.org/10.1016/j.ceca.2004.08.002

Fosque, B.F., Y. Sun, H. Dana, C.T. Yang, T. Ohyama, M.R. Tadross, R. Patel, M. Zlatic, D.S. Kim, M.B. Ahrens, et al. 2015. Neural circuits. Labeling of active neural circuits in vivo with designed calcium integrators. *Science.* 347:755–760. http://dx.doi.org/10.1126/science.1260922

Gadila, S.K.G., and K. Kim. 2016. Cargo trafficking from the trans-Golgi network towards the endosome. *Biol. Cell.* 108:205–218. http://dx.doi.org/10.1111/boc.201600001

Gaffield, M.A., and W.J. Betz. 2007. Imaging synaptic vesicle exocytosis and endocytosis with FM dyes. *Nat. Protoc.* 1:2916–2921. http://dx.doi.org/10.1038/nprot.2006.476

Gajewski, C.D., L. Yang, E.A. Schon, and G. Manfredi. 2003. New insights into the bioenergetics of mitochondrial disorders using intracellular ATP reporters. *Mol. Biol. Cell.* 14:3628–3635. http://dx.doi.org/10.1091/mbc.E02-12-0796

Gallegos, L.L., M.T. Kunkel, and A.C. Newton. 2006. Targeting protein kinase C activity reporter to discrete intracellular regions reveals spatiotemporal differences in agonist-dependent signaling. *J. Biol. Chem.* 281:30947–30956. http://dx.doi.org/10.1074/jbc.M603741200

Galperin, E., and A. Sorkin. 2003. Visualization of Rab5 activity in living cells by FRET microscopy and influence of plasma-membrane-targeted Rab5 on clathrin-dependent endocytosis. *J. Cell Sci.* 116:4799–4810. http://dx.doi.org/10.1242/jcs.00801

Gautier, A., A. Juillerat, C. Heinis, I.R. Corrêa Jr., M. Kindermann, F. Beaufils, and K. Johnsson. 2008. An engineered protein tag for multiprotein labeling in living cells. *Chem. Biol.* 15:128–136. http://dx.doi.org/10.1016/j.chembiol.2008.01.007

Germond, A., H. Fujita, T. Ichimura, and T.M. Watanabe. 2016. Design and development of genetically encoded fluorescent sensors to monitor intracellular chemical and physical parameters. *Biophys. Rev.* 8:121–138. http://dx.doi.org/10.1007/s12551-016-0195-9

Giacomello, M., I. Drago, M. Bortolozzi, M. Scorzeto, A. Gianelle, P. Pizzo, and T. Pozzan. 2010. Ca^{2+} hot spots on the mitochondrial surface are generated by Ca^{2+} mobilization from stores, but not by activation of store-operated Ca^{2+} channels. *Mol. Cell.* 38:280–290. http://dx.doi.org/10.1016/j.molcel.2010.04.003

Gilroy, S., and R.L. Jones. 1992. Gibberellic acid and abscisic acid coordinately regulate cytoplasmic calcium and secretory activity in barley aleurone protoplasts. *Proc. Natl. Acad. Sci. USA.* 89:3591–3595. http://dx.doi.org/10.1073/pnas.89.8.3591

Goldfarb, D.S., J. Gariépy, G. Schoolnik, and R.D. Kornberg. 1986. Synthetic peptides as nuclear localization signals. *Nature.* 322:641–644. http://dx.doi.org/10.1038/322641a0

González, J.E., and R.Y. Tsien. 1995. Voltage sensing by fluorescence resonance energy transfer in single cells. *Biophys. J.* 69:1272–1280. http://dx.doi.org/10.1016/S0006-3495(95)80029-9

Gould, S.J., G.A. Keller, N. Hosken, J. Wilkinson, and S. Subramani. 1989. A conserved tripeptide sorts proteins to peroxisomes. *J. Cell Biol.* 108:1657–1664. http://dx.doi.org/10.1083/jcb.108.5.1657

Grenier, V., A.S. Walker, and E.W. Miller. 2015. A small-molecule photoactivatable optical sensor of transmembrane potential. *J. Am. Chem. Soc.* 137:10894–10897. http://dx.doi.org/10.1021/jacs.5b05538

Greotti, E., A. Wong, T. Pozzan, D. Pendin, and P. Pizzo. 2016. Characterization of the ER-targeted low affinity Ca^{2+} probe D4ER. *Sensors (Basel).* 16:1419. http://dx.doi.org/10.3390/s16091419

Griesbeck, O., G.S. Baird, R.E. Campbell, D.A. Zacharias, and R.Y. Tsien. 2001. Reducing the environmental sensitivity of yellow fluorescent protein. Mechanism and applications. *J. Biol. Chem.* 276:29188–29194. http://dx.doi.org/10.1074/jbc.M102815200

Griffin, B.A., S.R. Adams, and R.Y. Tsien. 1998. Specific covalent labeling of recombinant protein molecules inside live cells. *Science.* 281:269–272. http://dx.doi.org/10.1126/science.281.5374.269

Gu, H., S. Lalonde, S. Okumoto, L.L. Looger, A.M. Scharff-Poulsen, A.R. Grossman, J. Kossmann, I. Jakobsen, and W.B. Frommer. 2006. A novel analytical method for in vivo phosphate tracking. *FEBS Lett.* 580:5885–5893. http://dx.doi.org/10.1016/j.febslet.2006.09.048

Gubernator, N.G., H. Zhang, R.G. Staal, E.V. Mosharov, D.B. Pereira, M. Yue, V. Balsanek, P.A. Vadola, B. Mukherjee, R.H. Edwards, et al. 2009. Fluorescent false neurotransmitters visualize dopamine release from individual presynaptic terminals. *Science.* 324:1441–1444. http://dx.doi.org/10.1126/science.1172278

Gutscher, M., A.L. Pauleau, L. Marty, T. Brach, G.H. Wabnitz, Y. Samstag, A.J. Meyer, and T.P. Dick. 2008. Real-time imaging of the intracellular glutathione redox potential. *Nat. Methods.* 5:553–559. http://dx.doi.org/10.1038/nmeth.1212

Hajnóczky, G., L.D. Robb-Gaspers, M.B. Seitz, and A.P. Thomas. 1995. Decoding of cytosolic calcium oscillations in the mitochondria. *Cell.* 82:415–424. http://dx.doi.org/10.1016/0092-8674(95)90430-1

Halls, M.L., and D.M. Cooper. 2011. Regulation by Ca^{2+}-signaling pathways of adenylyl cyclases. *Cold Spring Harb. Perspect. Biol.* 3:a004143. http://dx.doi.org/10.1101/cshperspect.a004143

Han, J., and K. Burgess. 2010. Fluorescent indicators for intracellular pH. *Chem. Rev.* 110:2709–2728. http://dx.doi.org/10.1021/cr900249z

Hanson, G.T., R. Aggeler, D. Oglesbee, M. Cannon, R.A. Capaldi, R.Y. Tsien, and S.J. Remington. 2004. Investigating mitochondrial redox potential with redox-sensitive green fluorescent protein indicators. *J. Biol. Chem.* 279:13044–13053. http://dx.doi.org/10.1074/jbc.M312846200

Harada, H., B. Becknell, M. Wilm, M. Mann, L.J. Huang, S.S. Taylor, J.D. Scott, and S.J. Korsmeyer. 1999. Phosphorylation and inactivation of BAD by mitochondria-anchored protein kinase A. *Mol. Cell.* 3:413–422. http://dx.doi.org/10.1016/S1097-2765(00)80469-4

Harbauer, A.B., R.P. Zahedi, A. Sickmann, N. Pfanner, and C. Meisinger. 2014. The protein import machinery of mitochondria-a regulatory hub in metabolism, stress, and disease. *Cell Metab.* 19:357–372. http://dx.doi.org/10.1016/j.cmet.2014.01.010

Hartl, F.U., N. Pfanner, D.W. Nicholson, and W. Neupert. 1989. Mitochondrial protein import. *Biochim. Biophys. Acta.* 988:1–45. http://dx.doi.org/10.1016/0304-4157(89)90002-6

Harvey, C.D., A.G. Ehrhardt, C. Cellurale, H. Zhong, R. Yasuda, R.J. Davis, and K. Svoboda. 2008. A genetically encoded fluorescent sensor of ERK activity. *Proc. Natl. Acad. Sci. USA.* 105:19264–19269. http://dx.doi.org/10.1073/pnas.0804598105

Hayes, J.S., L.L. Brunton, J.H. Brown, J.B. Reese, and S.E. Mayer. 1979. Hormonally specific expression of cardiac protein kinase activity. *Proc. Natl. Acad. Sci. USA.* 76:1570–1574. http://dx.doi.org/10.1073/pnas.76.4.1570

Hayes, J.S., L.L. Brunton, and S.E. Mayer. 1980. Selective activation of particulate cAMP-dependent protein kinase by isoproterenol and prostaglandin E1. *J. Biol. Chem.* 255:5113–5119.

Hazama, A., S. Hayashi, and Y. Okada. 1998. Cell surface measurements of ATP release from single pancreatic β cells using a novel biosensor technique. *Pflugers Arch.* 437:31–35. http://dx.doi.org/10.1007/s004240050742

Henderson, M.J., H.A. Baldwin, C.A. Werley, S. Boccardo, L.R. Whitaker, X. Yan, G.T. Holt, E.R. Schreiter, L.L. Looger, A.E. Cohen, et al. 2015. A low affinity GCaMP3 variant (GCaMPer) for imaging the endoplasmic reticulum calcium store. *PLoS One.* 10:e0139273. http://dx.doi.org/10.1371/journal.pone.0139273

Hikiji, T., J. Norisada, Y. Hirata, K. Okuda, H. Nagasawa, S. Ishigaki, G. Sobue, K. Kiuchi, and K. Oh-hashi. 2015. A highly sensitive assay of IRE1 activity using the small luciferase NanoLuc: Evaluation of ALS-related genetic and pathological factors. *Biochem. Biophys. Res. Commun.* 463:881–887. http://dx.doi.org/10.1016/j.bbrc.2015.05.132

Hochreiter, B., A.P. Garcia, and J.A. Schmid. 2015. Fluorescent proteins as genetically encoded FRET biosensors in life sciences. *Sensors (Basel).* 15:26281–26314. http://dx.doi.org/10.3390/s151026281

Hofer, A.M., W.R. Schlue, S. Curci, and T.E. Machen. 1995. Spatial distribution and quantitation of free luminal [Ca] within the InsP3-sensitive internal store of individual BHK-21 cells: ion dependence of InsP3-induced Ca release and reloading. *FASEB J.* 9:788–798.

Hofer, A.M., C. Fasolato, and T. Pozzan. 1998. Capacitative Ca^{2+} entry is closely linked to the filling state of internal Ca^{2+} stores: a study using simultaneous measurements of I_{CRAC} and intraluminal $[Ca^{2+}]$. *J. Cell Biol.* 140:325–334. http://dx.doi.org/10.1083/jcb.140.2.325

Hoffmann, C., G. Gaietta, M. Bünemann, S.R. Adams, S. Oberdorff-Maass, B. Behr, J.P. Vilardaga, R.Y. Tsien, M.H. Ellisman, and M.J. Lohse. 2005. A FlAsH-based FRET approach to determine G protein-coupled receptor activation in living cells. *Nat. Methods.* 2:171–176. http://dx.doi.org/10.1038/nmeth742

Hoi, H., T. Matsuda, T. Nagai, and R.E. Campbell. 2013. Highlightable Ca^{2+} indicators for live cell imaging. *J. Am. Chem. Soc.* 135:46–49. http://dx.doi.org/10.1021/ja310184a

Hoseki, J., A. Oishi, T. Fujimura, and Y. Sakai. 2016. Development of a stable ERroGFP variant suitable for monitoring redox dynamics in the ER. *Biosci. Rep.* 36:e00316. http://dx.doi.org/10.1042/BSR20160027

Hung, Y.P., J.G. Albeck, M. Tantama, and G. Yellen. 2011. Imaging cytosolic NADH-NAD^+ redox state with a genetically encoded fluorescent biosensor. *Cell Metab.* 14:545–554. http://dx.doi.org/10.1016/j.cmet.2011.08.012

Imamura, H., K.P. Nhat, H. Togawa, K. Saito, R. Iino, Y. Kato-Yamada, T. Nagai, and H. Noji. 2009. Visualization of ATP levels inside single living cells with fluorescence resonance energy transfer-based genetically encoded indicators. *Proc. Natl. Acad. Sci. USA.* 106:15651–15656. http://dx.doi.org/10.1073/pnas.0904764106

Iwawaki, T., R. Akai, K. Kohno, and M. Miura. 2004. A transgenic mouse model for monitoring endoplasmic reticulum stress. *Nat. Med.* 10:98–102. http://dx.doi.org/10.1038/nm970

Jankowski, A., J.H. Kim, R.F. Collins, R. Daneman, P. Walton, and S. Grinstein. 2001. In situ measurements of the pH of mammalian

peroxisomes using the fluorescent protein pHluorin. *J. Biol. Chem.* 276:48748–48753. http://dx.doi.org/10.1074/jbc.M109003200

Jean-Quartier, C., A.I. Bondarenko, M.R. Alam, M. Trenker, M. Waldeck-Weiermair, R. Malli, and W.F. Graier. 2012. Studying mitochondrial Ca^{2+} uptake - a revisit. *Mol. Cell. Endocrinol.* 353:114–127. http://dx.doi.org/10.1016/j.mce.2011.10.033

Jurevicius, J., and R. Fischmeister. 1996. cAMP compartmentation is responsible for a local activation of cardiac Ca2+ channels by beta-adrenergic agonists. *Proc. Natl. Acad. Sci. USA.* 93:295–299. http://dx.doi.org/10.1073/pnas.93.1.295

Kamiya, M., and K. Johnsson. 2010. Localizable and highly sensitive calcium indicator based on a BODIPY fluorophore. *Anal. Chem.* 82:6472–6479. http://dx.doi.org/10.1021/ac100741t

Kand, D., T. Saha, M. Lahiri, and P. Talukdar. 2015. Lysosome targeting fluorescence probe for imaging intracellular thiols. *Org. Biomol. Chem.* 13:8163–8168. http://dx.doi.org/10.1039/C5OB00889A

Kapoor, N., J.T. Maxwell, G.A. Mignery, D. Will, L.A. Blatter, and K. Banach. 2014. Spatially defined InsP3-mediated signaling in embryonic stem cell-derived cardiomyocytes. *PLoS One.* 9:e83715. http://dx.doi.org/10.1371/journal.pone.0083715

Kendall, J.M., R.L. Dormer, and A.K. Campbell. 1992. Targeting aequorin to the endoplasmic reticulum of living cells. *Biochem. Biophys. Res. Commun.* 189:1008–1016. http://dx.doi.org/10.1016/0006-291X(92)92304-G

Kim, H., M.C. Scimia, D. Wilkinson, R.D. Trelles, M.R. Wood, D. Bowtell, A. Dillin, M. Mercola, and Z.A. Ronai. 2011. Fine-tuning of Drp1/Fis1 availability by AKAP121/Siah2 regulates mitochondrial adaptation to hypoxia. *Mol. Cell.* 44:532–544. http://dx.doi.org/10.1016/j.molcel.2011.08.045

Kim, P.K., R.T. Mullen, U. Schumann, and J. Lippincott-Schwartz. 2006. The origin and maintenance of mammalian peroxisomes involves a de novo PEX16-dependent pathway from the ER. *J. Cell Biol.* 173:521–532. http://dx.doi.org/10.1083/jcb.200601036

Kipanyula, M.J., L. Contreras, E. Zampese, C. Lazzari, A.K. Wong, P. Pizzo, C. Fasolato, and T. Pozzan. 2012. Ca^{2+} dysregulation in neurons from transgenic mice expressing mutant presenilin 2. *Aging Cell.* 11:885–893. http://dx.doi.org/10.1111/j.1474-9726.2012.00858.x

Klarenbeek, J., J. Goedhart, A. van Batenburg, D. Groenewald, and K. Jalink. 2015. Fourth-generation epac-based FRET sensors for cAMP feature exceptional brightness, photostability and dynamic range: characterization of dedicated sensors for FLIM, for ratiometry and with high affinity. *PLoS One.* 10:e0122513. http://dx.doi.org/10.1371/journal.pone.0122513

Kneen, M., J. Farinas, Y. Li, and A.S. Verkman. 1998. Green fluorescent protein as a noninvasive intracellular pH indicator. *Biophys. J.* 74:1591–1599. http://dx.doi.org/10.1016/S0006-3495(98)77870-1

Komatsu, N., K. Aoki, M. Yamada, H. Yukinaga, Y. Fujita, Y. Kamioka, and M. Matsuda. 2011. Development of an optimized backbone of FRET biosensors for kinases and GTPases. *Mol. Biol. Cell.* 22:4647–4656. http://dx.doi.org/10.1091/mbc.E11-01-0072

Kornhauser, J.M., C.W. Cowan, A.J. Shaywitz, R.E. Dolmetsch, E.C. Griffith, L.S. Hu, C. Haddad, Z. Xia, and M.E. Greenberg. 2002. CREB transcriptional activity in neurons is regulated by multiple, calcium-specific phosphorylation events. *Neuron.* 34:221–233. http://dx.doi.org/10.1016/S0896-6273(02)00655-4

Kuner, T., and G.J. Augustine. 2000. A genetically encoded ratiometric indicator for chloride: capturing chloride transients in cultured hippocampal neurons. *Neuron.* 27:447–459. http://dx.doi.org/10.1016/S0896-6273(00)00056-8

Landolfi, B., S. Curci, L. Debellis, T. Pozzan, and A.M. Hofer. 1998. Ca^{2+} homeostasis in the agonist-sensitive internal store: functional interactions between mitochondria and the ER measured In situ in intact cells. *J. Cell Biol.* 142:1235–1243. http://dx.doi.org/10.1083/jcb.142.5.1235

Lasorsa, F.M., P. Pinton, L. Palmieri, P. Scarcia, H. Rottensteiner, R. Rizzuto, and F. Palmieri. 2008. Peroxisomes as novel players in cell calcium homeostasis. *J. Biol. Chem.* 283:15300–15308. http://dx.doi.org/10.1074/jbc.M800648200

Launikonis, B.S., J. Zhou, L. Royer, T.R. Shannon, G. Brum, and E. Ríos. 2005. Confocal imaging of [Ca^{2+}] in cellular organelles by SEER, shifted excitation and emission ratioing of fluorescence. *J. Physiol.* 567:523–543. http://dx.doi.org/10.1113/jphysiol.2005.087973

Lee, H., Z. Yang, Y. Wi, T.W. Kim, P. Verwilst, Y.H. Lee, G.I. Han, C. Kang, and J.S. Kim. 2015. BODIPY-Coumarin conjugate as an endoplasmic reticulum membrane fluidity sensor and its application to ER stress models. *Bioconjug. Chem.* 26:2474–2480. http://dx.doi.org/10.1021/acs.bioconjchem.5b00508

Lee, Y.H., N. Park, Y.B. Park, Y.J. Hwang, C. Kang, and J.S. Kim. 2014. Organelle-selective fluorescent Cu^{2+} ion probes: revealing the endoplasmic reticulum as a reservoir for Cu-overloading. *Chem. Commun. (Camb.).* 50:3197–3200. http://dx.doi.org/10.1039/c4cc00091a

Lefkimmiatis, K., D. Leronni, and A.M. Hofer. 2013. The inner and outer compartments of mitochondria are sites of distinct cAMP/PKA signaling dynamics. *J. Cell Biol.* 202:453–462. http://dx.doi.org/10.1083/jcb.201303159

Li, Y., and R.W. Tsien. 2012. pHTomato, a red, genetically encoded indicator that enables multiplex interrogation of synaptic activity. *Nat. Neurosci.* 15:1047–1053. http://dx.doi.org/10.1038/nn.3126

Li, D., K. Hérault, M. Oheim, and N. Ropert. 2009. FM dyes enter via a store-operated calcium channel and modify calcium signaling of cultured astrocytes. *Proc. Natl. Acad. Sci. USA.* 106:21960–21965. http://dx.doi.org/10.1073/pnas.0909109106

Lim, C.S., G. Masanta, H.J. Kim, J.H. Han, H.M. Kim, and B.R. Cho. 2011. Ratiometric detection of mitochondrial thiols with a two-photon fluorescent probe. *J. Am. Chem. Soc.* 133:11132–11135. http://dx.doi.org/10.1021/ja205081s

Lindenburg, L.H., A.M. Hessels, E.H. Ebberink, R. Arts, and M. Merkx. 2013a. Robust red FRET sensors using self-associating fluorescent domains. *ACS Chem. Biol.* 8:2133–2139. http://dx.doi.org/10.1021/cb400427b

Lindenburg, L.H., J.L. Vinkenborg, J. Oortwijn, S.J. Aper, and M. Merkx. 2013b. MagFRET: the first genetically encoded fluorescent Mg^{2+} sensor. *PLoS One.* 8:e82009. http://dx.doi.org/10.1371/journal.pone.0082009

Lissandron, V., P. Podini, P. Pizzo, and T. Pozzan. 2010. Unique characteristics of Ca^{2+} homeostasis of the trans-Golgi compartment. *Proc. Natl. Acad. Sci. USA.* 107:9198–9203. (published erratum appears in *Proc. Natl. Acad. Sci. USA.* 2011. 108:4512) http://dx.doi.org/10.1073/pnas.1004702107

Liu, S., J. Zhang, and Y.K. Xiang. 2011. FRET-based direct detection of dynamic protein kinase A activity on the sarcoplasmic reticulum in cardiomyocytes. *Biochem. Biophys. Res. Commun.* 404:581–586. http://dx.doi.org/10.1016/j.bbrc.2010.11.116

Liu, Z., A.M. Celotto, G. Romero, P. Wipf, and M.J. Palladino. 2012a. Genetically encoded redox sensor identifies the role of ROS in degenerative and mitochondrial disease pathogenesis. *Neurobiol. Dis.* 45:362–368. http://dx.doi.org/10.1016/j.nbd.2011.08.022

Liu, Z., C. Zhang, Y. Chen, W. He, and Z. Guo. 2012b. An excitation ratiometric Zn^{2+} sensor with mitochondria-targetability for monitoring of mitochondrial Zn^{2+} release upon different stimulations. *Chem. Commun. (Camb.).* 48:8365–8367. http://dx.doi.org/10.1039/c2cc33648k

Llopis, J., J.M. McCaffery, A. Miyawaki, M.G. Farquhar, and R.Y. Tsien. 1998. Measurement of cytosolic, mitochondrial, and Golgi pH in single living cells with green fluorescent proteins. *Proc.*

Natl. Acad. Sci. USA. 95:6803–6808. http://dx.doi.org/10.1073/pnas.95.12.6803

Loew, L.M. 2015. Design and use of organic voltage sensitive dyes. *Adv. Exp. Med. Biol.* 859:27–53. http://dx.doi.org/10.1007/978-3-319-17641-3_2

Loro, G., I. Drago, T. Pozzan, F.L. Schiavo, M. Zottini, and A. Costa. 2012. Targeting of Cameleons to various subcellular compartments reveals a strict cytoplasmic/mitochondrial Ca^{2+} handling relationship in plant cells. *Plant J.* 71:1–13. http://dx.doi.org/10.1111/j.1365-313X.2012.04968.x

Lukyanov, K.A., and V.V. Belousov. 2014. Genetically encoded fluorescent redox sensors. *Biochim. Biophys. Acta.* 1840:745–756. http://dx.doi.org/10.1016/j.bbagen.2013.05.030

Lv, H.S., S.Y. Huang, Y. Xu, X. Dai, J.Y. Miao, and B.X. Zhao. 2014. A new fluorescent pH probe for imaging lysosomes in living cells. *Bioorg. Med. Chem. Lett.* 24:535–538. http://dx.doi.org/10.1016/j.bmcl.2013.12.025

Malinouski, M., Y. Zhou, V.V. Belousov, D.L. Hatfield, and V.N. Gladyshev. 2011. Hydrogen peroxide probes directed to different cellular compartments. *PLoS One.* 6:e14564. http://dx.doi.org/10.1371/journal.pone.0014564

Manjarrés, I.M., P. Chamero, B. Domingo, F. Molina, J. Llopis, M.T. Alonso, and J. García-Sancho. 2008. Red and green aequorins for simultaneous monitoring of Ca^{2+} signals from two different organelles. *Pflugers Arch.* 455:961–970. http://dx.doi.org/10.1007/s00424-007-0349-5

Manno, C., L. Figueroa, R. Fitts, and E. Ríos. 2013a. Confocal imaging of transmembrane voltage by SEER of di-8-ANEPPS. *J. Gen. Physiol.* 141:371–387. http://dx.doi.org/10.1085/jgp.201210936

Manno, C., M. Sztretye, L. Figueroa, P.D. Allen, and E. Ríos. 2013b. Dynamic measurement of the calcium buffering properties of the sarcoplasmic reticulum in mouse skeletal muscle. *J. Physiol.* 591:423–442. http://dx.doi.org/10.1113/jphysiol.2012.243444

Mao, T., D.H. O'Connor, V. Scheuss, J. Nakai, and K. Svoboda. 2008. Characterization and subcellular targeting of GCaMP-type genetically-encoded calcium indicators. *PLoS One.* 3:e1796. http://dx.doi.org/10.1371/journal.pone.0001796

Marsault, R., M. Murgia, T. Pozzan, and R. Rizzuto. 1997. Domains of high Ca^{2+} beneath the plasma membrane of living A7r5 cells. *EMBO J.* 16:1575–1581. http://dx.doi.org/10.1093/emboj/16.7.1575

Martin-Urdiroz, M., M.J. Deeks, C.G. Horton, H.R. Dawe, and I. Jourdain. 2016. The exocyst complex in health and disease. *Front. Cell Dev. Biol.* 4:24. http://dx.doi.org/10.3389/fcell.2016.00024

Maruyama, Y., O.H. Petersen, P. Flanagan, and G.T. Pearson. 1983. Quantification of Ca2+-activated K+ channels under hormonal control in pig pancreas acinar cells. *Nature.* 305:228–232. http://dx.doi.org/10.1038/305228a0

Marvin, J.S., B.G. Borghuis, L. Tian, J. Cichon, M.T. Harnett, J. Akerboom, A. Gordus, S.L. Renninger, T.W. Chen, C.I. Bargmann, et al. 2013. An optimized fluorescent probe for visualizing glutamate neurotransmission. *Nat. Methods.* 10:162–170. http://dx.doi.org/10.1038/nmeth.2333

Masanta, G., C.S. Lim, H.J. Kim, J.H. Han, H.M. Kim, and B.R. Cho. 2011. A mitochondrial-targeted two-photon probe for zinc ion. *J. Am. Chem. Soc.* 133:5698–5700. http://dx.doi.org/10.1021/ja200444t

Matsuda, T., K. Horikawa, K. Saito, and T. Nagai. 2013. Highlighted Ca^{2+} imaging with a genetically encoded 'caged' indicator. *Sci. Rep.* 3:1398. http://dx.doi.org/10.1038/srep01398

McCue, H.V., J.D. Wardyn, R.D. Burgoyne, and L.P. Haynes. 2013. Generation and characterization of a lysosomally targeted, genetically encoded Ca^{2+}-sensor. *Biochem. J.* 449:449–457. http://dx.doi.org/10.1042/BJ20120898

Meinig, J.M., L. Fu, and B.R. Peterson. 2015. Synthesis of fluorophores that target small molecules to the endoplasmic reticulum of living mammalian cells. *Angew. Chem. Int. Ed. Engl.* 54:9696–9699. http://dx.doi.org/10.1002/anie.201504156

Mellman, I., and W.J. Nelson. 2008. Coordinated protein sorting, targeting and distribution in polarized cells. *Nat. Rev. Mol. Cell Biol.* 9:833–845. http://dx.doi.org/10.1038/nrm2525

Merksamer, P.I., A. Trusina, and F.R. Papa. 2008. Real-time redox measurements during endoplasmic reticulum stress reveal interlinked protein folding functions. *Cell.* 135:933–947. http://dx.doi.org/10.1016/j.cell.2008.10.011

Miao, F., G. Song, Y. Sun, Y. Liu, F. Guo, W. Zhang, M. Tian, and X. Yu. 2013. Fluorescent imaging of acidic compartments in living cells with a high selective novel one-photon ratiometric and two-photon acidic pH probe. *Biosens. Bioelectron.* 50:42–49. http://dx.doi.org/10.1016/j.bios.2013.05.060

Miesenböck, G., D.A. De Angelis, and J.E. Rothman. 1998. Visualizing secretion and synaptic transmission with pH-sensitive green fluorescent proteins. *Nature.* 394:192–195. http://dx.doi.org/10.1038/28190

Minta, A., J.P. Kao, and R.Y. Tsien. 1989. Fluorescent indicators for cytosolic calcium based on rhodamine and fluorescein chromophores. *J. Biol. Chem.* 264:8171–8178.

Miranda, J.G., A.L. Weaver, Y. Qin, J.G. Park, C.I. Stoddard, M.Z. Lin, and A.E. Palmer. 2012. New alternately colored FRET sensors for simultaneous monitoring of Zn^{2+} in multiple cellular locations. *PLoS One.* 7:e49371. http://dx.doi.org/10.1371/journal.pone.0049371

Mitchell, K.J., P. Pinton, A. Varadi, C. Tacchetti, E.K. Ainscow, T. Pozzan, R. Rizzuto, and G.A. Rutter. 2001. Dense core secretory vesicles revealed as a dynamic Ca^{2+} store in neuroendocrine cells with a vesicle-associated membrane protein aequorin chimaera. *J. Cell Biol.* 155:41–52. http://dx.doi.org/10.1083/jcb.200103145

Miyamoto, T., E. Rho, V. Sample, H. Akano, M. Magari, T. Ueno, K. Gorshkov, M. Chen, H. Tokumitsu, J. Zhang, and T. Inoue. 2015. Compartmentalized AMPK signaling illuminated by genetically encoded molecular sensors and actuators. *Cell Reports.* 11:657–670. http://dx.doi.org/10.1016/j.celrep.2015.03.057

Miyawaki, A., and R.Y. Tsien. 2000. Monitoring protein conformations and interactions by fluorescence resonance energy transfer between mutants of green fluorescent protein. *Methods Enzymol.* 327:472–500. http://dx.doi.org/10.1016/S0076-6879(00)27297-2

Miyawaki, A., J. Llopis, R. Heim, J.M. McCaffery, J.A. Adams, M. Ikura, and R.Y. Tsien. 1997. Fluorescent indicators for Ca^{2+} based on green fluorescent proteins and calmodulin. *Nature.* 388:882–887. http://dx.doi.org/10.1038/42264

Mohsin, M., A. Ahmad, and M. Iqbal. 2015. FRET-based genetically-encoded sensors for quantitative monitoring of metabolites. *Biotechnol. Lett.* 37:1919–1928. http://dx.doi.org/10.1007/s10529-015-1873-6

Mongillo, M., T. McSorley, S. Evellin, A. Sood, V. Lissandron, A. Terrin, E. Huston, A. Hannawacker, M.J. Lohse, T. Pozzan, et al. 2004. Fluorescence resonance energy transfer-based analysis of cAMP dynamics in live neonatal rat cardiac myocytes reveals distinct functions of compartmentalized phosphodiesterases. *Circ. Res.* 95:67–75. http://dx.doi.org/10.1161/01.RES.0000134629.84732.11

Montero, M., M. Brini, R. Marsault, J. Alvarez, R. Sitia, T. Pozzan, and R. Rizzuto. 1995. Monitoring dynamic changes in free Ca2+ concentration in the endoplasmic reticulum of intact cells. *EMBO J.* 14:5467–5475.

Montero, M., J. Alvarez, W.J. Scheenen, R. Rizzuto, J. Meldolesi, and T. Pozzan. 1997. Ca^{2+} homeostasis in the endoplasmic reticulum: coexistence of high and low [Ca^{2+}] subcompartments in intact

HeLa cells. *J. Cell Biol.* 139:601–611. http://dx.doi.org/10.1083/jcb.139.3.601

Morgan, A.J. 2016. Ca^{2+} dialogue between acidic vesicles and ER. *Biochem. Soc. Trans.* 44:546–553. http://dx.doi.org/10.1042/BST20150290

Morgan, D., M. Capasso, B. Musset, V.V. Cherny, E. Ríos, M.J. Dyer, and T.E. DeCoursey. 2009. Voltage-gated proton channels maintain pH in human neutrophils during phagocytosis. *Proc. Natl. Acad. Sci. USA.* 106:18022–18027. http://dx.doi.org/10.1073/pnas.0905565106

Mukherjee, S., V. Jansen, J.F. Jikeli, H. Hamzeh, L. Alvarez, M. Dombrowski, M. Balbach, T. Strünker, R. Seifert, U.B. Kaupp, and D. Wachten. 2016. A novel biosensor to study cAMP dynamics in cilia and flagella. *eLife.* 5:e14052. http://dx.doi.org/10.7554/eLife.14052

Mukhtarov, M., L. Liguori, T. Waseem, F. Rocca, S. Buldakova, D. Arosio, and P. Bregestovski. 2013. Calibration and functional analysis of three genetically encoded Cl^-/pH sensors. *Front. Mol. Neurosci.* 6:9. http://dx.doi.org/10.3389/fnmol.2013.00009

Mutoh, H., A. Perron, W. Akemann, Y. Iwamoto, and T. Knöpfel. 2011. Optogenetic monitoring of membrane potentials. *Exp. Physiol.* 96:13–18. http://dx.doi.org/10.1113/expphysiol.2010.053942

Nachury, M.V., E.S. Seeley, and H. Jin. 2010. Trafficking to the ciliary membrane: how to get across the periciliary diffusion barrier? *Annu. Rev. Cell Dev. Biol.* 26:59–87. http://dx.doi.org/10.1146/annurev.cellbio.042308.113337

Nagai, T., A. Sawano, E.S. Park, and A. Miyawaki. 2001. Circularly permuted green fluorescent proteins engineered to sense Ca^{2+}. *Proc. Natl. Acad. Sci. USA.* 98:3197–3202. http://dx.doi.org/10.1073/pnas.051636098

Nakahashi, Y., E. Nelson, K. Fagan, E. Gonzales, J.L. Guillou, and D.M. Cooper. 1997. Construction of a full-length Ca^{2+}-sensitive adenylyl cyclase/aequorin chimera. *J. Biol. Chem.* 272:18093–18097. http://dx.doi.org/10.1074/jbc.272.29.18093

Nakajima, T., M. Sato, N. Akaza, and Y. Umezawa. 2008. Cell-based fluorescent indicator to visualize brain-derived neurotrophic factor secreted from living neurons. *ACS Chem. Biol.* 3:352–358. http://dx.doi.org/10.1021/cb800052v

Nakano, M., H. Imamura, T. Nagai, and H. Noji. 2011. Ca^{2+} regulation of mitochondrial ATP synthesis visualized at the single cell level. *ACS Chem. Biol.* 6:709–715. http://dx.doi.org/10.1021/cb100313n

Navas-Navarro, P., J. Rojo-Ruiz, M. Rodriguez-Prados, M.D. Ganfornina, L.L. Looger, M.T. Alonso, and J. García-Sancho. 2016. GFP-Aequorin protein sensor for ex vivo and in vivo imaging of Ca^{2+} dynamics in high-Ca^{2+} organelles. *Cell Chem. Biol.* 23:738–745. http://dx.doi.org/10.1016/j.chembiol.2016.05.010

Nguyen, Q.T., L.F. Schroeder, M. Mank, A. Muller, P. Taylor, O. Griesbeck, and D. Kleinfeld. 2010. An in vivo biosensor for neurotransmitter release and in situ receptor activity. *Nat. Neurosci.* 13:127–132. http://dx.doi.org/10.1038/nn.2469

Nicholls, D.G. 2012. Fluorescence measurement of mitochondrial membrane potential changes in cultured cells. *Methods Mol. Biol.* 810:119–133. http://dx.doi.org/10.1007/978-1-61779-382-0_8

Niehörster, T., A. Löschberger, I. Gregor, B. Krämer, H.J. Rahn, M. Patting, F. Koberling, J. Enderlein, and M. Sauer. 2016. Multi-target spectrally resolved fluorescence lifetime imaging microscopy. *Nat. Methods.* 13:257–262. http://dx.doi.org/10.1038/nmeth.3740

Nikolaev, V.O., A. Moshkov, A.R. Lyon, M. Miragoli, P. Novak, H. Paur, M.J. Lohse, Y.E. Korchev, S.E. Harding, and J. Gorelik. 2010. β_2-adrenergic receptor redistribution in heart failure changes cAMP compartmentation. *Science.* 327:1653–1657. http://dx.doi.org/10.1126/science.1185988

Ohara-Imaizumi, M., Y. Nakamichi, T. Tanaka, H. Katsuta, H. Ishida, and S. Nagamatsu. 2002. Monitoring of exocytosis and endocytosis of insulin secretory granules in the pancreatic beta-cell line MIN6 using pH-sensitive green fluorescent protein (pHluorin) and confocal laser microscopy. *Biochem. J.* 363:73–80. http://dx.doi.org/10.1042/bj3630073

Oheim, M., M. van 't Hoff, A. Feltz, A. Zamaleeva, J.M. Mallet, and M. Collot. 2014. New red-fluorescent calcium indicators for optogenetics, photoactivation and multi-color imaging. *Biochim. Biophys. Acta.* 1843:2284–2306. http://dx.doi.org/10.1016/j.bbamcr.2014.03.010

Oldach, L., and J. Zhang. 2014. Genetically encoded fluorescent biosensors for live-cell visualization of protein phosphorylation. *Chem. Biol.* 21:186–197. http://dx.doi.org/10.1016/j.chembiol.2013.12.012

Omura, T. 1998. Mitochondria-targeting sequence, a multi-role sorting sequence recognized at all steps of protein import into mitochondria. *J. Biochem.* 123:1010–1016. http://dx.doi.org/10.1093/oxfordjournals.jbchem.a022036

Osipchuk, Y.V., M. Wakui, D.I. Yule, D.V. Gallacher, and O.H. Petersen. 1990. Cytoplasmic Ca2+ oscillations evoked by receptor stimulation, G-protein activation, internal application of inositol trisphosphate or Ca2+: simultaneous microfluorimetry and Ca2+ dependent Cl- current recording in single pancreatic acinar cells. *EMBO J.* 9:697–704.

Palmer, A.E., C. Jin, J.C. Reed, and R.Y. Tsien. 2004. Bcl-2-mediated alterations in endoplasmic reticulum Ca^{2+} analyzed with an improved genetically encoded fluorescent sensor. *Proc. Natl. Acad. Sci. USA.* 101:17404–17409. http://dx.doi.org/10.1073/pnas.0408030101

Palmer, A.E., M. Giacomello, T. Kortemme, S.A. Hires, V. Lev-Ram, D. Baker, and R.Y. Tsien. 2006. Ca^{2+} indicators based on computationally redesigned calmodulin-peptide pairs. *Chem. Biol.* 13:521–530. http://dx.doi.org/10.1016/j.chembiol.2006.03.007

Pap, E.H., T.B. Dansen, and K.W. Wirtz. 2001. Peptide-based targeting of fluorophores to peroxisomes in living cells. *Trends Cell Biol.* 11:10–12. http://dx.doi.org/10.1016/S0962-8924(00)01829-8

Paramonov, V.M., V. Mamaeva, C. Sahlgren, and A. Rivero-Müller. 2015. Genetically-encoded tools for cAMP probing and modulation in living systems. *Front. Pharmacol.* 6:196. http://dx.doi.org/10.3389/fphar.2015.00196

Park, Y.U., J. Jeong, H. Lee, J.Y. Mun, J.H. Kim, J.S. Lee, M.D. Nguyen, S.S. Han, P.G. Suh, and S.K. Park. 2010. Disrupted-in-schizophrenia 1 (DISC1) plays essential roles in mitochondria in collaboration with Mitofilin. *Proc. Natl. Acad. Sci. USA.* 107:17785–17790. http://dx.doi.org/10.1073/pnas.1004361107

Pasti, L., M. Zonta, T. Pozzan, S. Vicini, and G. Carmignoto. 2001. Cytosolic calcium oscillations in astrocytes may regulate exocytotic release of glutamate. *J. Neurosci.* 21:477–484.

Pédelacq, J.D., S. Cabantous, T. Tran, T.C. Terwilliger, and G.S. Waldo. 2006. Engineering and characterization of a superfolder green fluorescent protein. *Nat. Biotechnol.* 24:79–88. http://dx.doi.org/10.1038/nbt1172

Pellegatti, P., S. Falzoni, P. Pinton, R. Rizzuto, and F. Di Virgilio. 2005. A novel recombinant plasma membrane-targeted luciferase reveals a new pathway for ATP secretion. *Mol. Biol. Cell.* 16:3659–3665. http://dx.doi.org/10.1091/mbc.E05-03-0222

Peterka, D.S., H. Takahashi, and R. Yuste. 2011. Imaging voltage in neurons. *Neuron.* 69:9–21. http://dx.doi.org/10.1016/j.neuron.2010.12.010

Pierzyńska-Mach, A., P.A. Janowski, and J.W. Dobrucki. 2014. Evaluation of acridine orange, LysoTracker Red, and quinacrine as fluorescent probes for long-term tracking of acidic vesicles. *Cytometry A.* 85:729–737. http://dx.doi.org/10.1002/cyto.a.22495

Pinton, P., T. Pozzan, and R. Rizzuto. 1998. The Golgi apparatus is an inositol 1,4,5-trisphosphate-sensitive Ca2+ store, with functional properties distinct from those of the endoplasmic reticulum. *EMBO J.* 17:5298–5308. http://dx.doi.org/10.1093/emboj/17.18.5298

Pizzo, P., V. Lissandron, P. Capitanio, and T. Pozzan. 2011. Ca^{2+} signalling in the Golgi apparatus. *Cell Calcium.* 50:184–192. http://dx.doi.org/10.1016/j.ceca.2011.01.006

Poburko, D., J. Santo-Domingo, and N. Demaurex. 2011. Dynamic regulation of the mitochondrial proton gradient during cytosolic calcium elevations. *J. Biol. Chem.* 286:11672–11684. http://dx.doi.org/10.1074/jbc.M110.159962

Poenie, M., R.Y. Tsien, and A.M. Schmitt-Verhulst. 1987. Sequential activation and lethal hit measured by [Ca2+]i in individual cytolytic T cells and targets. *EMBO J.* 6:2223–2232.

Porcelli, A.M., A. Ghelli, C. Zanna, P. Pinton, R. Rizzuto, and M. Rugolo. 2005. pH difference across the outer mitochondrial membrane measured with a green fluorescent protein mutant. *Biochem. Biophys. Res. Commun.* 326:799–804. http://dx.doi.org/10.1016/j.bbrc.2004.11.105

Prasad, R.M., X. Jin, and S.M. Nauli. 2014. Sensing a sensor: identifying the mechanosensory function of primary cilia. *Biosensors (Basel).* 4:47–62. http://dx.doi.org/10.3390/bios4010047

Qin, Y., P.J. Dittmer, J.G. Park, K.B. Jansen, and A.E. Palmer. 2011. Measuring steady-state and dynamic endoplasmic reticulum and Golgi Zn^{2+} with genetically encoded sensors. *Proc. Natl. Acad. Sci. USA.* 108:7351–7356. http://dx.doi.org/10.1073/pnas.1015686108

Rapizzi, E., P. Pinton, G. Szabadkai, M.R. Wieckowski, G. Vandecasteele, G. Baird, R.A. Tuft, K.E. Fogarty, and R. Rizzuto. 2002. Recombinant expression of the voltage-dependent anion channel enhances the transfer of Ca^{2+} microdomains to mitochondria. *J. Cell Biol.* 159:613–624. http://dx.doi.org/10.1083/jcb.200205091

Raspe, M., K.M. Kedziora, B. van den Broek, Q. Zhao, S. de Jong, J. Herz, M. Mastop, J. Goedhart, T.W. Gadella, I.T. Young, and K. Jalink. 2016. siFLIM: single-image frequency-domain FLIM provides fast and photon-efficient lifetime data. *Nat. Methods.* 13:501–504. http://dx.doi.org/10.1038/nmeth.3836

Reddy G, U., A.H. A, F. Ali, N. Taye, S. Chattopadhyay, and A. Das. 2015. FRET-based probe for monitoring pH changes in lipid-dense region of Hct116 cells. *Org. Lett.* 17:5532–5535. http://dx.doi.org/10.1021/acs.orglett.5b02568

Rehberg, M., A. Lepier, B. Solchenberger, P. Osten, and R. Blum. 2008. A new non-disruptive strategy to target calcium indicator dyes to the endoplasmic reticulum. *Cell Calcium.* 44:386–399. http://dx.doi.org/10.1016/j.ceca.2008.02.002

Remus, T.P., A.V. Zima, J. Bossuyt, D.J. Bare, J.L. Martin, L.A. Blatter, D.M. Bers, and G.A. Mignery. 2006. Biosensors to measure inositol 1,4,5-trisphosphate concentration in living cells with spatiotemporal resolution. *J. Biol. Chem.* 281:608–616. http://dx.doi.org/10.1074/jbc.M509645200

Rich, T.C., K.A. Fagan, H. Nakata, J. Schaack, D.M. Cooper, and J.W. Karpen. 2000. Cyclic nucleotide-gated channels colocalize with adenylyl cyclase in regions of restricted cAMP diffusion. *J. Gen. Physiol.* 116:147–162. http://dx.doi.org/10.1085/jgp.116.2.147

Rich, T.C., W. Xin, S.J. Leavesley, and M.S. Taylor. 2015. Channel-based reporters for cAMP detection. *Methods Mol. Biol.* 1294:71–84. http://dx.doi.org/10.1007/978-1-4939-2537-7_6

Richards, M., O. Lomas, K. Jalink, K.L. Ford, R.D. Vaughan-Jones, K. Lefkimmiatis, and P. Swietach. 2016. Intracellular tortuosity underlies slow cAMP diffusion in adult ventricular myocytes. *Cardiovasc. Res.* 110:395–407. http://dx.doi.org/10.1093/cvr/cvw080

Rizzuto, R., and T. Pozzan. 2006. Microdomains of intracellular Ca^{2+}: molecular determinants and functional consequences. *Physiol. Rev.* 86:369–408. http://dx.doi.org/10.1152/physrev.00004.2005

Rizzuto, R., A.W. Simpson, M. Brini, and T. Pozzan. 1992. Rapid changes of mitochondrial Ca^{2+} revealed by specifically targeted recombinant aequorin. *Nature.* 358:325–327. http://dx.doi.org/10.1038/358325a0

Rizzuto, R., M. Brini, M. Murgia, and T. Pozzan. 1993. Microdomains with high Ca^{2+} close to IP3-sensitive channels that are sensed by neighboring mitochondria. *Science.* 262:744–747. http://dx.doi.org/10.1126/science.8235595

Rizzuto, R., C. Bastianutto, M. Brini, M. Murgia, and T. Pozzan. 1994. Mitochondrial Ca^{2+} homeostasis in intact cells. *J. Cell Biol.* 126:1183–1194. http://dx.doi.org/10.1083/jcb.126.5.1183

Rizzuto, R., P. Pinton, W. Carrington, F.S. Fay, K.E. Fogarty, L.M. Lifshitz, R.A. Tuft, and T. Pozzan. 1998. Close contacts with the endoplasmic reticulum as determinants of mitochondrial Ca^{2+} responses. *Science.* 280:1763–1766. http://dx.doi.org/10.1126/science.280.5370.1763

Robinson, K.M., M.S. Janes, M. Pehar, J.S. Monette, M.F. Ross, T.M. Hagen, M.P. Murphy, and J.S. Beckman. 2006. Selective fluorescent imaging of superoxide in vivo using ethidium-based probes. *Proc. Natl. Acad. Sci. USA.* 103:15038–15043. http://dx.doi.org/10.1073/pnas.0601945103

Röder, I.V., K.R. Choi, M. Reischl, Y. Petersen, M.E. Diefenbacher, M. Zaccolo, T. Pozzan, and R. Rudolf. 2010. Myosin Va cooperates with PKA RIα to mediate maintenance of the endplate in vivo. *Proc. Natl. Acad. Sci. USA.* 107:2031–2036. http://dx.doi.org/10.1073/pnas.0914087107

Rodriguez, P.C., D.B. Pereira, A. Borgkvist, M.Y. Wong, C. Barnard, M.S. Sonders, H. Zhang, D. Sames, and D. Sulzer. 2013. Fluorescent dopamine tracer resolves individual dopaminergic synapses and their activity in the brain. *Proc. Natl. Acad. Sci. USA.* 110:870–875. http://dx.doi.org/10.1073/pnas.1213569110

Rodriguez-Garcia, A., J. Rojo-Ruiz, P. Navas-Navarro, F.J. Aulestia, S. Gallego-Sandin, J. Garcia-Sancho, and M.T. Alonso. 2014. GAP, an aequorin-based fluorescent indicator for imaging Ca^{2+} in organelles. *Proc. Natl. Acad. Sci. USA.* 111:2584–2589. http://dx.doi.org/10.1073/pnas.1316539111

Rodríguez-Prados, M., J. Rojo-Ruiz, F.J. Aulestia, J. García-Sancho, and M.T. Alonso. 2015. A new low-Ca^{2+} affinity GAP indicator to monitor high Ca^{2+} in organelles by luminescence. *Cell Calcium.* 58:558–564. http://dx.doi.org/10.1016/j.ceca.2015.09.002

Roise, D., and G. Schatz. 1988. Mitochondrial presequences. *J. Biol. Chem.* 263:4509–4511.

Ronco, V., D.M. Potenza, F. Denti, S. Vullo, G. Gagliano, M. Tognolina, G. Guerra, P. Pinton, A.A. Genazzani, L. Mapelli, et al. 2015. A novel Ca^{2+}-mediated cross-talk between endoplasmic reticulum and acidic organelles: implications for NAADP-dependent Ca^{2+} signalling. *Cell Calcium.* 57:89–100. http://dx.doi.org/10.1016/j.ceca.2015.01.001

Rost, B.R., F. Schneider, M.K. Grauel, C. Wozny, C.G. Bentz, A. Blessing, T. Rosenmund, T.J. Jentsch, D. Schmitz, P. Hegemann, and C. Rosenmund. 2015. Optogenetic acidification of synaptic vesicles and lysosomes. *Nat. Neurosci.* 18:1845–1852. http://dx.doi.org/10.1038/nn.4161

Russwurm, M., F. Mullershausen, A. Friebe, R. Jäger, C. Russwurm, and D. Koesling. 2007. Design of fluorescence resonance energy transfer (FRET)-based cGMP indicators: a systematic approach. *Biochem. J.* 407:69–77. http://dx.doi.org/10.1042/BJ20070348

Salahpour, A., S. Espinoza, B. Masri, V. Lam, L.S. Barak, and R.R. Gainetdinov. 2012. BRET biosensors to study GPCR biology, pharmacology, and signal transduction. *Front. Endocrinol. (Lausanne).* 3:105.

San Martín, A., S. Ceballo, I. Ruminot, R. Lerchundi, W.B. Frommer, and L.F. Barros. 2013. A genetically encoded FRET lactate sensor and its use to detect the Warburg effect in single cancer cells. *PLoS One.* 8:e57712. http://dx.doi.org/10.1371/journal.pone.0057712

San Martín, A., S. Ceballo, F. Baeza-Lehnert, R. Lerchundi, R. Valdebenito, Y. Contreras-Baeza, K. Alegría, and L.F. Barros. 2014. Imaging mitochondrial flux in single cells with a FRET sensor for pyruvate. *PLoS One.* 9:e85780. http://dx.doi.org/10.1371/journal.pone.0085780

Sarkar, A.R., C.H. Heo, L. Xu, H.W. Lee, H.Y. Si, J.W. Byun, and H.M. Kim. 2016. A ratiometric two-photon probe for quantitative imaging of mitochondrial pH values. *Chem. Sci.* 7:766–773. http://dx.doi.org/10.1039/C5SC03708E

Sasaki, K., M. Sato, and Y. Umezawa. 2003. Fluorescent indicators for Akt/protein kinase B and dynamics of Akt activity visualized in living cells. *J. Biol. Chem.* 278:30945–30951. http://dx.doi.org/10.1074/jbc.M212167200

Sato, M. 2014. Genetically encoded fluorescent biosensors for live cell imaging of lipid dynamics. *Methods Mol. Biol.* 1071:73–81. http://dx.doi.org/10.1007/978-1-62703-622-1_6

Sato, M., Y. Ueda, M. Shibuya, and Y. Umezawa. 2005. Locating inositol 1,4,5-trisphosphate in the nucleus and neuronal dendrites with genetically encoded fluorescent indicators. *Anal. Chem.* 77:4751–4758. http://dx.doi.org/10.1021/ac040195j

Sato, M., Y. Ueda, and Y. Umezawa. 2006. Imaging diacylglycerol dynamics at organelle membranes. *Nat. Methods.* 3:797–799. http://dx.doi.org/10.1038/nmeth930

Saucerman, J.J., E.C. Greenwald, and R. Polanowska-Grabowska. 2014. Mechanisms of cyclic AMP compartmentation revealed by computational models. *J. Gen. Physiol.* 143:39–48. http://dx.doi.org/10.1085/jgp.201311044

Schlatterer, C., G. Knoll, and D. Malchow. 1992. Intracellular calcium during chemotaxis of *Dictyostelium discoideum*: a new fura-2 derivative avoids sequestration of the indicator and allows long-term calcium measurements. *Eur. J. Cell Biol.* 58:172–181.

Shen, D., X. Wang, X. Li, X. Zhang, Z. Yao, S. Dibble, X.P. Dong, T. Yu, A.P. Lieberman, H.D. Showalter, and H. Xu. 2012. Lipid storage disorders block lysosomal trafficking by inhibiting a TRP channel and lysosomal calcium release. *Nat. Commun.* 3:731. http://dx.doi.org/10.1038/ncomms1735

Si, F., Y. Liu, K. Yan, and W. Zhong. 2015. A mitochondrion targeting fluorescent probe for imaging of intracellular superoxide radicals. *Chem. Commun. (Camb.).* 51:7931–7934. http://dx.doi.org/10.1039/C5CC01075F

Siegel, M.S., and E.Y. Isacoff. 1997. A genetically encoded optical probe of membrane voltage. *Neuron.* 19:735–741. http://dx.doi.org/10.1016/S0896-6273(00)80955-1

Simonetti, M., A.M. Hagenston, D. Vardeh, H.E. Freitag, D. Mauceri, J. Lu, V.P. Satagopam, R. Schneider, M. Costigan, H. Bading, and R. Kuner. 2013. Nuclear calcium signaling in spinal neurons drives a genomic program required for persistent inflammatory pain. *Neuron.* 77:43–57. http://dx.doi.org/10.1016/j.neuron.2012.10.037

Smith, G.A., R.T. Hesketh, J.C. Metcalfe, J. Feeney, and P.G. Morris. 1983. Intracellular calcium measurements by 19F NMR of fluorine-labeled chelators. *Proc. Natl. Acad. Sci. USA.* 80:7178–7182. http://dx.doi.org/10.1073/pnas.80.23.7178

Snapp, E.L., R.S. Hegde, M. Francolini, F. Lombardo, S. Colombo, E. Pedrazzini, N. Borgese, and J. Lippincott-Schwartz. 2003. Formation of stacked ER cisternae by low affinity protein interactions. *J. Cell Biol.* 163:257–269. http://dx.doi.org/10.1083/jcb.200306020

Sprenger, J.U., R.K. Perera, J.H. Steinbrecher, S.E. Lehnart, L.S. Maier, G. Hasenfuss, and V.O. Nikolaev. 2015. In vivo model with targeted cAMP biosensor reveals changes in receptor-microdomain communication in cardiac disease. *Nat. Commun.* 6:6965. http://dx.doi.org/10.1038/ncomms7965

Sreenath, K., J.R. Allen, M.W. Davidson, and L. Zhu. 2011. A FRET-based indicator for imaging mitochondrial zinc ions. *Chem. Commun. (Camb.).* 47:11730–11732. http://dx.doi.org/10.1039/c1cc14580k

Storace, D., M. Sepehri Rad, B. Kang, L.B. Cohen, T. Hughes, and B.J. Baker. 2016. Toward better genetically encoded sensors of membrane potential. *Trends Neurosci.* 39:277–289.

St-Pierre, F., J.D. Marshall, Y. Yang, Y. Gong, M.J. Schnitzer, and M.Z. Lin. 2014. High-fidelity optical reporting of neuronal electrical activity with an ultrafast fluorescent voltage sensor. *Nat. Neurosci.* 17:884–889. http://dx.doi.org/10.1038/nn.3709

St-Pierre, F., M. Chavarha, and M.Z. Lin. 2015. Designs and sensing mechanisms of genetically encoded fluorescent voltage indicators. *Curr. Opin. Chem. Biol.* 27:31–38. http://dx.doi.org/10.1016/j.cbpa.2015.05.003

Su, S., S.C. Phua, R. DeRose, S. Chiba, K. Narita, P.N. Kalugin, T. Katada, K. Kontani, S. Takeda, and T. Inoue. 2013. Genetically encoded calcium indicator illuminates calcium dynamics in primary cilia. *Nat. Methods.* 10:1105–1107. http://dx.doi.org/10.1038/nmeth.2647

Summerville, J.B., J.F. Faust, E. Fan, D. Pendin, A. Daga, J. Formella, M. Stern, and J.A. McNew. 2016. The effects of ER morphology on synaptic structure and function in Drosophila melanogaster. *J. Cell Sci.* 129:1635–1648. http://dx.doi.org/10.1242/jcs.184929

Suzuki, J., K. Kanemaru, K. Ishii, M. Ohkura, Y. Okubo, and M. Iino. 2014. Imaging intraorganellar Ca^{2+} at subcellular resolution using CEPIA. *Nat. Commun.* 5:4153. http://dx.doi.org/10.1038/ncomms5153

Szent-Gyorgyi, C., B.F. Schmidt, Y. Creeger, G.W. Fisher, K.L. Zakel, S. Adler, J.A. Fitzpatrick, C.A. Woolford, Q. Yan, K.V. Vasilev, et al. 2008. Fluorogen-activating single-chain antibodies for imaging cell surface proteins. *Nat. Biotechnol.* 26:235–240. http://dx.doi.org/10.1038/nbt1368

Sztretye, M., J. Yi, L. Figueroa, J. Zhou, L. Royer, and E. Ríos. 2011. D4cpv-calsequestrin: a sensitive ratiometric biosensor accurately targeted to the calcium store of skeletal muscle. *J. Gen. Physiol.* 138:211–229. http://dx.doi.org/10.1085/jgp.201010591

Tang, S., H.C. Wong, Z.M. Wang, Y. Huang, J. Zou, Y. Zhuo, A. Pennati, G. Gadda, O. Delbono, and J.J. Yang. 2011. Design and application of a class of sensors to monitor Ca^{2+} dynamics in high Ca^{2+} concentration cellular compartments. *Proc. Natl. Acad. Sci. USA.* 108:16265–16270. http://dx.doi.org/10.1073/pnas.1103015108

Tantama, M., Y.P. Hung, and G. Yellen. 2011. Imaging intracellular pH in live cells with a genetically encoded red fluorescent protein sensor. *J. Am. Chem. Soc.* 133:10034–10037. http://dx.doi.org/10.1021/ja202902d

Tantama, M., J.R. Martínez-François, R. Mongeon, and G. Yellen. 2013. Imaging energy status in live cells with a fluorescent biosensor of the intracellular ATP-to-ADP ratio. *Nat. Commun.* 4:2550. http://dx.doi.org/10.1038/ncomms3550

Tavaré, J.M., L.M. Fletcher, and G.I. Welsh. 2001. Using green fluorescent protein to study intracellular signalling. *J. Endocrinol.* 170:297–306. http://dx.doi.org/10.1677/joe.0.1700297

Terrin, A., G. Di Benedetto, V. Pertegato, Y.F. Cheung, G. Baillie, M.J. Lynch, N. Elvassore, A. Prinz, F.W. Herberg, M.D. Houslay, and M. Zaccolo. 2006. PGE_1 stimulation of HEK293 cells generates multiple contiguous domains with different [cAMP]: role of compartmentalized phosphodiesterases. *J. Cell Biol.* 175:441–451. http://dx.doi.org/10.1083/jcb.200605050

Terrin, A., S. Monterisi, A. Stangherlin, A. Zoccarato, A. Koschinski, N.C. Surdo, M. Mongillo, A. Sawa, N.E. Jordanides, J.C.

Mountford, and M. Zaccolo. 2012. PKA and PDE4D3 anchoring to AKAP9 provides distinct regulation of cAMP signals at the centrosome. *J. Cell Biol.* 198:607–621. http://dx.doi.org/10.1083/jcb.201201059

Thomas, D., S.C. Tovey, T.J. Collins, M.D. Bootman, M.J. Berridge, and P. Lipp. 2000. A comparison of fluorescent Ca^{2+} indicator properties and their use in measuring elementary and global Ca^{2+} signals. *Cell Calcium.* 28:213–223. http://dx.doi.org/10.1054/ceca.2000.0152

Tinel, H., J.M. Cancela, H. Mogami, J.V. Gerasimenko, O.V. Gerasimenko, A.V. Tepikin, and O.H. Petersen. 1999. Active mitochondria surrounding the pancreatic acinar granule region prevent spreading of inositol trisphosphate-evoked local cytosolic Ca^{2+} signals. *EMBO J.* 18:4999–5008. http://dx.doi.org/10.1093/emboj/18.18.4999

Tripathi, D.N., and C.L. Walker. 2016. The peroxisome as a cell signaling organelle. *Curr. Opin. Cell Biol.* 39:109–112. http://dx.doi.org/10.1016/j.ceb.2016.02.017

Tsai, F.C., A. Seki, H.W. Yang, A. Hayer, S. Carrasco, S. Malmersjö, and T. Meyer. 2014. A polarized Ca^{2+}, diacylglycerol and STIM1 signalling system regulates directed cell migration. *Nat. Cell Biol.* 16:133–144. http://dx.doi.org/10.1038/ncb2906

Tsien, R.Y. 1981. A non-disruptive technique for loading calcium buffers and indicators into cells. *Nature.* 290:527–528. http://dx.doi.org/10.1038/290527a0

Tsien, R.Y., T. Pozzan, and T.J. Rink. 1982. T-cell mitogens cause early changes in cytoplasmic free Ca^{2+} and membrane potential in lymphocytes. *Nature.* 295:68–71. http://dx.doi.org/10.1038/295068a0

van Lith, M., S. Tiwari, J. Pediani, G. Milligan, and N.J. Bulleid. 2011. Real-time monitoring of redox changes in the mammalian endoplasmic reticulum. *J. Cell Sci.* 124:2349–2356. http://dx.doi.org/10.1242/jcs.085530

van Unen, J., A.D. Stumpf, B. Schmid, N.R. Reinhard, P.L. Hordijk, C. Hoffmann, T.W. Gadella Jr., and J. Goedhart. 2016. A New generation of FRET sensors for robust measurement of Gαi1, Gαi2 and Gαi3 activation kinetics in single cells. *PLoS One.* 11:e0146789. http://dx.doi.org/10.1371/journal.pone.0146789

Villaseñor, R., Y. Kalaidzidis, and M. Zerial. 2016. Signal processing by the endosomal system. *Curr. Opin. Cell Biol.* 39:53–60. http://dx.doi.org/10.1016/j.ceb.2016.02.002

Vinkenborg, J.L., T.J. Nicolson, E.A. Bellomo, M.S. Koay, G.A. Rutter, and M. Merkx. 2009. Genetically encoded FRET sensors to monitor intracellular Zn^{2+} homeostasis. *Nat. Methods.* 6:737–740. http://dx.doi.org/10.1038/nmeth.1368

Violin, J.D., J. Zhang, R.Y. Tsien, and A.C. Newton. 2003. A genetically encoded fluorescent reporter reveals oscillatory phosphorylation by protein kinase C. *J. Cell Biol.* 161:899–909. http://dx.doi.org/10.1083/jcb.200302125

Vishnu, N., M. Jadoon Khan, F. Karsten, L.N. Groschner, M. Waldeck-Weiermair, R. Rost, S. Hallström, H. Imamura, W.F. Graier, and R. Malli. 2014. ATP increases within the lumen of the endoplasmic reticulum upon intracellular Ca^{2+} release. *Mol. Biol. Cell.* 25:368–379. http://dx.doi.org/10.1091/mbc.E13-07-0433

Vorndran, C., A. Minta, and M. Poenie. 1995. New fluorescent calcium indicators designed for cytosolic retention or measuring calcium near membranes. *Biophys. J.* 69:2112–2124. http://dx.doi.org/10.1016/S0006-3495(95)80082-2

Waldeck-Weiermair, M., H. Bischof, S. Blass, A.T. Deak, C. Klec, T. Graier, C. Roller, R. Rost, E. Eroglu, B. Gottschalk, et al. 2015. Generation of red-shifted cameleons for imaging Ca^{2+} dynamics of the endoplasmic reticulum. *Sensors (Basel).* 15:13052–13068. http://dx.doi.org/10.3390/s150613052

Wandinger-Ness, A., and M. Zerial. 2014. Rab proteins and the compartmentalization of the endosomal system. *Cold Spring Harb. Perspect. Biol.* 6:a022616. http://dx.doi.org/10.1101/cshperspect.a022616

Wang, Q., L. Zhou, L. Qiu, D. Lu, Y. Wu, and X.B. Zhang. 2015. An efficient ratiometric fluorescent probe for tracking dynamic changes in lysosomal pH. *Analyst (Lond.).* 140:5563–5569. http://dx.doi.org/10.1039/C5AN00683J

Wang, X., H. Fang, Z. Huang, W. Shang, T. Hou, A. Cheng, and H. Cheng. 2013. Imaging ROS signaling in cells and animals. *J. Mol. Med.* 91:917–927. http://dx.doi.org/10.1007/s00109-013-1067-4

Wang, Z., D. Liu, A. Varin, V. Nicolas, D. Courilleau, P. Mateo, C. Caubere, P. Rouet, A.M. Gomez, G. Vandecasteele, et al. 2016. A cardiac mitochondrial cAMP signaling pathway regulates calcium accumulation, permeability transition and cell death. *Cell Death Dis.* 7:e2198. http://dx.doi.org/10.1038/cddis.2016.106

Ward, M.W., H.J. Huber, P. Weisová, H. Düssmann, D.G. Nicholls, and J.H. Prehn. 2007. Mitochondrial and plasma membrane potential of cultured cerebellar neurons during glutamate-induced necrosis, apoptosis, and tolerance. *J. Neurosci.* 27:8238–8249. http://dx.doi.org/10.1523/JNEUROSCI.1984-07.2007

Wong, A.K., P. Capitanio, V. Lissandron, M. Bortolozzi, T. Pozzan, and P. Pizzo. 2013. Heterogeneity of Ca^{2+} handling among and within Golgi compartments. *J. Mol. Cell Biol.* 5:266–276. http://dx.doi.org/10.1093/jmcb/mjt024

Wu, M.M., J. Llopis, S. Adams, J.M. McCaffery, M.S. Kulomaa, T.E. Machen, H.P. Moore, and R.Y. Tsien. 2000. Organelle pH studies using targeted avidin and fluorescein-biotin. *Chem. Biol.* 7:197–209. http://dx.doi.org/10.1016/S1074-5521(00)00088-0

Yang, P.C., B.W. Boras, M.T. Jeng, S.S. Docken, T.J. Lewis, A.D. McCulloch, R.D. Harvey, and C.E. Clancy. 2016. A Computational modeling and simulation approach to investigate mechanisms of subcellular cAMP compartmentation. *PLOS Comput. Biol.* 12:e1005005. http://dx.doi.org/10.1371/journal.pcbi.1005005

Yano, T., M. Oku, N. Akeyama, A. Itoyama, H. Yurimoto, S. Kuge, Y. Fujiki, and Y. Sakai. 2010. A novel fluorescent sensor protein for visualization of redox states in the cytoplasm and in peroxisomes. *Mol. Cell. Biol.* 30:3758–3766. http://dx.doi.org/10.1128/MCB.00121-10

Yapici, N.B., Y. Bi, P. Li, X. Chen, X. Yan, S.R. Mandalapu, M. Faucett, S. Jockusch, J. Ju, K.M. Gibson, et al. 2015. Highly stable and sensitive fluorescent probes (LysoProbes) for lysosomal labeling and tracking. *Sci. Rep.* 5:8576. http://dx.doi.org/10.1038/srep08576

Yousif, L.F., K.M. Stewart, and S.O. Kelley. 2009. Targeting mitochondria with organelle-specific compounds: strategies and applications. *ChemBioChem.* 10:1939–1950. http://dx.doi.org/10.1002/cbic.200900185

Zaccolo, M., and T. Pozzan. 2002. Discrete microdomains with high concentration of cAMP in stimulated rat neonatal cardiac myocytes. *Science.* 295:1711–1715. http://dx.doi.org/10.1126/science.1069982

Zaccolo, M., F. De Giorgi, C.Y. Cho, L. Feng, T. Knapp, P.A. Negulescu, S.S. Taylor, R.Y. Tsien, and T. Pozzan. 2000. A genetically encoded, fluorescent indicator for cyclic AMP in living cells. *Nat. Cell Biol.* 2:25–29. http://dx.doi.org/10.1038/71345

Zacharias, D.A., J.D. Violin, A.C. Newton, and R.Y. Tsien. 2002. Partitioning of lipid-modified monomeric GFPs into membrane microdomains of live cells. *Science.* 296:913–916. http://dx.doi.org/10.1126/science.1068539

Zhang, Y., M.K. So, A.M. Loening, H. Yao, S.S. Gambhir, and J. Rao. 2006. HaloTag protein-mediated site-specific conjugation of bioluminescent proteins to quantum dots. *Angew. Chem. Int. Ed. Engl.* 45:4936–4940. http://dx.doi.org/10.1002/anie.200601197

Zhao, Y., J. Jin, Q. Hu, H.M. Zhou, J. Yi, Z. Yu, L. Xu, X. Wang, Y. Yang, and J. Loscalzo. 2011. Genetically encoded fluorescent

sensors for intracellular NADH detection. *Cell Metab.* 14:555–566. http://dx.doi.org/10.1016/j.cmet.2011.09.004

Zhou, X., T.L. Clister, P.R. Lowry, M.M. Seldin, G.W. Wong, and J. Zhang. 2015. Dynamic visualization of mTORC1 activity in living cells. *Cell Reports.* 10:1767–1777. http://dx.doi.org/10.1016/j.celrep.2015.02.031

Zhu, H., J. Fan, Q. Xu, H. Li, J. Wang, P. Gao, and X. Peng. 2012. Imaging of lysosomal pH changes with a fluorescent sensor containing a novel lysosome-locating group. *Chem. Commun. (Camb.).* 48:11766–11768. http://dx.doi.org/10.1039/c2cc36785h

Zhu, Y., J. Xu, and S.F. Heinemann. 2009. Two pathways of synaptic vesicle retrieval revealed by single-vesicle imaging. *Neuron.* 61:397–411. http://dx.doi.org/10.1016/j.neuron.2008.12.024